Earth, wind, water, fire: Interactions between land-use and natural disturbance in tropical second-growth forest landscapes

Naomi Schwartz

Submitted in partial fulfillment of the
requirements for the degree of
Doctor of Philosophy
in the Graduate School of Arts and Sciences

COLUMBIA UNIVERSITY

2017

ABSTRACT

Earth, wind, water, fire: Interactions between land-use and natural disturbance in tropical second-growth forest landscapes

Naomi Schwartz

Climate models predict changes to the frequency and intensity of extreme events, with large effects on tropical forests likely. Predicting these impacts requires understanding how landscape configuration and land-use change influence the susceptibility of forests to disturbances such as wind, drought, and fire. This is important because most tropical forests are regenerating from anthropogenic disturbance, and are located in landscape mosaics of forest, agriculture, and other land use. This dissertation consists of four chapters that combine remote sensing and field data to examine causes and consequences of disturbance and land-use change in tropical second-growth forests. In Chapter 1, I use satellite data to identify factors associated with permanence of second-growth forest, and assess how estimates of carbon sequestration vary under different assumptions about second-growth forest permanence. I show that most second-growth forest is cleared when young, limiting carbon sequestration. In Chapter 2, I combine data from weather stations, remote sensing, and landowner surveys to model fire activity on 732 farms in the study area over ten years. The relative importance of these factors differs across scales and depending on the metric of fire activity being considered, illustrating how implications for fire prevention and mitigation can be different depending on the metric considered. Chapter 3 combines Landsat imagery and field data to map wind damage from a severe convective storm, providing strong empirical evidence that vulnerability to wind disturbance is elevated in tropical forest fragments. Finally, in Chapter 4 I integrate annual forest census data with LiDAR-derived topography

metrics and tree functional traits in a hierarchical Bayesian modeling framework to explore how drought, topography, and neighborhood crowding affect tree growth, and how functional traits modulate those effects. The results from these studies demonstrate innovative approaches to understanding spatial variation in forest vulnerability to disturbance at multiple scales, and the results have implications for managing forests in a changing climate.

TABLE OF CONTENTS

LIST OF FIGURES AND TABLES

Chapter 1

Chapter 2

Chapter 3

Chapter 4

ACKNOWLEDGEMENTS

Doing my Ph.D. at Columbia was a privilege and a pleasure, made possible only by contributions, support, encouragement, and love from a huge number of people. First and foremost, I must thank my co-advisors, Ruth DeFries and Maria Uriarte. Both Maria and Ruth have provided me with time, intellectual energy, and financial support throughout my Ph.D., and I'm grateful to have had the opportunity to work with two such accomplished scientists (who also happen to be terrific mentors). Maria's quantitative skills and deep insight into tropical forest ecology made for excellent scientific training, and I thank her for weekly meetings that kept me on track and for giving just the right amount of "push" to keep me productive and hardworking. Ruth has always encouraged me to think hard about why my science matters and what science can do for conservation and people, making me a better scientist and a better citizen, and her remote sensing expertise and integrative landscape perspective greatly enhanced this work.

I also thank my committee members, Duncan Menge, Laura Schneider, and Louis Verchot. Duncan has taught me more than I ever dreamed I'd know about nitrogen fixation and logarithms, and has provided lots of helpful scientific and life advice over impromptu lunchtime chats. I thank Laura for her insight into disturbance ecology and human influences in tropical forest landscapes, and Lou for helping me think about my work in a global and policy context. I am deeply grateful to Miguel Pinedo-Vasquez, my unofficial sixth committee member, for his unparalleled insight into the Peruvian study landscape, helping me get financial and on-the-ground support for my fieldwork in Peru, and for his comments and contributions to this dissertation. I also thank collaborators who contributed time, data, and their ideas and perspectives to this research, including Victor Gutierrez-Velez, Katia Fernandes, Kris Bedka,

and Walter Baethgen. I thank CIFOR for financially supporting my fieldwork, and acknowledge funding from NSF grant 0909475, an E3B dissertation research travel grant, and the Columbia Institute for Latin American Studies.

Conducting fieldwork was one of the most challenging parts of my dissertation, and I am forever grateful to the people who made it easier. I cannot overstate how much Aoife Bennett helped me, from finding me a place to live, connecting me with field assistants, and helping me learn and understand Amazonian Spanish, to introducing me to the coolest pet I'll ever have. I am being completely truthful when I say that I couldn't have completed my fieldwork without her. I also thank Medardo Miranda Ruiz, Gabriel Hidalgo, Luis Calderon Vasquez, Orlando Sanchez and other assistants for their help collecting field data and for safely driving me around the Peruvian countryside on a beat-up Chinese dirt bike. Thank you to all the landowners who welcomed me into their forests and shared guaba and oranges with me at the end of long, hot field days.

E3B has been a wonderful home over the past five years. Lourdes, Jae, Alex, and all the administrators keep the department running smoothly – we wouldn't function without you! Current and former members of the DeFries, Uriarte, and Menge labs have given helpful feedback and exposed me to new and interesting scientific ideas and approaches. The students, postdocs, and faculty in this department have created a supportive and intellectually stimulating environment and I've benefitted greatly from being a part of this community. In particular, I thank friends and fellow inhabitants of Schermerhorn Extension for afternoon coffee runs, office beers, and listening to me think out loud, especially: Ben Taylor, Andrew Quebbeman, Case Prager, Brian Weeks, Nicole Thompson, Amrita Neelakantan, Andrew Budsock, Bob Muscarella, Bene Bachelot, Jesse Lasky, Matt Fagan, Meha Jain, Megan Cattau, Carla Staver,

and many others. Bianca Lopez, my ecology partner-in-crime, has read drafts, shared ideas, and been a great friend from afar. Other friends have made living in New York so much fun, and have provided excellent distractions from working on this dissertation, especially Simma Reingold, Kaity and Jeremy Lloyd-Styles, Neil Satterlund, and Megan Ines.

Finally I thank my family. To Ryan, my partner and future husband, your love, support, and friendship made this process so much easier and more fun and it wouldn't have been the same without you. My family has provided me with unending support, and I'm so glad I got to live near them while I did my Ph.D. My siblings, Daniel and Rebecca, have provided friendship and humor all along. Mom, Dad, and Opa, you have always encouraged me to ask questions and look critically at the world, which I'm sure is the reason I became a scientist. Thank you.

To my dad, Aron, who gave me the idea to study ecology

INTRODUCTION

Climate models consistently predict changes in the frequency and intensity of extreme events, such as tropical cyclones, heavy precipitation, droughts, and fires (Knutson et al. 2010, Pechony and Shindell 2010, Moritz et al. 2012, Feng et al. 2013, IPCC 2013, Duffy et al. 2015). These events have implications for the global carbon cycle, ecosystem services, biodiversity, human health, and the economy. For example, biomass burning releases up to 2.2 Pg carbon into the atmosphere every year (Jacobson 2014), and tree mortality from wind, floods, and droughts can also lead to significant emissions (Juárez et al. 2008, Phillips et al. 2009). Though disturbance is an integral part of many ecosystems, shifts in disturbance regimes can lead to drastic ecological changes (Nepstad et al. 2008, Malhi et al. 2009). Disturbance and extreme events also affect human health and have major economic impacts (de Mendonça et al. 2004, Marlier et al. 2012).

Ecological impacts of disturbance tend to be patchy, with patterns resulting from natural environmental gradients and anthropogenic modifications to the environment. Variation in topography, elevation, and soil type creates heterogeneity in moisture conditions, forest structure, and species composition (Stephenson 1990), which leads to spatial variation in disturbance impacts. For example, drought-induced mortality is sometimes higher in drier landscape positions, such as steep and southwest-facing slopes (Fekedulegn et al. 2003, Guarín and Taylor 2005), and fire regimes can be strongly influenced by topography as well (e.g. Bradstock et al. 2010, Flatley et al. 2011, Taylor and Skinner 2011). Forest stand characteristics, such as forest structure and species composition, can also mediate the effects of disturbance. For example, forest flammability often varies with forest structure (Harrod et al. 2000, Ray et al. 2005, 2010), and vulnerability to fire-induced mortality depends on tree size and species traits,

such as bark thickness and wood density (Pinard and Huffman 1997, Barlow et al. 2003, Balch et al. 2011, Brando et al. 2012). Extreme wind impacts in forests also depend on individual characteristics such as tree size and life history strategy (Everham and Brokaw 1996, Canham et al. 2010, Uriarte et al. 2012a), and stand structure variables like canopy height and total basal area (McGroddy et al. 2013). Drought effects also depend on individual and species characteristics: pioneer species, species with low wood density, and larger trees tend to suffer more severe drought effects (Nepstad et al. 2007, Phillips et al. 2010, Greenwood et al. 2017).

Anthropogenic factors, such as land use, forest fragmentation, and the presence of roads, modulate disturbance severity and spatial patterns. For example, land use, land management, and other anthropogenic drivers are key determinants of patterns of fire frequency and intensity, especially in tropical regions (Nepstad et al. 1999, Van Der Werf et al. 2008, Archibald et al. 2009, Uriarte et al. 2012b). Forest fragmentation can increase vulnerability to wind damage via edge effects on forest structure, microclimate, and species composition (Broadbent et al. 2008, Laurance and Curran 2008). Ultimately, climate variability is filtered through these landscape, forest stand, species, and individual tree characteristics to generate observed patterns of disturbance impacts, the drivers of which vary across spatial scales.

Today, about 57% of forests are secondary or "naturally regenerating;" that is, they show clear signs of logging, agricultural use, or other human activities (FAO 2010). Recent studies have highlighted the potential for carbon mitigation from rapid biomass recovery in regrowing tropical forests (Poorter et al. 2016): in Latin America alone, second-growth forests could offset 21 years of the region's emissions from fossil fuels and other industrial processes (Chazdon et al. 2016). Furthermore, second growth forests can provide benefits for biodiversity conservation, livelihood strategies, and other ecosystem services such as flood or erosion control (Brown and

Lugo 1990, Barlow et al. 2007, Chazdon et al. 2009, Locatelli et al. 2015). However, second growth forests are particularly vulnerable to disturbance and clearing, making the likelihood that they will contribute substantially to climate change mitigation highly uncertain.

Exposure to natural disturbances such as extreme winds, fires, or drought can cause large losses of carbon and affect successional trajectories in regenerating forests (Flynn et al. 2010, Anderson-Teixeira et al. 2013, Uriarte et al. 2016b), influencing the degree to which the carbon sequestration potential of second-growth forests is achieved. Second-growth forests are typically located in landscapes subject to human influence that are mosaics of old growth, second growth, and other land cover types (Brown and Lugo 1990), and regrowth often happens along existing forest margins (Asner et al. 2009b, Sloan et al. 2016), making second-growth forests highly exposed to edge effects, impacts of fragmentation, and anthropogenic disturbances such as fire and logging. Second growth forests also contain a high proportion of pioneer and fast growing tree species, whose characteristics may make them more vulnerable to drought, wind disturbance, or fire (Bazzaz and Pickett 1980, Phillips et al. 2010, Ouédraogo et al. 2013, Lohbeck et al. 2013). Furthermore, most second-growth forests are not under formal protection, and rates of clearing of second-growth forest tend to be higher than old-growth forest (Heinimann et al. 2007, Gutiérrez-Vélez et al. 2011). The carbon benefits, conservation value, and other services associated with tropical second-growth forests require long-term permanence and protection from frequent disturbance (Liebsch et al. 2008, Chazdon et al. 2009). Accurately predicting successional trajectories and biomass recovery in these forests requires that we understand their disturbance ecology and how their disturbance regimes are influenced by the landscapes in which they are situated.

This dissertation aims to understand the drivers of vulnerability to disturbance in tropical second-growth forests, and specifically, how landscape characteristics influence observed patterns of disturbance impacts. The research was conducted in two regions with unique and distinct land-use histories and landscape dynamics. Chapters 1 through 3 focus on the heterogeneous and rapidly changing landscape near Pucallpa, Peru, in the western Amazon. The landscape is a mosaic of forest patches (old-growth and naturally regenerating, plus a small number of forest plantations) surrounded by pastures, oil palm plantations, and smallholder farms. Pucallpa is connected to Lima, the capital city, by road, and has been an important transport center and a hotspot for in-migration, settlement, and land conversion since the 1960s (Oliveira et al. 2007). Agricultural fire-use is common, and these fires occasionally escape, burning large areas of the landscape, including forests (Uriarte et al. 2012b, Gutiérrez-Velez et al. 2014). A severe windstorm passed through the study area in 2013, and caused widespread blowdowns and tree mortality. This region thus provides a useful example for considering second-growth forest dynamics in a changing tropical landscape, and given the wind and fire disturbances in recent years, an ideal region in which to assess the drivers of fire activity and wind damage.

Chapter 4 was conducted in field plots located in El Verde National Forest, Puerto Rico. Puerto Rico was once almost entirely deforested, but due to agricultural abandonment forest cover increased from 9% to 37% of the island from 1950 to 1990 (Rudel et al. 2000). The El Verde Chronosequence Plots represent a range of forest ages from 35 to 76 years since agricultural abandonment, and old-growth forest, and are located across variable topography, enabling research about landscape influences on successional forest dynamics.

In this dissertation, I developed new methods combining satellite and airborne remote sensing and field data to examine causes and consequences of disturbance and land-use change in tropical second-growth forests. I consider four types of disturbance to which second-growth forests are exposed: clearing, fire, extreme wind, and drought. Chapter 1 aims to characterize the landscape context of the study area in Peru, and to identify landscape factors that increase the likelihood of forest regrowth and clearing. In Chapter 2, I synthesize data on climate, landowner residency, and land cover to model drivers of fire activity, and determine how multiple interacting factors at different scales influence fire probability and fire size. Chapter 3 combines satellite imagery and field data to map wind damage from a severe convective storm, assessing the degree to which vulnerability to wind disturbance is elevated in tropical forest fragments and varies with forest age. In Chapter 4, I explore how drought and topography interact to influence tree demographics in a tropical second-growth forest. Together, the results from these studies demonstrate innovative, interdisciplinary approaches to understanding spatial variation in forest vulnerability to disturbance at multiple scales, and the results have implications for managing forests in a changing climate.

CHAPTER 1: LAND-USE DYNAMICS INFLUENCE ESTIMATES OF CARBON SEQUESTRATION POTENTIAL IN TROPICAL SECOND-GROWTH FOREST

Naomi Schwartz, María Uriarte, Ruth DeFries, Victor Gutierrez-Velez, Miguel Pinedo-Vasquez

Abstract

Many countries have made major commitments to carbon sequestration through reforestation under the Paris Climate Agreement, and recent studies have illustrated the potential for large amounts of carbon sequestration in tropical second-growth forests. However, carbon gains in second-growth forests are threatened by non-permanence, i.e. release of carbon into the atmosphere from clearing or disturbance. The benefits of second-growth forests require long-term persistence on the landscape, but estimates of carbon potential rarely consider the spatio-temporal landscape dynamics of second-growth forests. In this study, we used remotely sensed imagery from a landscape in the Peruvian Amazon to examine patterns of second-growth forest regrowth and permanence over 28 years (1985-2013). By 2013, 44% of all forest cover in the study area was second growth and more than 50% of second-growth forest pixels were less than 5 years old. We modeled probabilities of forest regrowth and clearing as a function of landscape factors. The amount of neighboring forest and variables related to pixel position (i.e. distance to edge) were important for predicting both clearing and regrowth. Forest age was the strongest predictor of clearing probability and suggests a threshold response of clearing probability to age. Finally, we simulated future trajectories of carbon sequestration using the parameters from our models. We compared this with the amount of biomass that would accumulate under the assumption of second-growth permanence. Estimates differed by 900,000 tonnes, equivalent to over 80% of Peru's commitment to carbon sequestration through "community reforestation" under the Paris Agreement. Though the study area has more than 40,000 hectares of second-

growth forest, only a small proportion is likely to accumulate significant carbon. Instead, cycles between forest and non-forest are common. Our results illustrate the importance of considering landscape dynamics when assessing the carbon sequestration potential of second-growth forests.

Introduction

Recent studies have highlighted the potential for carbon mitigation from rapid biomass recovery in regrowing tropical forests (Poorter et al. 2016). In Latin America alone, second-growth forests could offset 21 years of the region's emissions from fossil fuels and other industrial processes (Chazdon et al. 2016). Carbon sequestration through reforestation (including active restoration and natural regeneration) comprises a major contribution in many countries' Intended Nationally Determined Contributions (iNDCs) to emissions reductions in the UN Framework Convention on Climate Change (UNFCCC). However, carbon sequestration in forests can be temporary, since forests are always at risk of being cleared or otherwise disturbed. Though the UNFCCC recognizes the risk of non-permanence and reversal of carbon gains from reforestation (UNFCCC 2014), estimates of potential benefits from second-growth forests typically consider just a snapshot of a landscape, without explicit analysis of the spatio-temporal dynamics of second-growth forest regrowth and clearing.

The carbon benefits and other services associated with tropical second-growth forests require the forests persist long-term (Chazdon et al. 2009). Accumulating biomass equivalent to 90% that of old-growth forest takes a median time of 66 years (Poorter et al. 2016). Long-term persistence of second-growth forest allows long-lived species and old-growth taxa to regenerate, enhancing long-term carbon storage and conservation value (Liebsch et al. 2008, Chazdon et al. 2009). Therefore, an estimate of the amount of second-growth forest in a region or the amount of

land available for reforestation is not enough to quantify these benefits. Predictions of the likelihood of forest regrowth and persistence and an understanding of their drivers are necessary as well.

Drivers of forest regrowth range from global macroeconomic conditions to local management strategies, and vary across scales. Commodity prices, demand for agricultural and forest products, and other global macroeconomic drivers influence rates of deforestation and regrowth (Grau and Aide 2008, Lambin and Meyfroidt 2011, Aide et al. 2013). At national scales, forest transition theory describes the shift from net deforestation to net increase in forest cover that has occurred in many countries as their economies have developed (Mather 1992). Mechanisms for forest transitions include agricultural intensification and adjustment to land quality, shortages of forest products, or demographic shifts such as rural-to-urban migration and associated remittances (Mather 1992, Hecht et al. 2006, Meyfroidt and Lambin 2011). However, forest transitions can reverse (Jeon et al. 2014). At sub-national scales, forest regrowth tends to occur first in regions with marginal suitability for agriculture (Rudel et al. 2000, Asner et al. 2009a, Yackulic et al. 2011). Within landscapes, forest regrowth is more likely far from roads (Rudel et al. 2002) or closer to forest (Crk et al. 2009, Sloan et al. 2016). Finally, forest regrowth may be intertwined in local management strategies, particularly shifting cultivation (Rudel et al. 2002).

Far less research has assessed if, when, and why second-growth forests persist. Most second-growth forests are not under formal protection, and rates of clearing of second-growth forest tend to be higher than old-growth forest (Heinimann et al. 2007, Gutiérrez-Vélez et al. 2011), though the probability of clearing tends to decline with increasing forest age (Etter et al. 2005, Helmer et al. 2008). Because regrowth tends to occur along forest margins (Asner et al.

2009b, Sloan et al. 2016) and in small fragments (Helmer 2000), second-growth forests are highly vulnerable to fire (Alencar et al. 2004, Armenteras et al. 2013) and wind disturbance (Laurance and Curran 2008, Schwartz et al. in review). Regrowth forests associated with shifting cultivation practices are unlikely to persist longer than the length of the fallow period, often as few as 5-7 years (Pinedo-Vasquez et al. 1992, Coomes et al. 2000). Furthermore, many drivers of regrowth are transitory. For example, commodity prices fluctuate and economic downturns affect the amount of remittances arriving in rural areas (Tilly 2011). These and other changes can lead to deforestation and shifts in land-use practices, affecting the likelihood that second-growth forests persist and influencing estimates of the carbon sequestration potential of second-growth forests.

In this study, we used remotely sensed imagery to examine patterns of second-growth forest development and permanence over 28 years (1985-2013) in a western Amazonian landscape. We investigated temporal variation in the amount of second-growth forest, and rates of forest regrowth and clearing. We also assess spatial variation in where second-growth forest develops and persists within the study landscape. Specifically, we ask:

1) How has the amount of second-growth forest in the study area changed over the last three decades?
2) What landscape factors are associated with forest regrowth?
3) What landscape factors are associated with clearing of second-growth forest?
4) How do estimates of carbon sequestration potential vary under different assumptions about second-growth forest persistence?

Better understanding the dynamics associated with second-growth forest development and persistence will allow more realistic estimation of the carbon potential of second-growth forest,

and will allow managers interested in promoting forest regrowth to target efforts most effectively.

Materials and methods

Study area

This research focuses on an area of 215,800 ha near Pucallpa, the capital of the Ucayali region of Peru (Figure 1). The landscape is a mosaic of forest (old-growth and naturally regenerating, plus a small number of forest plantations) surrounded by pastures, oil palm plantations, and smallholder farms. Pucallpa is connected to Lima, the capital city, by road, and has been an important transport center and a hotspot for in-migration, settlement, and land conversion since the 1960s. Recently, rural-to-urban migration has increased (Instituto Nacional de Estadistica e Informatica 2009), which has been associated with cessation of cultivation on land owned by absentee landowners and an increase in fire activity in areas with high levels of landowner absenteeism (Uriarte et al. 2012b, Schwartz et al. 2015). More recently, there has also been expansion of more intensive commodity crops, especially oil palm and cacao, in response to government policies incentivizing their cultivation, often into un-protected second-growth forest areas (Gutiérrez-Vélez et al. 2011). Shifting cultivation is still a common form of smallholder production, with the typical fallow time being around 4-7 years (Pinedo-Vasquez et al. 1992). The study area is in the midst of a transition from frontier clearing to small-scale farming and intensive agriculture, a common dynamic in some tropical landscapes (DeFries et al. 2004). This region thus provides a useful example for considering second-growth forest dynamics in a changing tropical landscape.

Data collection

We developed a 28-year land cover time series with Landsat data spanning from 1985-2013 (Appendix 1: Table 1). The classification differentiates between old-growth/high-biomass forest, young or low-biomass forest, pasture, fallow, oil palm and other land-cover types with an overall accuracy of 93%. Methods for the classification are detailed in Gutiérrez-Vélez and DeFries (2013) and in Appendix 1.

Second-growth forest was defined as woody vegetation growing on land that was previously classified as non-forest at some point since 1985. Second-growth forest age was determined as the number of years since a non-forest land cover type was replaced by forest. We identified regrowth events as a transition from non-forest to forest. To be classified as second-growth forest, we required that a pixel must have been classified as non-forest for at least two consecutive years prior, and that the new forest must have persisted for at least two consecutive years, to minimize the influence of random noise or classification error on our results. We also used the land cover layers to generate a number of predictor variables (Table 1). Predictor variables were related to either pixel position on the landscape (distance to roads, rivers, and settlements, distance to forest edge, forest patch size, and the amount of forest in the neighborhood around the pixel) or pixel history (forest age, number of years cleared before regrowth occurred, whether or not the pixel was ever classified as forest, Table 1).

To develop a relationship between forest biomass and forest age, we collected data on above ground biomass in 30 field plots (Schwartz et al. in revision, see SI). We identified the age of each plot using the land cover time series. Plots that were classified as forest for the entire study period were assigned an age of 30 years, which is a lower bound. We fit a linear model

predicting biomass from log-transformed age, as the rate of biomass accumulation tends to slow with age (Poorter *et al* 2016, Appendix 1: Figure 1). The parameters from this model and their 95% confidence intervals were used to estimate biomass accumulated in second-growth forest pixels and associated uncertainty.

Statistical analysis

Modeling forest regeneration

To assess the factors associated with forest regrowth, we first sampled pixels every 600 m from a regular grid overlaid across the study area; this sampling scheme facilitates computation and avoids spatial autocorrelation. Pixels classified as non-forest were included in analyses, with the response variable determined as whether or not that pixel transitioned into forest (i.e. regrew) in the subsequent year. Sampled pixels that were always classified as forest during the 28-year time-series were not included in analysis. Ultimately, a total of 54,718 pixel-years were included in analysis, from 4,223 unique pixels. We used the R package 'lme4' (Bates et al. 2015) to fit generalized linear mixed effects models to assess what landscape characteristics best predicted forest regrowth. Fixed effects covariates are listed in Table 1, and pixel ID and year were both included as random effects to account for year-to-year variation and repeated measures of individual pixels. To ensure that spatial autocorrelation did not bias our results, we tested for spatial autocorrelation in the residuals by calculating Moran's I. To assess goodness of fit, we calculated marginal and conditional R^2 values using the R package MuMIn, and compared predicted probability of regrowth with the proportion of pixels that did regrow (Appendix 1: Figure 2).

Modeling second-growth forest permanence

To analyze the degree to which second-growth forests persist and the factors associated with persistence, we sampled one pixel from every new second-growth forest patch greater than 1 ha for all years. For each sampled pixel, we tracked the fate of the pixel (whether it persisted as second-growth forest, or was cleared) for each year until the pixel was classified as non-forest, or until the end of the study period, whichever came first. This resulted in a total of 142,487 pixel-years included in analysis, from 19,805 unique pixels. We fit generalized linear mixed effects models including random effects for year and pixel ID, to account for repeated measures of individual pixels. Predictors included variables related to pixel position and pixel history (Table 1). We tested for spatial autocorrelation and assessed goodness of fit using the same procedures described above.

Simulating future forest regrowth trajectories

To assess how estimates of carbon sequestration potential vary under different assumptions of second-growth forest persistence, we simulated future forest regrowth trajectories from the end of the study period until 2050. For each annual time step from 2013 to 2050, we recalculated predictor variables. Distance to road, river, and settlement were assumed to remain constant over time for pixels, because projections for how the location or number of these features will change over time are not available. Then, we calculated the probability of regrowth (for non-forest cells) or the probability of clearing (for the second-growth forest cells) using the model parameters from the models described above. Because we were interested specifically in dynamics surrounding regrowth forest, we assumed all "old-growth" pixels (i.e. pixels that were

never detected as a non-forest land cover class) remained old growth forest throughout the simulation. However, we included old-growth forest pixels in our simulated landscapes so they would be factored in as forest for variables like distance to forest edge and proportion of neighborhood made up of forest. To calculate total second-growth forest biomass over time, we applied the parameters from the model of biomass vs. forest age to all second-growth forest pixels and summed across the landscape (SI). We compared these calculations to the amount of biomass that would accumulate on the landscape if the regrowth forest present in the landscape at the end of the observation period (2013) was assumed to persist and continue to accumulate biomass until 2050.

Results

Forest regrowth and clearing, 1985-2013

From 1985-2013, total forest cover decreased from 162,725 hectares to 97,455 ha (Figure 2). By 2013, 42,756 hectares of second-growth forest were present in the study area, while only 54,698 ha of old growth remained (Figure 2). Most of this forest was young, with 57.4% of second-growth forest less than 5 years of age, and only 4.3% over 20 years of age (Appendix 1: Figure 4).

The model of forest regrowth reproduced the patterns observed in the data, but slightly over-predicted forest regrowth (R^2=0.64, Table 1, Appendix 1: Figure 2). Spatial autocorrelation in the model residuals was low (Moran's $I < 0.001$, $p < 0.05$). Both pixel position and pixel history were important for predicting forest regrowth (Table 1). The proportion of neighboring forest around a focal pixel was the most important predictor of forest regrowth (Table 1), suggesting that forest cover is contagious. Distance to nearest road and to nearest settlement

were also important predictors of the probability of regrowth, with regrowth more likely to occur further from roads, but closer to settlements. Whether a pixel had previously been classified as forest was the second most important predictor of regrowth probability, with probability of regrowth higher for pixels that were previously classified as forest.

The model of second-growth forest clearing somewhat under-predicted clearing of second-growth forest (Appendix 1: Figure 3), but explained 35% of the variation in observed clearing (Table 1). Spatial autocorrelation in residuals was low (Moran's I =0.02, $p < 0.05$). Again, both pixel position and pixel history were significant predictors of the likelihood of clearing, but the relative importance of predictors differed from the model of regrowth. Age was the strongest predictor of clearing, with the probability of clearing first increasing with age, until peaking approximately at 5 years of age, and then declining steeply (Figure 3). The number of years pixels remained cleared before regrowing was also an important predictor of clearing likelihood, with pixels that had been cleared for shorter periods of time more likely to persist as second-growth forest. As expected, second-growth forest pixels farther from forest edges were more likely to persist, but counter to expectations, pixels in larger patches were more likely to be cleared. Pixels far from roads and far from rivers were less likely to be cleared, but these effects were weak relative to other significant predictors.

Forest regrowth trajectories and biomass accumulation

Simulations of future forest regrowth trajectories predicted a further increase in the total cover of second-growth forest, from 42,756 hectares in 2013 to 50,636 hectares in 2050 (Figure 2). However, 52% of second-growth forest in 2050 was still under 20 years old in our simulations, and only 35% was over 30 (Figure 4). Our simulations predicted that by 2050, total carbon stored in second-growth forest in the study area was 2.724 million tonnes (CI = 0.300,

5.536, Figure 4). Under the assumption that all second-growth forest on the landscape in 2013 persists and continues to age and accumulate carbon, but no new forest emerges, 3.649 (95% CI = 0.619, 6.614) million tonnes C are stored in the second-growth forest by 2050 (Fig 5).

Discussion

Reforestation is frequently cited as a promising strategy for removing CO_2 from the atmosphere (Rhodes and Keith 2008, van Vuuren et al. 2013), particularly in the humid tropics where second-growth forest can accumulate as much as 225 Mg biomass (113 Mg carbon) per hectare in just 20 years (Poorter et al. 2016). Furthermore, forest cover is increasing in many countries as forest transitions take place, offering a cost-effective carbon mitigation strategy (Rudel et al. 2005, Meyfroidt et al. 2010, Aide et al. 2013). Although reforestation is an attractive option, it is also risky: carbon sequestration from reforestation can be rapidly reversed because forests are inherently vulnerable to both natural and anthropogenic disturbance (Fuss et al. 2014). Our study highlights the role that land-use and land-cover change play in influencing carbon sequestration potential of reforestation in tropical landscapes.

Peru estimates that community-based reforestation could provide up to 1.069 million tonnes CO_2 equivalent in emissions reductions (Peru 2015). We found that within our relatively small study area (0.16% of the area of Peru), estimates of carbon storage potential differed by nearly 925,000 tonnes of carbon depending on assumptions made about land-use change and disturbance. Though there are more than 40,000 hectares of second-growth forest present in the study landscape, only a small proportion of that forest is likely to persist long enough to accumulate significant amounts of carbon. Instead, rapid cycles between forest and non-forest

land-cover types are the norm. Managing tropical landscapes for climate mitigation will require a deeper understanding of the factors that drive these dynamics.

Regrowth and clearing varied considerably both temporally and spatially. Rates of regrowth and clearing strongly fluctuated from year to year (Figure 4). Large-scale processes, such as regional variation in climate and ecological conditions, land-use policies, and demographics, likely drive temporal fluctuations in rates of clearing and regrowth. Forest disturbance linked with climate conditions, specifically fire activity, could be an important driver of observed dynamics. The highest rate of clearing occurred in 2005, coincident with a severe drought and the highest levels of fire activity observed in the study area (Appendix 1: Figure 4, Fernandes *et al* 2011). Fire is commonly used for land management, and during dry years it frequently burns second-growth forest and can cause conversion to non-forest (Gutiérrez-Velez et al. 2014).

Changes in land-use policies may also underlie temporal fluctuations in regrowth and clearing. For example, the Peruvian government has promoted oil palm cultivation in Ucayali since 1991 (Potter 2015), and oil palm is often planted in second-growth forest (Gutiérrez-Vélez et al. 2011). Up to 42% of smallholder oil palm plantations in Ucayali have been abandoned due to crop disease and poor road access (Potter 2015), and abandoned oil palm plantations may convert to second-growth forest. Past rural development projects, such as those promoting pepper plantations, sugar cane, and rice may also have influenced fluctuations in second-growth forest cover and dynamics. However, land-use practices in the study area are particularly diverse and heterogeneous (Fujisaka and White 1998), so it may be difficult to distinguish the role of any particular policy or practice at the scale of the entire landscape.

Demographic changes and associated shifts in demand for forest products also influence forest dynamics in the study area. Pucallpa, the city adjacent to our study area, has rapidly grown since the 1960s (Padoch et al. 2008). This growth has driven increased demand for cheap construction products, which has encouraged smallholder farmers who practice shifting cultivation to increase the size of their fallows and manage them to promote cheap and fast-growing timber species (Padoch et al. 2008). These trees are harvested after four years of growth, which corresponds with the maximum probability of clearing occurring at about 4-5 years of age observed in our dataset.

The observed decline in probability of clearing with age is probably also influenced by changes in the way that people use and value forest with forest age. In a study nearby in the Peruvian Amazon, de Jong et al. (2001) found that 27 percent of land owners intended to conserve at least some of their second-growth forest, often with the intention of extracting wood or non-timber forest products. Conservation plans were more common for older second-growth forest than for young forest. In our study area, once second-growth forests reach about 20 years of age the probability of clearing is low, suggesting that the economic or conservation value of second-growth forests increases with age.

Second-growth dynamics also vary spatially. Variables related to pixel remoteness were important, but not always in the direction expected. Pixels far from forest edges were less likely to be cleared. Regrowth was more likely and clearing less likely far from roads. Similarly, Rudel et al. (2002) found that dynamics differed depending on distance to the road: close to roads, cyclical dynamics associated with swidden agriculture were common, while regrowth was more permanent far from roads. Surprisingly, regrowth was more likely close to settlements, possibly because shifting cultivation is more commonly practiced near settlements. However, there was

no significant effect of distance to settlement on probability of clearing. This suggests that more permanent regrowth may be more common near settlements, possibly because people conserve some second-growth forest for ecosystem services beyond carbon storage (de Jong *et al* 2001). Also surprising was our finding that the probability of second-growth forest clearing increased with forest patch size. On the national and regional scales that are typically associated with forest transitions, increases in forest cover can result from scarcity of forest resources and forest cover (Rudel et al. 2005). A similar dynamic, in which small forest patches are more protected because forest is locally scarce, might play out on a smaller scale within the study landscape, and could explain the fact that second-growth pixels in larger patches were more likely to be cleared than those in smaller patches.

The simulation results indicate that realistic scenarios of forest regrowth and clearing lead to much lower estimates of future carbon storage in the landscape. Our simulations predicted over 900,000 tonnes less carbon than the static land-use dynamics scenario, or 25% (Figure 5). This is likely a conservative estimate of the discrepancy for several reasons. First, our models slightly over-predict regrowth and under-predict clearing (Figures S2, S3). Furthermore, our models assume that when a pixel is forested, it continuously accumulates biomass and does not experience any disturbance other than clear-cutting, which results in being classified as non-forest. We do not consider variation in land-use history or in vulnerability to disturbance, important factors that affect rates and quantities of biomass accumulation. In the Amazon, the legacy of fire can reduce rates of carbon accumulation in second-growth forests (Zarin et al. 2005). Fire is commonly used for clearing and agricultural management in our study area (Schwartz *et al* 2015) and might be an important factor influencing rates and quantities of biomass accumulation. Second-growth forests in our study area also tend to be highly

fragmented and close to forest edges (Schwartz et al. in revision). Fragmented forests are more susceptible to wind damage (Schwartz et al. in revision) and forest edges tend to have lower biomass (Laurance et al. 1997, Haddad et al. 2015). In general, plot-based estimates of biomass accumulation rates such as in this study may underestimate disturbance and morality, and therefore overestimate biomass accumulation (Fisher et al. 2008, Chambers et al. 2009, Di Vittorio et al. 2014). This discrepancy might be particularly important in second-growth forests, which are more prone to disturbance. Finally, feedbacks with future climate change could affect successional trajectories and rates of biomass accumulation (Anderson-Teixeira et al. 2013, Uriarte et al. 2016a). Still, our results illustrate the importance of considering land-use/land-cover change and landscape dynamics when considering the carbon sequestration potential of second-growth forest.

Conclusions

Many countries, including Peru, have ambitious reforestation goals in their iNDCs. Peru predicts 1.069 million tonnes carbon sequestration via community reforestation (Peru 2015). Brazil plans 12 million ha reforestation (Brazil 2015), China plans 50-100 million ha reforestation, equivalent to 1 gigaton carbon (Fransen et al 2015), and India plans 5 million ha reforestation (100 million tonnes carbon, India 2015). These are non-trivial contributions to the carbon reductions these countries pledged under the Paris Climate Agreement, but the assumptions about land-use dynamics and methods to ensure second-growth forest permanence are not made clear in the iNDCs. Land-use dynamics reduced projected C storage potential by 25% in our study area; a similar discrepancy in China's estimates would lead to 250 million tonnes additional emissions. Because land-use dynamics vary across regions, the specific results of our study do not apply everywhere, but the approach and predictors we used are generalizable

across landscapes. Looking to past dynamics of second-growth forests can help identify where second-growth forest is threatened by non-permanence and where to focus reforestation programs. Monitoring the fate of new second-growth forests will also be important to ensure that the carbon promise of second-growth forests can be achieved.

Acknowledgements

This work was supported by National Science Foundation grant 0909475 and by the Center for International Forestry Research (CIFOR). We thank the Menge and DeFries lab groups for helpful comments on this manuscript.

Figures and tables

Figure 1: Location of study area in Peru, and location/extent of second-growth forest in study area in 2013.

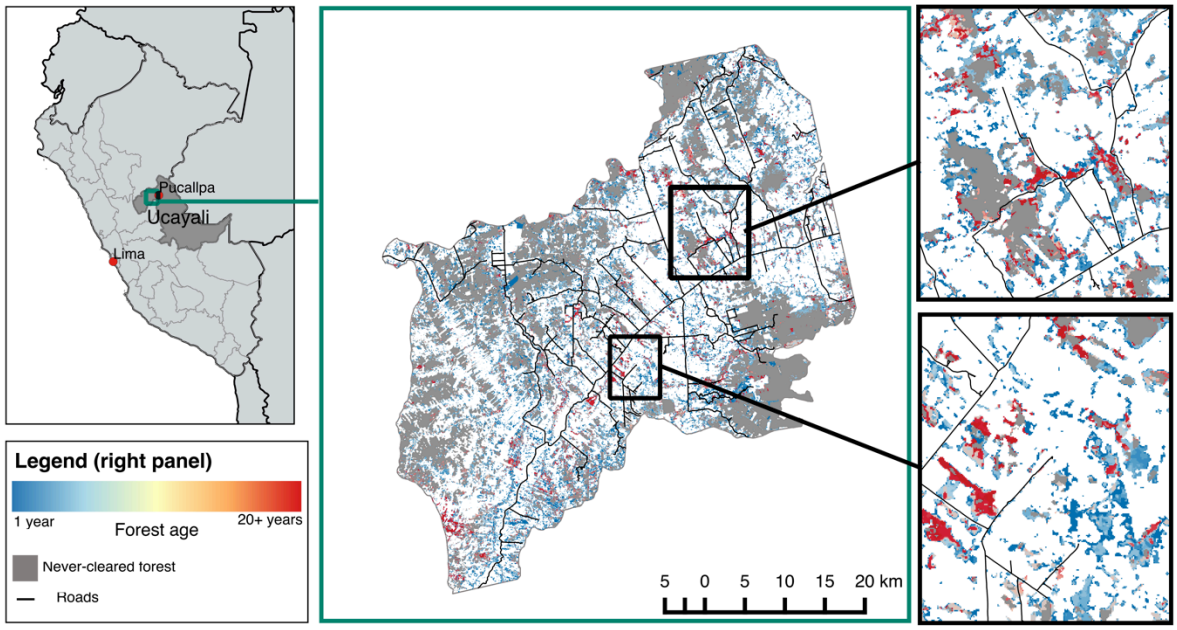

Figure 2: Forest cover in the study area from 1985-2013.

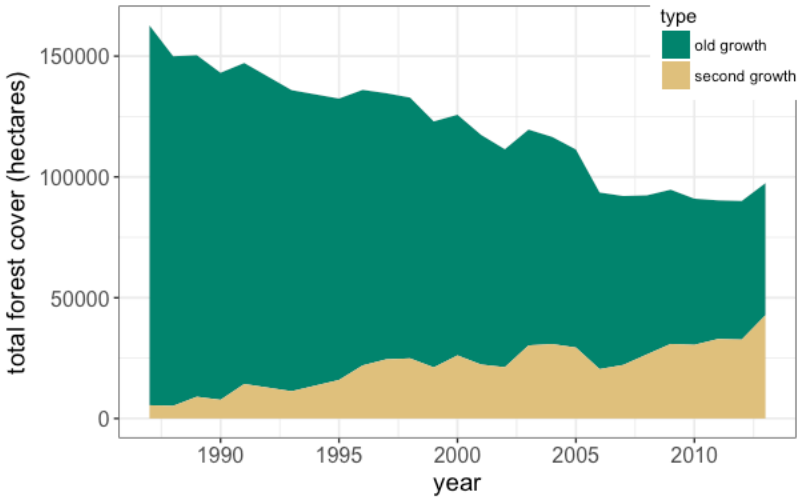

Figure 3: Predicted probability of clearing vs. age based on the coefficients from the model of second-growth forest clearing. Bars represent proportion cleared in different age classes in 2010.

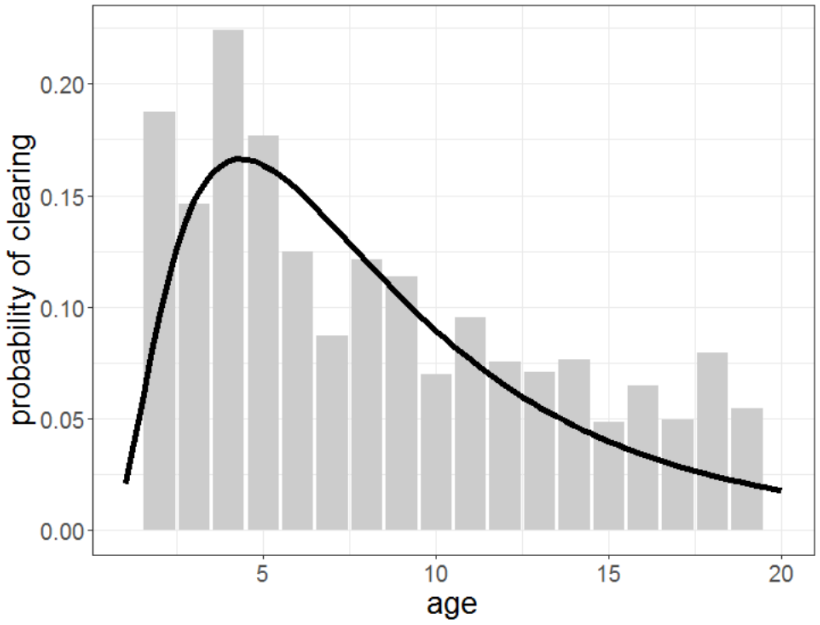

Figure 4: Observed and projected trajectories for area (top panels) and biomass (bottom panels) in different second-growth forest age classes (note: over 30 does not include old-growth forest). Left panels illustrate scenario in which all forest present in 2013 is presumed to persist and age until 2050 and right panel shows trajectories results from simulations using model parameters.

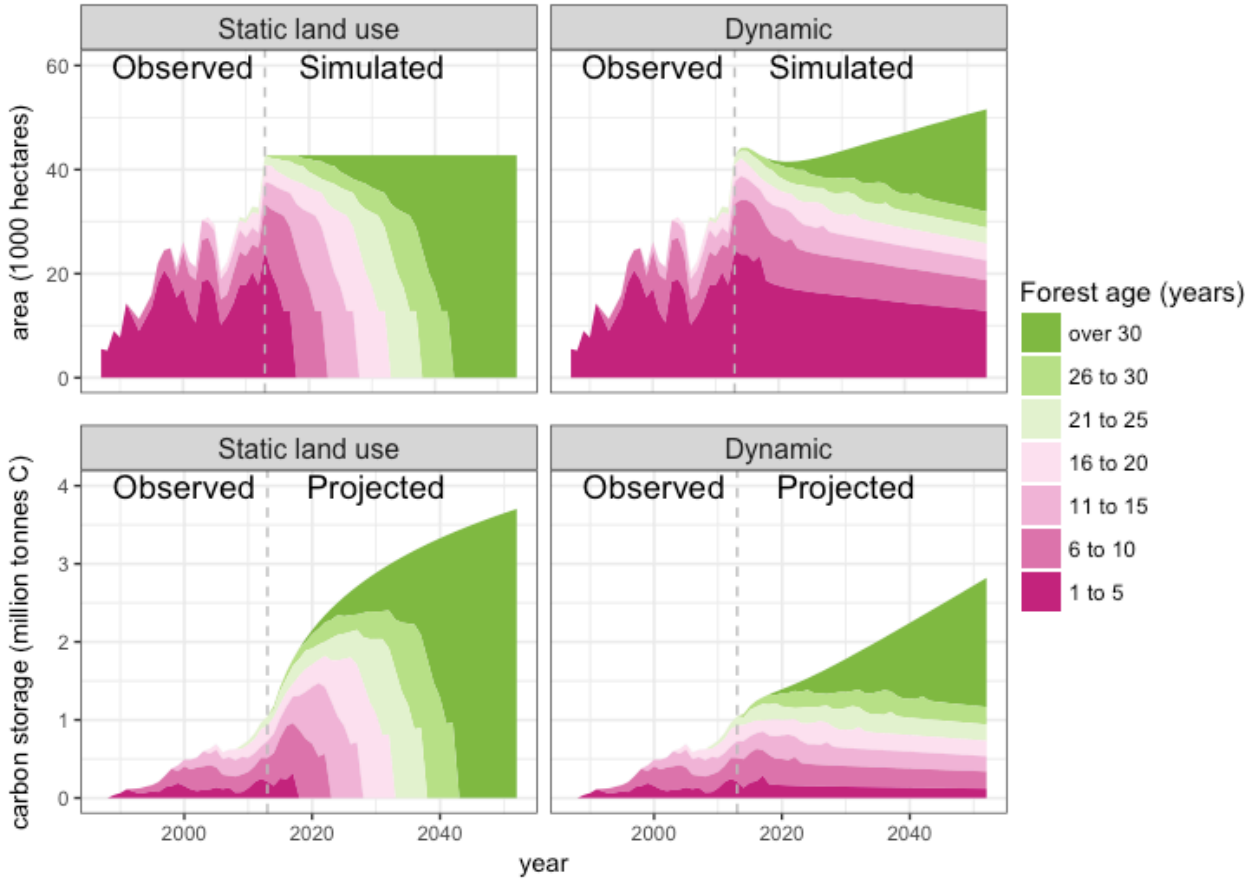

Table 1: Predictor variable descriptions, and results from the mixed effects models predicting forest regrowth in cleared areas and clearing of second-growth forest. N.a. indicates parameter not included in model, as some parameters (e.g. patch size, distance to edge) were relevant for only one of the models. Predictors were standardized to facilitate parameter comparison. Standard error values are in parentheses. Parameter significance: ***p<0.001, **p<0.05, n.s. not significant.

R^2	**Description**	**Regrowth**	**Clearing**
$R^2_{marginal}$		0.31	0.22
$R^2_{conditional}$		0.64	0.35
Predictor		**Model parameters**	
Distance to road	Pixel distance to nearest road. Constant over time because historic roads maps were not available.	0.28 (0.05)***	-0.05 (0.01)***
Distance to river	Pixel distance to nearest river or stream. Constant over time.	$0.01^{n.s.}$	-0.02 (0.01)**
Distance to settlement	Pixel distance to nearest settlement. Constant over time because historic data on the existence or location of settlements unavailable.	-0.18 (0.04)***	$-0.01^{n.s.}$
Proportion of forest in neighborhood	Amount of forest (old growth and second growth) in a 30x30 pixel window around focal pixel	1.56 (.04)***	-0.11 (0.01)***
Ever forest	Binary variable variable for whether the pixel was ever previously classified as forest before time t.	0.50 (.10)***	n.a.
Distance to edge	For forest pixels, the distance to the nearest forest edge.	n.a.	-0.60 (0.02)***
Clear length	Number of consecutive years that pixel was classified as non-forest before regrowth event.	n.a.	0.3 (0.01)**
Patch size	For forest pixels, the size of the forest patch in which the pixel was located.	n.a.	0.15 (0.01)***
Age	Number of consecutive years classified as forest, up to and including present year (log-transformed).	n.a.	2.48 (0.04)***
Age^2	Quadratic log-transformed age.	n.a.	-2.17 (0.04)***

CHAPTER 2: CLIMATE, LANDOWNER RESIDENCY AND LAND COVER PREDICT LOCAL SCALE FIRE ACTIVITY IN THE WESTERN AMAZON

Published as: Schwartz, N.B., M. Uriarte, V.H. Guiterrez-Velez, W. Baethgen, R. DeFries, K. Fernandes, and M.A. Pinedo-Vazquez (2015) Climate, landowner residency, and land cover predict local scale fire activity in the Western Amazon. *Global Environmental Change* 31, 144-153.

Abstract

The incidence of escaped agricultural fire has recently been increasing in the Western Amazon, driven by climate variability, land use change, and changes in patterns of residency and land occupation. Preventing and mitigating the negative impacts of fire in the Amazon require a comprehensive understanding not only of what the drivers of fire activity are, but also how these drivers interact and vary across scales. Here, we combine multi-scalar data on land use, climate, and landowner residency to disentangle the drivers of fire activity over ten years (2001-2010) on individual landholdings in a fire-prone region of the Peruvian Amazon. We examined the relative importance of and interactions between climate variability (drought intensity), land occupation (in particular, landowner absenteeism), and land cover variables (cover of fallow and pasture) for predicting both fire occurrence (whether or not fire was detected on a farm in a given year) and fire size. Drought intensity was the most important predictor of fire occurrence, but land-cover type and degree of landowner absenteeism increased fire probability when conditions were dry enough. On the other hand, drought intensity did not stand out relative to other significant predictors in the fire size model, where degree of landowner absenteeism in a village and percent cover of fallow in a village were also strongly associated with fire size. We also investigated to what extent these variables measured at the individual landholding versus the village scale influenced fire activity. While the predictors measured at the landholding and village scales were approximately of equal importance for modeling fire occurrence, only village scale predictors

were important in the model of fire size. These results demonstrate that the relative importance of various drivers of fire activity can vary depending on the scale at which they are measured and the scale of analysis. Additionally, we highlight how a full understanding of the drivers of fire activity should go beyond fire occurrence to consider other metrics of fire activity such as fire size, as implications for fire prevention and mitigation can be different depending on the model considered. Drought early warning systems may be most effective for preventing fire in dry years, but management to address the impacts of landowner absenteeism, such as bolstering community fire control efforts in high-risk areas, could help minimize the size of fires when they do occur. Thus, interventions should focus on minimizing fire size as well as preventing fires altogether, especially because fire is an inexpensive and effective management tool that has been in use for millennia.

Introduction

Although humans have long influenced fire regimes on earth, recent anthropogenic drivers are causing major shifts in fire activity in some parts of the world and are expected to further alter global fire regimes in the near future (Krawchuk et al. 2009, Turner 2010, Bowman et al. 2011). These changes will have consequences for biodiversity, conservation, and ecosystem processes, along with human health, economics, and wellbeing (Lohman et al. 2007, Bowman et al. 2009). Adapting to and mitigating the effects of changing fire regimes requires an understanding of the drivers of both broad scale and local heterogeneity in fire activity, and of the links, interactions, and interdependencies of the multiple drivers of these changes.

An ideal region in which to examine such questions is the western Amazon. Although humans have used fire to clear land for agriculture and improve hunting grounds in the Amazon

for thousands of years (Bush et al. 2008, Bowman et al. 2008), the incidence of escaped agricultural fires has been increasing in recent decades (Aragão et al. 2007, Aragão and Shimabukuro 2010, Asner and Alencar 2010, Alencar et al. 2011, Armenteras and Retana 2012). Because there are few natural ignitions, fires are associated with human activities (Nepstad et al. 2001, Cochrane and Laurance 2008). Fire is still a common tool used to prepare land for agriculture or grazing, but today, these fires are prone to escaping into adjacent forest or non-forested land, particularly in dry years (Nepstad et al. 1999, Alencar et al. 2004). Amazonian fires can be major sources of greenhouse gas emissions (DeFries et al. 2002, 2008), degrade forests, affect biodiversity and ecosystem services (Cochrane and Schulze 1999, Gerwing 2002), and cause property loss and respiratory disease (de Mendonça et al. 2004). Although fire is most prevalent in the southern and eastern parts of the Amazon basin, its incidence is growing in the western Amazon as well (Brown et al. 2011). For example, in the 2005 drought, 22,000 ha burned in the Ucayali region of Peru (Gobierno regional de Ucayali 2006).

Fire can only occur when conditions are favorable; it requires fuels, an ignition source, and sufficiently dry weather conditions to ignite and spread. Fire regimes, the spatial and temporal patterns of fire observed in an ecosystem, are the result of vegetation, climate, and ignition controls acting simultaneously (Moritz et al. 2005). Human activities can affect fire regimes by interfering with any of these controls. For example, land use and management activities can change fuel amounts, composition, and configuration and affect the number and spatiotemporal patterns of ignitions (Nepstad et al. 1999), while roads can act as fire breaks, but also can be a source of anthropogenic ignitions (Cardille and Ventura 2001, Archibald et al. 2009, Bowman et al. 2011, Hawbaker et al. 2013). Promoting grazing, introducing exotic plants,

engaging in fire suppression, and other activities can similarly affect patterns of fire (Bowman et al. 2011).

The degree to which various controls on fire activity limit fire depends on the study location (Bowman et al. 2009, Krawchuk et al. 2009, Parisien and Moritz 2009, Krawchuk and Moritz 2011). For example, in places with wet climates where productivity, and thus fuel availability, is high, fire is limited by fuel moisture. In very dry climates where fuels are almost always dry enough to burn, fuel quantity can be limiting instead (Krawchuk and Moritz 2011). Where natural ignitions are very rare, the availability of anthropogenic ignitions changes the degree to which ignitions limit fire (Nepstad et al. 2001, Cochrane and Laurance 2008).

The spatial scale of analysis also affects which drivers best explain patterns of fire activity (Parisien and Moritz 2009, Parks et al. 2012). Climate exerts control across broad areas, while topography and vegetation are important in driving finer scale heterogeneity. Within broad fire-prone regions there can be considerable spatial and temporal heterogeneity in frequency, intensity, and severity of fires, and local patterns of fire activity are the result of climate, fuel, and ignition controls acting simultaneously and to different degrees, and reflect the ways humans influence each of these controls. Thorough understanding of a fire regime requires examining patterns of fire at a number of different spatial scales: focusing on broad scales might blur out the drivers of local scale heterogeneity, while focusing only on very local scales may miss informative and important regional patterns in fire activity. For example, a focus on climate may overlook the role of topography in driving local variation in fire regimes, while a focus on the way topography influences patterns of fire might not detect the role of interannual climate variability in driving regional synchrony and year-to-year variability in fire activity.

Similarly, the most important biophysical factors predicting fire occurrence (defined as whether a particular place burns or not) may be different from those predicting other metrics of fire activity such as fire intensity or fire size. In ecosystems where natural ignitions are rare, availability of ignitions could be the most important driver of fire occurrence, but once a fire starts, fuel quantity could be the strongest predictor of fire intensity and the spatial configuration or connectivity of fuels could be most important for fire size. In ecosystems where ignitions are frequent but conditions are rarely dry enough for fires to start, fuel moisture might be the most important factor limiting fire occurrence, intensity, and size.

Here, we combine multi-scalar data on land use, climate, and landowner residence from remote sensing, meteorological stations and socio-economic surveys to further disentangle the drivers of two different metrics of fire activity – fire occurrence and fire size – over ten years on individual landholdings in a fire prone region of the Peruvian Amazon. We focused on the following questions:

1) *What is the relative importance of climate, landowner place of residence, and land cover for predicting fire activity in the Ucayali region of the Peruvian Amazon and how do these drivers interact?*

   We expected that climate would exert the strongest control on fire, but in dry years, variables related to human activities would play an important role in determining finer scale patterns of fire activity.

2) *To what extent do characteristics of a particular landholding, as opposed to characteristics of the village or region around it, predict fire activity on that landholding?*

Because most landholdings are relatively small and thus potentially highly susceptible to fire spread from adjacent properties, we expected that characteristics of the village around a landholding would be a stronger predictor of fire activity than conditions on a landholding itself.

3) *Are the drivers of fire occurrence different from those of fire size?*

We expected that the predictors of fire occurrence would be different from those of fire size: fire occurrence would be more closely associated with spatial and temporal patterns of ignition sources (related to patterns of human activity) while fire size would be associated with variables that affect fuel quantity and moisture, in particular land cover and drought intensity, and that reflect social control, in particular the number of landowners present in the village.

Materials and methods

Study area

This study focused on an area within the Ucayali region of Peru, near the urban areas of Pucallpa and Campo Verde (Figure 1). Elevation ranges from 150 to 250 m, and annual mean precipitation averages 1500 to 2500 mm/year with an annual dry season from July-September (Gutiérrez-Vélez and DeFries 2013). The study region has been connected to Lima and other urban centers in the coast and mountains of Peru by a highway and networks of roads for more than six decades. It has attracted many migrants from elsewhere in Peru in recent years (Uriarte et al., 2012) and has undergone extensive land-use change and deforestation including conversion of forest to oil palm (Oliveira et al. 2007, Gutiérrez-Vélez and DeFries 2013). Since the early 1980s, there has been significant rural-to-urban migration, with 75% of the population

living in cities as of 2007, up from 56% in 1972 (Instituto Nacional de Estadistica e Informatica 2009). Many households are multi-sited, with property and activities in rural and urban areas (Padoch et al. 2008).

Several studies have examined the drivers of recent fire activity in the western Amazon, and have found it is correlated with repeated droughts over the 2000s, which in turn are associated with positive anomalies in the North Atlantic sea surface temperature (Fernandes et al. 2011, Chen et al. 2011). Recent fires in the Peruvian Amazon have been concentrated in provinces where rural-to-urban migration is high, and, within the study area, in villages with high levels of landowner absenteeism (Uriarte et al. 2012b). This may be due to decreased capacity to control fires in areas where landowners are rarely present on their land, and/or to an increase in flammable fallow land. Gutiérrez-Vélez et al. (2014) found that land cover composition is significantly correlated with fire probability in individual burned pixels but that the magnitude and sign of the correlation depends strongly on drought intensity, successional stage of regrowing vegetation and oil palm age. Here, we build on these findings to further disentangle the drivers of fire occurrence over ten years on the scale of individual landholdings in the Peruvian Amazon. Previous analyses of drivers of fire activity in the region have been on disparate scales: province, village, burned 250 m pixel. Conducting analyses on the scale of individual landholdings allows us to simultaneously compare the relative importance of the climate, residency, and land cover drivers previously identified as important, at a scale relevant for local management and prediction of finer scale patterns of fire occurrence.

Data were compiled from a number of sources including weather stations, satellites, and farmer surveys (Table 1). We focused our analyses on 732 farms within 37 villages in the region (Figure 1).

Climate data

Drought is a major climatic driver of fire in the Amazon (Nepstad et al. 2004, Alencar et al. 2006, Fernandes et al. 2011). To quantify drought intensity, we used the Standardized Precipitation Index (SPI), calculated as the number of standard deviations that cumulative precipitation over a defined period deviates from the long-term average: here, 1970-2010. SPI values < -1 indicate drought, while SPI > 1 wet years. We used a map of SPI at 0.25° spatial resolution developed by Fernandes et al (2011) to assess the relative and interactive influence of drought intensity on fire occurrence and size. The map was derived by interpolating meteorological stations' precipitation data from the Peruvian Meteorological Service (Servicio Nacional de Meteorologia e Hidrologia - SENAMHI) and the Brazilian Agência Nacional de Águas (http://hidroweb.ana.gov.br/) using the Cressman method (Cressman 1959). Previous analyses have shown that July-August-September (JAS) SPI is the most accurate predictor of fire activity for the Peruvian Amazon (Fernandes et al. 2011), so we used JAS SPI as the climate variable in our analyses to predict fire activity. Because of the coarse spatial resolution of the SPI data, there were only 6 different values of SPI across the study area each year. Thus, variation in SPI mainly represents inter-annual variation in precipitation, as opposed to spatial variation.

Fire mapping

Annual burn scar maps for every year between 2001 and 2010 were obtained from a previous study (Gutiérrez-Vélez et al. 2014). Burn scars were mapped using the daily surface reflectance product from the Moderate Resolution Imaging Spectrometer (MODIS) satellite

(MOD09GQ) at 250 x 250 m resolution, based on temporal changes in NDVI and in bands 1 (620-670 nm) and 2 (841-876 nm). The presence of smoke, haze, and clouds during burning can prevent the detection of fires at the time of burning. The method used for burn scar mapping minimizes these effects in a number of ways. First, the MODIS surface reflectance product incorporates an algorithm that reduces the effects of smoke and other aerosols (Vermote et al. 2002). Second, the method implements a filtering algorithm to remove unreliable pixel observations. Third, the method takes into consideration minimum NDVI values measured throughout the entire dry season, July through November. Detection of fires that occur towards the end of this period may be reduced somewhat, but relatively few fires occur during this time period (Gutiérrez-Vélez et al. 2014).

Due to the minimum pixel size required for detection, sub pixel-sized fires, such as controlled agricultural fires, are not likely to be detected, and the method is most reliable for burn scars larger than 10 ha (Gutiérrez-Vélez et al. 2014). Therefore, though it is not possible to discriminate controlled vs. escaped fires using this method, the majority of fires included in our models likely represent large escaped fires, as controlled agricultural fires are generally smaller than 2 ha (Gutierrez-Velez et al. 2014). Therefore, this method allows us to detect and model the drivers of large fires; the drivers of small fires may be different.

In addition, there may be some error in the size of mapped burn scars in both directions, due to the lack of information on date of burning. The same fire event may correspond to multiple separate mapped burn scars if they are connected through areas smaller than the minimum detectable burn scars, leading to some underestimation of fire size. On the other hand, single burn scars could correspond to areas burned in different fire events during the same year and close enough to be mapped as an individual burn scar, leading to some overestimation.

Land cover mapping

Land cover maps were obtained from a previous study (Gutiérrez-Vélez and DeFries 2013). They were classified at the 30x30 m resolution using a combination of Landsat TM and ETM optical data and ALOS-PALSAR radar data. We excluded 2007 from analyses because there was not a suitable Landsat TM image of the region available. Each pixel was classified as oil palm, deforested, fallow, forest, pasture, secondary vegetation, bare, or water with an overall accuracy of 93%.

Socio-economic data

During 2010 and 2011, we conducted semi-structured interviews at 732 farms in 37 villages across the study area (Figure 1). A farm is defined here as one spatially continuous landholding with one owner. Villages are defined as communities with more than 40 school-aged children (the minimum number needed for a private school) and are delineated by the local government. We selected these 37 villages via a preliminary survey of fire history and landholding types (smallholders versus large holdings). Households were selected from within these communities from the population who potentially used fire as a management tool or were potentially affected by escaped fires using snowball sampling, in which individual respondents helped recruit future respondents from their acquaintances (Goodman 1961). Only heads of households or individuals actively involved with farm management were interviewed. Each individual was asked about the landowner's place of residence and fire use and management practices. If the current landowner acquired the farm more recently than ten years ago, they were included in analyses for all years after they acquired it. Otherwise, they were included for all ten

years of the study. This resulted in 5,387 farm-year observations. We assumed that their answers in 2010-2011 reflect conditions since the acquisition.

Farm boundaries were mapped using GPS points. Mean farm size was 32.5 ha. If any burn scar overlapped with a farm in a given year, that farm was classified as "burned" for that year, for the model of fire occurrence. Otherwise landholdings were marked as unburned. For farms that burned, we calculated the total area of the burn scars that overlapped with the farm for use in the model of fire size. For each farm, we tallied the proportion in each land cover class for each year between 2001 and 2010. In addition, we calculated the proportion of land cover class in each village and the proportion of landowners residing on their property to use as community-scale predictors in our models of fire activity.

Statistical analysis

We used a hierarchical Bayesian modeling framework to predict annual fire activity from 2001-2010 at the scale of individual farms. We expected that the predictors of fire occurrence would be different from those of fire size. Therefore, we built two models to predict fire activity: first, to predict the probability that fire occurs on a farm in a given year, and second, for the subset of farms that did burn in a particular year (n=1095), the total area of burn scars overlapping with each farm. Considering fire size in this way allows us to understand the characteristics of farms that are associated with large escaped fires.

Predictors varied at the regional (i.e. whole study area), village, and individual farm scale and comprised drought intensity (SPI), farm-level land cover (proportion of pasture and fallow), place of residence of landowner (on the farm or elsewhere), village land cover (proportion pasture and fallow), and percent of landowners residing within the village (Table 1). We also

included interactions between SPI and each other predictor. Because we were interested in how the relative importance of predictors varied across models, and not in finding the best model to predict each metric of fire occurrence, we fit a full model for both fire probability and fire size. Farm size (hectares) was included as a covariate to control for the fact that fire is more probable in large farms because they cover more area. We included only the fallow and pasture land cover classes as predictors to avoid collinearity between land cover predictors and because both have been identified as being associated with fire in previous analyses (Gutiérrez-Vélez et al. 2014). Collinearity was less than 0.36 for all pairs of predictors (Appendix 2: Table 1).

Fire occurrence (y_{occ}) was modeled as a Bernoulli process as follows:

$$y_{occ,ij} \sim Bernoulli(p_{ij}) \quad \text{(Eq. 1)}$$

where p_{ij} is the probability of fire on farm *I* in year *j*. We modeled the logit of p_{ij} as a linear combination of the predictors (x), regression coefficients β, and a farm-specific intercept α_i:

$$\ln\left(\frac{p_{ij}}{1-p_{ij}}\right) = \alpha_{ij} + \beta_1 x_{1,ij} + \cdots + \beta_n x_{n,ij} \quad \text{(Eq. 2)}$$

The size of fires overlapping with a farm was log transformed, as a few very large fires resulted in a long-tailed distribution. We modeled fire size (y_{fs}) using a gamma density function as follows:

$$y_{fs} \sim gamma(\frac{\mu_{ij}^2}{\sigma}, \frac{\mu_{ij}}{\sigma}) \quad \text{(Eq. 3)}$$

$$\mu_{ij} = \alpha_{ij} + \beta_1 x_{1,ij} + \cdots + \beta_n x_{n,ij} \quad \text{(Eq. 4)}$$

where μ_{ij} is the predicted fire size associated with farm *I* in year *j* and σ is the estimated variance. In all models for both fire occurrence and fire size, we modeled random effects (α_i) for farm *I* in community *k* drawn from a normal distribution with parameters μ_k and τ_k determined by the community in which they were located. These parameters were in turn derived from a normal

distribution whose mean (μ_{com}) and precision (τ_{com}) were estimated as hyperparameters. Including random effects for village helps account for the fact that a farm may be more likely to burn simply because it is located in a more fire-prone village.

Models were specified using uninformative priors. Posterior distributions for parameters were estimated using Markov Chain Monte Carlo (MCMC) sampling. Models were run for 3 chains and 10,000 iterations burn-in, and then for 10,000 total iterations. Convergence was assessed visually by examining chains and the shapes of the posterior distributions of parameters and using the Gelman and Rubin Diagnostics (Brooks and Gelman 1998). If the 95% credible interval of the posterior distribution of a parameter did not overlap with 0, that parameter was determined to be statistically significant. The estimated parameters were used to calculate predicted values of fire probability and fire size for each landholding; the predictions were plotted against observations to assess model predictive ability (Appendix 2: Figures 1 and 2). All statistical analyses were conducted in R (R Development Core Team 2014) using the rjags interface (Plummer 2003).

Results

Fire occurrence model

The model of fire occurrence was able to reproduce the patterns observed in the data (Appendix 2: Figure 1). Main effects for all predictors were significantly different from zero (Figure 2). Consistent with expectations, greater drought intensity (lower SPI values) was associated with greater fire occurrence (Figure 2), and the magnitude of the effect of drought intensity on fire probability stood out as far larger than the effects of any other predictors; it was more than double the magnitude of the next largest effect (farm size). The probability of fire

increased with the percent of the farm in fallow and to a slightly lesser extent, in pasture. The presence of a landowner on a farm decreased the probability of fire, and fire was less likely on farms located in villages with a higher percentage of landowners residing in that village. The predicted probability of fire was higher on farms located in villages with a larger percent in fallow, but was reduced in villages with a large proportion of pasture.

There were significant interactions between the index of drought intensity and both percent fallow on the farm and village-scale landowner absenteeism. The magnitude of the effect of percent fallow on a farm on the probability of fire was higher in drought years (Figure 3a). In wet years, probability of fire increases only slightly as the percent of a farm in fallow increases. In dry years, the overall probability of fire is much higher, but also increases more quickly as the percent fallow on a farm increases. There was a positive interaction between drought intensity and the percent of landowners in a village who live locally. In dry years, farms located in villages with high levels of landowner absenteeism were more likely to burn than those in villages where more landowners are present (Figure 3b).

Fire size model

Results from the model to predict fire size (the total area of fires overlapping with an individual farm in a given year) were qualitatively different from the results from the fire occurrence model (Figure 4). While the model of fire size accurately reproduced the trend in the observed data, the model under-predicted the size of large fires (Appendix 2: Figure 2). SPI was negatively correlated with fire size, meaning that fires are larger in drier years. However, unlike the model of fire occurrence, here there were other predictors that had effects of almost the same magnitude as that SPI. Several of the village level predictors had effects comparable in

magnitude to that of SPI, with larger fires associated with farms within villages with a high percent cover of fallow and in villages with fewer landowners residing on site. The only farm-level predictor that was significant was percent of farm in fallow, with farms with a large percent in fallow being associated with larger fires.

As in the previous model, there were several significant interactions between SPI and the other predictors, but the nature of these interactions was different. The negative interaction term between percent of a village in fallow and SPI means that farms located in villages with a high percent of fallow land cover tend to be associated with large fires regardless of SPI, whereas when there is small area of fallow in a village, climate is more important in determining fire size (Figure 5). In other words, the relative effect of SPI is greater in villages with less percent cover of fallow.

Discussion

We combined data from meteorological stations, remote sensing, and landowner surveys to examine the relative importance of and interactions between multiple drivers of fire activity in the Peruvian Amazon. As expected, drought intensity is an important predictor of fire occurrence and fire size, although its relative importance compared to other significant predictors is far greater in the model of fire occurrence than in that of fire size. We also found that the relative importance of predictors varies depending on the scale at which they are measured: in the model of fire occurrence, the predictors at both household and village scales are important, but in the model of fire size, the importance of village scale predictors outweighs that of the household scale predictors. These differences across scales and across metrics of fire activity have

implications for understanding future fire regimes and for fire prevention and mitigation activities.

Relative importance of climate, patterns of landowner residency, and land cover for predicting fire activity

Other studies have shown that because much of the Amazon is so wet, climate exerts a strong control on fire (Alencar et al. 2004, 2011, Nepstad et al. 2004, Fernandes et al. 2011). Because almost all ignitions are caused by human activities, at some level fire occurrence is limited by whether or not there are people present and whether or not they are using fire. However, in dry years, fires are more likely to escape, spread further and burn a larger area, which increases the likelihood that any given farm is burned by a fire large enough to be detected by satellites. While variables associated with human activities were important in our models, we found that climate was the most important driver of fire occurrence. In the model of fire occurrence, the effect of drought intensity overwhelms the effects of other predictors, with an effect about twice the magnitude of any others. Fire is more common in the drier and more seasonal eastern Amazon than it is in the more humid western Amazon (DeFries et al. 2008, van der Werf et al. 2009), so the constraint of climate on fire occurrence may be particularly strong in Ucayali and other regions of western Amazonia. This is consistent with the varying constraints hypothesis, which implies that in wet regions fire should be constrained by fuel moisture conditions (Krawchuk and Moritz 2011). If it is too wet, agricultural fires will rarely escape control, regardless of land cover type, landowner place of residence, or management practices. Climate also exerts a strong influence on fire size, with big fires more likely in dry years.

However, within dry years, there is still considerable heterogeneity in spatial patterns of fire, driven by factors other than climate. Our results were consistent with other studies that have examined the role of human activities in driving patterns of fire in the Amazon. While conventional wisdom has said that more people and more land preparation mean more fires in the Amazon, recent findings, including those presented here, indicate that this relationship is more complex than previously thought. In the Brazilian Amazon, fire occurrence has increased in the majority of the areas where deforestation rates have declined (Aragão and Shimabukuro 2010). Morton et al. (2013) found high levels of understory fire activity in Mato Grosso, even as deforestation rates were some of the lowest in recent decades. Uriarte et al. (2012) found that fire activity in the Peruvian Amazon was more extensive in provinces with high levels of rural-to-urban migration and in villages with high levels of landowner absenteeism. Our results extend this finding to a finer spatial scale, demonstrating that fine scale analysis can help explain the mechanism behind the observed broad scale trends.

Land cover type was significantly related to fire activity in both the fire occurrence and size models, although the role of land cover was weaker than that of climate in the model predicting fire occurrence. Although not all measures of land cover were significant in both models, fallow and pasture were both correlated with fire activity. There are multiple plausible mechanisms for the relationship between land cover and fire activity, which could be biophysical or related to human activities and decisions. The biophysical explanations relate to differences in flammability: fallow land could be more flammable because there are more fuels that can dry out relatively quickly compared to forest (Gutiérrez-Vélez et al. 2014). Alternatively, the reason fallow land is more prone to fire could be because people frequently burn fallow land for various management purposes. Fire is a common tool for land preparation and agricultural management

in the Amazon (Bowman et al. 2008, Carmenta et al. 2013), and so the association between fallow land and fire could represent people's uses of fire for land preparation or pasture management. However, because of the minimum fire size necessary for satellite detection, the fires mapped for this research likely represent escaped fires, suggesting that factors that affect the likelihood of fire escaping, i.e. biophysical factors not directly related to ignitions, are responsible for this association (Gutiérrez-Vélez et al. 2014).

There were significant interaction terms in both models. These interactions illustrate that the nature of the relationships between local-scale variables and fire can change depending on the prevailing climate conditions within a year. For example, percent of farm in fallow has little effect on the probability of fire in wet years, but once it starts getting drier, the amount of the farm in fallow can greatly increase the probability of fire (Figure 3a). Gutiérrez-Vélez et al. (2014) found that the relationship between land cover types and fire on the pixel scale covaried with climate. They found a particularly strong interaction between secondary forest and fire activity: the direction of the relationship between secondary forest and fire occurrence switches from a negative correlation during wet years to a positive correlation during dry years. In the Brazilian Amazon, human activity is key for determining seasonal and annual trends in fire occurrence, but the effect of drought can overwhelm that of anthropogenic activities, leading to high-fire years when land conversion is low (Aragão et al. 2008). Our results are consistent with these findings, which demonstrate a strong interaction between the effects of human activities and the effects of climate.

Importance of conditions within vs. around a farm

Fire can occur on a farm in two ways: the ignition can occur in the landholding, or it can spread onto a property from a fire ignited in the area surrounding it. For that reason, we included land cover and landowner residency predictors calculated at both the individual landholding and the village scale, to compare to what degree landscape context (i.e. characteristics of the village in which farms are located) versus characteristics of a property itself are important.

The importance of variables at the village and individual landholding scale varied depending on which metric of fire occurrence was being considered. In the fire occurrence model, the parameters for variables measured at the individual farm and village scale were approximately of the same magnitude. On the other hand, in the model for predicting fire size, the effects of variables at the village scale (percent of landowners living in village and percent of village in fallow) were much larger than those at the individual farm scale, of which only one predictor, percent of property in fallow, is significant. This suggests that efforts to control fire size should target communities, perhaps working to build fire control and firefighting capacity or working to manage fallows in a way that would reduce flammability, in addition to targeting management practices of individual households. This also corroborates the hypothesis that large fires are related to a limited capacity to control fire (Uriarte et al. 2012), as fire control can be a community effort (Brondizio and Moran 2008, Bowman et al. 2008).

Drivers of fire occurrence vs. fire size

As expected, there were differences between the models predicting fire occurrence and fire size (total area of fires overlapping a farm), mostly in terms of differences in the relative magnitudes of the coefficients of the various predictors. Fewer of the predictors found to be

significant in the model of fire occurrence were significant in the model of fire size. This could relate to the fact that the model of fire size in general did a poorer job predicting the observed data (Appendix 2: Figure 2) and suggests that there may be factors important for predicting the size of fires overlapping with a farm that we did not measure or include in our model, such as landscape configuration or fuel connectivity on or around a farm. Gutiérrez-Vélez et al. (2014) found that the degree of aggregation and patchiness of some land cover types affected fire spread, i.e. the number of pixels burned around a focal pixel. Including such a measure of the degree of connectivity or fragmentation of particular fuel types might have improved our predictions of fire size. A lower predictability of fire size might also be influenced by limitations in fire detection given the relatively coarse resolution of the satellite source (250 m pixel size) used for burn scar mapping, the absence of data on the time of burning, and possible errors in estimation of fire size, as discussed in section 2.3.

One key difference between the models of fire occurrence versus fire size was the difference in the strength of the effect of climate relative to the strength of the other significant predictors. Climate is an important predictor of fire occurrence and size, but its influence relative to other predictors is smaller in the model of fire size. Fires are bigger in dry years, but several other predictors also have quite large contributions; in particular, larger fires are associated with landholdings located in villages with high levels of landowner absenteeism and in villages with a high percent cover in fallow.

The significant interaction terms in the model predicting fire size also illustrate that the dynamics in models of fire size are different than in those for fire occurrence (Figure 5). Once a fire is ignited, it is likely to be large in villages with a high percent cover in fallow regardless of a year's climate conditions. On the other hand, if there is small area of fallow, predicted fire size

is much smaller overall, but is significantly larger in dry years than in wet years. In this case, local conditions are more important in determining fire size, with big fires happening when village conditions are favorable with comparatively less influence of climate conditions. This is in contrast to the dynamics observed in models predicting fire probability, where only in dry years do conditions such as landowner place of residence and land cover type elevate the probability of fire.

These results suggest that studies should consider multiple aspects of fire regimes to gain full understanding of the relative importance of and interactions between different drivers of fire activity. In our study area, conclusions about which fire prevention and mitigation activities are most likely to be effective could vary depending on the model being considered. The model of fire occurrence suggests that management to lower the probability of fire should mainly focus on responding to anticipated climate conditions. Fire prevention interventions to this end include early warning systems meant to inform farmers of extreme weather conditions that create high risk of escaped fires (Goldammer 1998), coupled with education about how drought affects the risk of escaped fire and under what conditions it is safer to burn. However, other variables, which could imply different management responses, become equally relevant when fire size is considered. For example, targeting fire-fighting efforts and building community fire-control capacity in areas with high levels of absenteeism, or building fire breaks in areas with extensive fallow land may also be effective at minimizing the occurrence, size and effects of escaped fires. Area burned, not just fire occurrence, is important for emissions and property loss. Management interventions could usefully focus on minimizing fire size and not just preventing people from using fire, especially because fire is an inexpensive and effective management tool that has been in use for millennia (Bowman et al. 2008, Carmenta et al. 2013).

Future research

By simultaneously using data on climate variability, landowner residence and land cover type to model two different metrics of fire activity, this study provides a deepened understanding of the relative importance and interactions between the multi-scalar drivers of fire activity. Yet we still require a further understanding of the sources, numbers, and spatio-temporal patterns of ignitions. Fires cannot occur without ignitions, and all ignitions in this region come from human activities. Changing the spatial and temporal patterns of ignitions could have a major effect on patterns of fire activity. While some of the predictors considered in this analysis may reflect differences in ignitions – for example, ignitions might be more common in pasture as it is frequently burned for management – a more direct examination of the sources and patterns of ignitions would help our understanding of the degree to which ignitions are limiting in the region.

Additionally, fire activity may have positive feedbacks: a place that burns once may be more likely to burn again in the future because of fire-induced changes to fuel structure. This phenomenon has been observed elsewhere in the Amazon (Nepstad et al. 2001); however, it has not been investigated in this region. Alternatively, in places that burn frequently, there may be a negative fire feedback as fine fuels may become slower to accumulate (Balch et al. 2008). Analyses of repeat burns could provide insights into whether or not this phenomenon occurs in the wetter Peruvian Amazon as well, which would have implications for our understanding of fire regimes in the region and for fire management.

Conclusions

Climate variability and change, land use change, and other shifts in human activity and demographics are expected to alter future fire regimes around the world (Krawchuk et al. 2009, Bowman et al. 2011), and are projected to lead to increases in future fire activity in the Amazon (Silvestrini et al. 2011, Chen et al. 2011). Better understanding of the drivers of fine scale patterns of fire activity provides insight into appropriate actions to minimize the risk of escaped fires and decrease the risk of property loss to fire in these landscapes (Sorrensen 2009, Carmenta et al. 2013). By focusing on the individual farm scale, we were able to combine climate and land cover data, along with data on patterns of landowner occupation to better elucidate how these variables affect patterns of fire on a relatively fine scale. This study adds to the growing literature demonstrating that fire in the wet tropics is not simply a byproduct of deforestation and may continue to spread even as deforestation declines (Aragão and Shimabukuro 2010, Uriarte et al. 2012b, Morton et al. 2013). Additionally, the differences we found between the models of fire occurrence and fire size demonstrate that the metric of fire activity being considered can influence results, and highlight the importance of considering multiple aspects of fire regimes. A full understanding of drivers of fire, their relative importance, and their interactions can help to identify the most effective interventions to prevent and mitigate escaped fires in the tropics.

Acknowledgements

This work was supported by National Science Foundation grant 0909475 and by the Center for International Forestry Research (CIFOR). We thank Medardo Miranda Ruiz, Isaac Perez, and Walter Rios Perez for assistance with field data collection. We also thank Meha Jain, Jesse Lasky, Bob Muscarella, Benton Taylor, and two anonymous reviewers for their helpful feedback.

Figures and tables

Figure 1: Map of study area. Inset shows location in Peru (black rectangle).

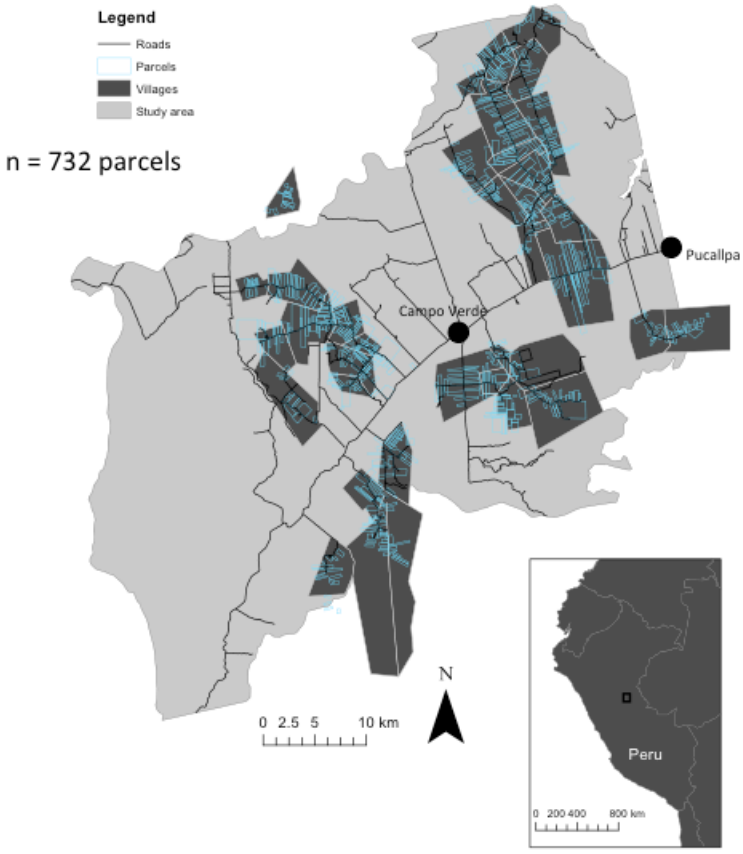

Figure 2: Standardized regression coefficients for model predicting fire occurrence.

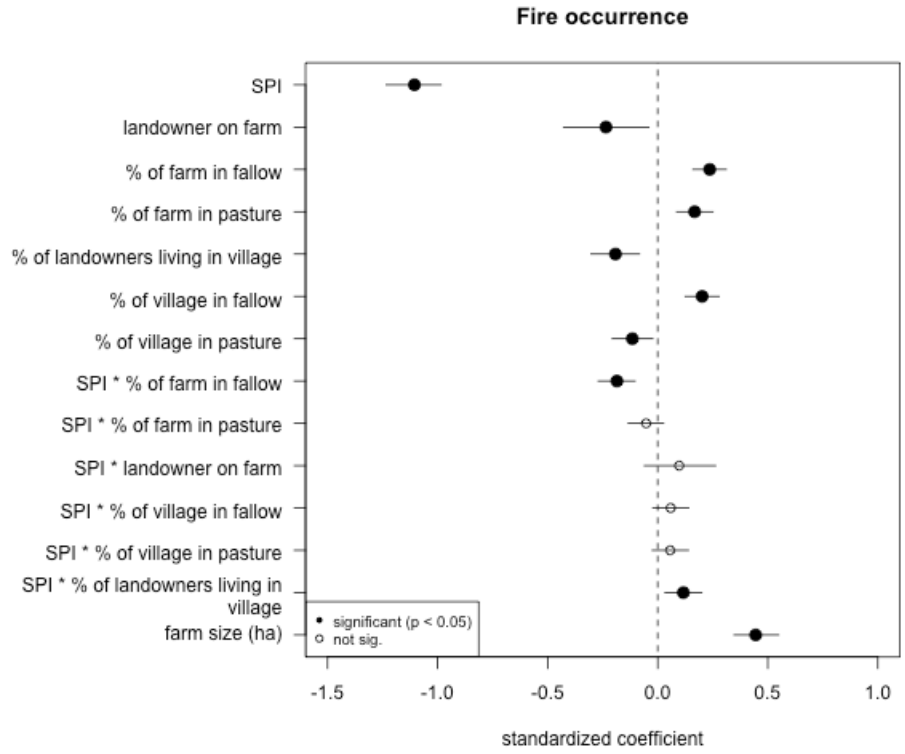

Figure 3: Predictions to illustration interaction terms. A) Predictions for probability of fire as a function of percent farm in fallow. When SPI is high (wet year), fire probability is low regardless. In wet years, fire probability is higher overall, but increases with percent fallow on a parcel. B) Predicted probability of fire as a function of SPI. Blue line depicts predictions for village with a high percent of landowners residing in the village (90th percentile) while orange line is for villages with a low percentage of farmers residing in village (10th percentile).

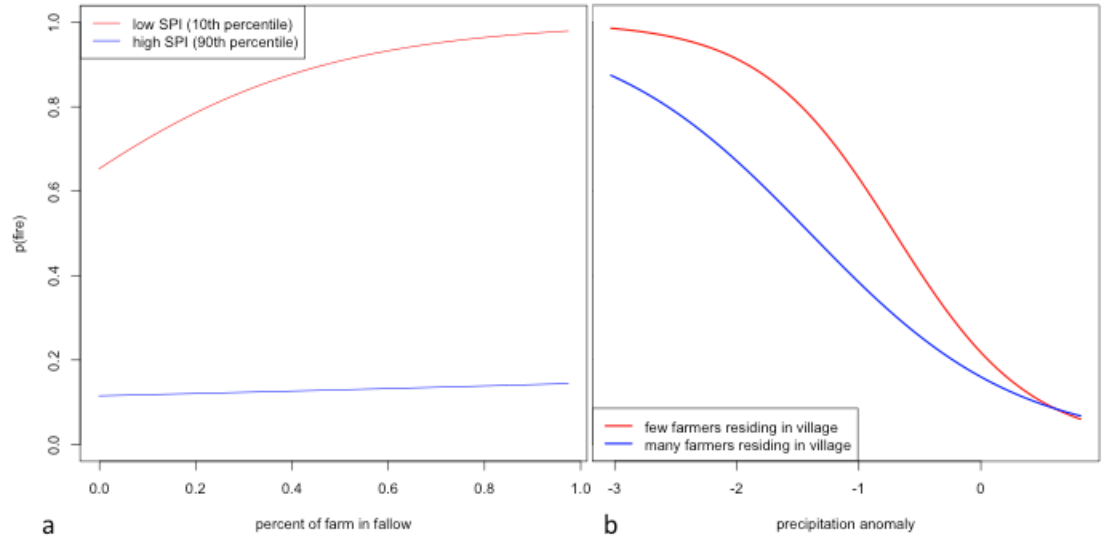

Figure 4: Standardized regression coefficients from the model to predict fire size

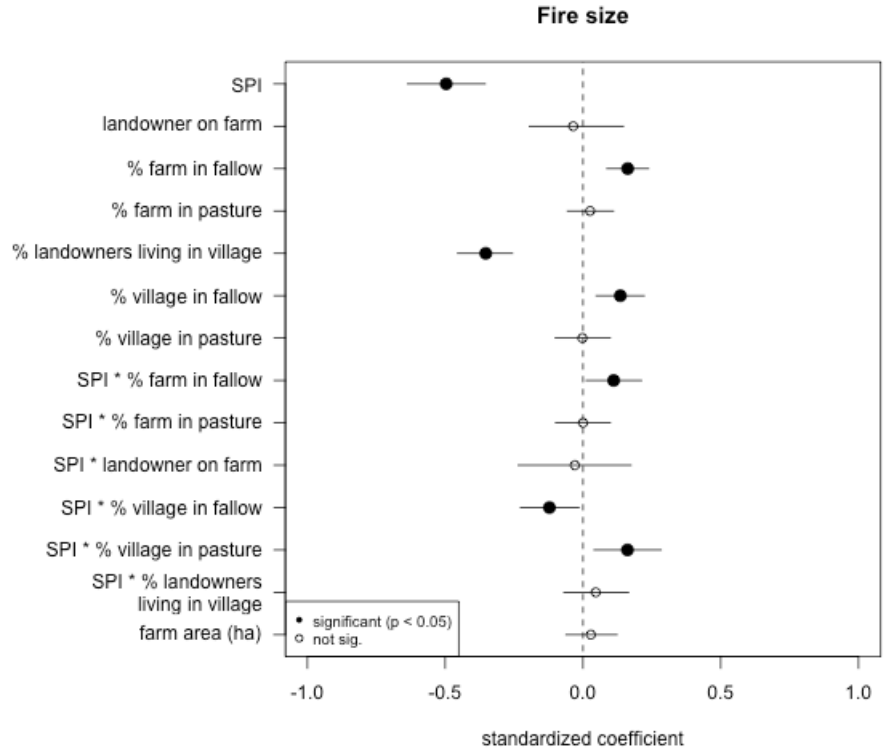

Figure 5: Predicted fire size as a function of the proportion of a village in fallow. Red line shows predictions for a dry year (10th percentile SPI) and blue line shows predictions for a wet year (90th percentile SPI).

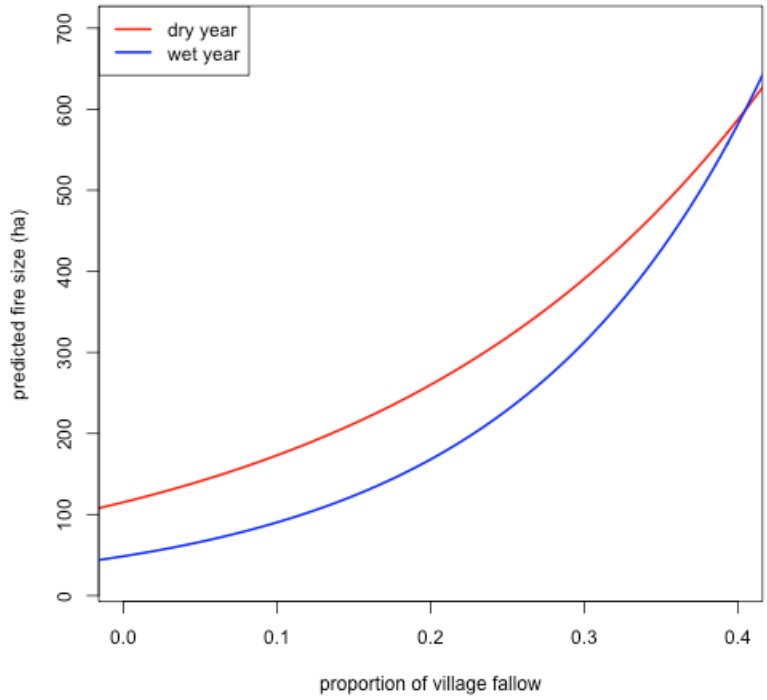

Table 1: Variables used and their sources.

Variable	**Source**	**Citation**
Response variables		
Fire occurrence	MODIS	Gutiérrez-Vélez et al. *2014*
Burn scar size	MODIS	Gutiérrez-Vélez et al. *2014*
Predictors – household scale		
Land cover (focal landholding)	Landsat	Gutiérrez-Vélez and DeFries 2013
Does landowner live on farm?	Landowner survey	Uriarte et al. 2012
Farm size	Landowner survey	Uriarte et al. 2012
Predictors – village scale		
Land cover (village)	Landsat	Gutiérrez-Vélez and DeFries 2013
% landowners residing in village	Landowner survey	Uriarte et al. 2012
Predictors – regional scale		
Climate (SPI)	Peruvian Meteorological Service and Brazilian Agência Nacional de Águas	Fernandes et al. 2011

CHAPTER 3: FRAGMENTATION INCREASES WIND DISTURBANCE IMPACTS ON FOREST STRUCTURE AND CARBON STOCKS IN A WESTERN AMAZONIAN LANDSCAPE

Naomi B. Schwartz, Maria Uriarte, Ruth DeFries, Kristopher Bedka,

Katia Fernandes, Victor Gutierrez-Velez, Miguel Pinedo-Vasquez

Abstract

Tropical second-growth forests could help mitigate climate change, but the degree to which their carbon potential is achieved will depend on exposure to disturbance. Wind disturbance is common in tropical forests, shaping structure, composition, and function, and influencing successional trajectories. However, little is known about the impacts of extreme winds on second-growth forests in fragmented landscapes, though these ecosystems are often located in mosaics of forest, pasture, cropland, and other land cover types. Indirect evidence suggests that fragmentation increases risk of wind damage in tropical forests, but no studies have found such impacts following severe storms. In this study, we ask whether fragmentation and forest type (old vs. second growth) were associated with variation in wind damage after a severe convective storm in a fragmented production landscape in western Amazonia. We applied linear spectral unmixing to Landsat 8 imagery from before and after the storm, and combined it with field observations of damage to map wind effects on forest structure and biomass. We also used Landsat 8 imagery to map land cover with the goals of identifying old- and second-growth forest and characterizing fragmentation. We used these data to assess variation in wind disturbance across 95,596 hectares of forest, distributed over 6,110 patches. We find that fragmentation is significantly associated with wind damage, with damage severity higher at forest edges and in

edgier, more isolated patches. Damage was also more severe in old-growth than in second-growth forests, but this effect was weaker than that of fragmentation. These results illustrate the importance of considering landscape context in planning tropical forest restoration and natural regeneration projects. Assessments of long-term carbon sequestration potential need to consider spatial variation in disturbance exposure. Where risk of extreme winds is high, minimizing fragmentation and isolation could increase carbon sequestration potential.

Introduction

Tropical second-growth forests, defined here as forests growing on previously cleared land, can recover biomass quickly and sequester large amounts of carbon (Poorter et al. 2016). These forests could play an important role in mitigating climate change; for example, if allowed to grow undisturbed, existing Latin American second-growth forests could accumulate an additional 8.48 Pg C in the next 40 years, enough to offset all carbon emissions from fossil fuel use and industrial processes in Latin America and the Caribbean from 1993-2014 (Chazdon et al. 2016). Many factors, including past land use, climate, and soil characteristics influence rates and quantities of carbon sequestration in second-growth forests (Anderson-Teixeira et al. 2013, Jakovac et al. 2016, Poorter et al. 2016, Uriarte et al. 2016b). In particular, exposure to natural disturbances such as extreme winds, fires, or drought can affect successional trajectories in regenerating forests (Flynn et al. 2010, Anderson-Teixeira et al. 2013, Uriarte et al. 2016b), influencing the degree to which the carbon sequestration potential of second-growth forests is achieved. Furthermore, second-growth forests are typically located in landscapes subject to human influence that are mosaics of old growth, second growth, and other land cover types (Brown and Lugo 1990). Regrowth often happens along existing forest margins (Asner et al.

2009b, Sloan et al. 2016), making second-growth forests highly exposed to edge effects, impacts of fragmentation, and anthropogenic disturbances such as fire and logging. Accurately predicting biomass recovery in these forests requires that we understand their disturbance ecology and how their disturbance regimes are influenced by the landscapes in which they are situated.

Wind is a major disturbance in the tropics and has both short-term impacts and lasting legacies in tropical forests (Everham and Brokaw 1996, Laurance and Curran 2008, Lugo 2008). Tropical forests are exposed to extreme winds from tropical storms or via convective downdrafts, squall lines and isolated cold fronts. Convective downdrafts and squall lines are relatively common in the Amazon basin (Garstang et al. 1994, 1998), and associated extreme winds can cause large-scale forest disturbance and tree mortality (Espirito-Santo et al. 2010, Negrón-Juárez et al. 2010). Tropical storms and heavy precipitation events are expected to become more intense with climate change (Knutson et al. 2010, Orlowsky and Seneviratne 2012, IPCC 2013), and warming and land use change will affect future convection patterns (Del Genio et al. 2007, da Silva et al. 2008). Understanding the determinants of forest susceptibility to extreme winds is thus important for modeling and monitoring future impacts of forest disturbance (US DOE 2012).

The spatial distribution and size of blowdowns have important consequences for understanding biomass dynamics in tropical forests (Fisher et al. 2008, Chambers et al. 2009, Di Vittorio et al. 2014, Magnabosco Marra et al. 2016). A number of studies have quantified the frequency, return interval, rotation period, and carbon impacts of large blowdowns in the Amazon across expanses of old-growth forest (Nelson 1994, Negrón-Juárez et al. 2010, Chambers et al. 2013, Espirito-Santo et al. 2014). However, little is known about the impacts of extreme winds in the fragmented, mosaic landscapes in which tropical second-growth forests

occur. If forest fragmentation increases the impacts of wind disturbance, this difference could affect estimates of potential carbon sequestration in tropical second-growth forest.

Impacts of extreme wind on both individual trees and stand-level carbon balance differ depending on species composition and forest structure. Damage is most severe for pioneer species, species with low wood density, taller trees, and trees with higher slenderness coefficient, i.e. a larger height for a given diameter (Zimmerman et al. 1994, Everham and Brokaw 1996, Curran et al. 2008a, Canham et al. 2010, Uriarte et al. 2012a, McGroddy et al. 2013, Ribeiro et al. 2016, Rifai et al. 2016). Stand structure characteristics such as canopy height, canopy density, basal area, and median diameter are positively correlated with the amount of wind damage in a stand (Everham and Brokaw 1996, Uriarte et al. 2004c, McGroddy et al. 2013). Susceptibility to damage also increases with stand age in earlier stages of succession, but may decline in older stands (Everham and Brokaw 1996). These shifts are due to both changes in forest structure and changes in species composition: though canopy height, density, and basal area increase over succession, species composition often shifts away from low wood-density pioneers towards late-successional species with higher wood density (Bazzaz and Pickett 1980, Lohbeck et al. 2013).

Though second-growth forests are often highly fragmented and located in mosaic landscapes, few studies have considered the influence of landscape and patch structure on wind damage. Fragmentation may influence exposure to strong winds because landscape variability influences the way wind moves, and generates heterogeneity in wind speeds and wind exposure through a number of mechanisms. Wind speeds vary with surface roughness, with winds gaining more speed over low-roughness vegetation such as open grassland, brush, or agricultural crops (Fons 1940, Oliver 1971, Davies-Colley et al. 2000). Accordingly, wind speeds decline with distance from forest-pasture edges (Davies-Colley et al. 2000), and there is strong wind

turbulence at high-contrast forest edges (Somerville 1980, Morse et al. 2002). Wind also moves more quickly though open forest (Somerville 1980, Kanowski et al. 2008). Forest edges have lower biomass and a more open canopy (de Casenave et al. 1995, Laurance et al. 1997, Harper et al. 2005), implying that wind speeds should be higher at forest edges than in the interior. Furthermore, pioneer species are more common close to forest edges, elevating the vulnerability of edge forest to windthrow (Oosterhoorn and Kappelle 2000, Laurance et al. 2006).

Despite variation in exposure and vulnerability to extreme winds, evidence for impacts of fragmentation on wind damage in tropical forests is lacking. Several studies in temperate silvicultural systems have detected edge effects on wind damage (Peltola 1996, Talkkari et al. 2000, Zeng et al. 2004) but this effect has been more challenging to detect in diverse tropical forests. The Biological Dynamics of Forest Fragments experiment in the Brazilian Amazon found high tree mortality close to forest edges, with uprooting more frequent relative to standing dead trees (Ferreira and Laurance 1997, Mesquita et al. 1999). However, this mortality was not linked to specific extreme wind events and could have resulted from other factors (e.g., desiccation). Several studies have examined fragmentation effects on wind damage after tropical storms, and have found little evidence that damage varies with fragmentation (Catterall et al. 2008, Grimbacher et al. 2008). The degree to which fragmentation increases the risk of damage from extreme winds in tropical forests thus remains an open question.

Detecting effects of fragmentation on wind damage may be difficult with a field sampling approach. Extreme winds can be highly patchy (Bellingham et al. 1992, Imbert et al. 1996, Grove et al. 2000, Pohlman et al. 2008). Detecting spatial patterns within heterogeneous, patchy phenomena requires large sample sizes, and inadequate sampling can make it difficult or impossible to detect patterns (Loehle 1991). Estimates of landscape level mortality based on field

plot observations may miss up to 17% of mortality (Chambers et al. 2013), and field plot studies may lack the statistical power to detect the effect of fragmentation on wind damage (Grimbacher et al. 2008). However, remote sensing allows detection of patterns that may be unfeasible or impossible in ground-based studies (Chambers et al. 2007). Recently developed remote sensing techniques can detect small blowdowns (Negrón-Juárez et al. 2011). Unlike plot-based approaches, remote sensing allows estimation of wind damage across broad areas, and in combination with field data can improve our understanding of disturbance and carbon dynamics in tropical mosaic landscapes.

Here, we use remotely sensed data to quantify damage from a mesoscale convective storm system across a fragmented production landscape in the Peruvian Amazon. We use these data in combination with land cover maps to ask:

1) Are second-growth forests more severely fragmented than old-growth forests?
2) How does fragmentation influence forest vulnerability to extreme winds?
3) Does wind damage severity vary in old-growth versus second-growth forests?

We predict that second-growth forests in our study area will be more severely fragmented than old-growth forests, and hypothesize that severity of wind damage will be highest in small, isolated forest fragments and close to forest edges. We expect that second-growth forests, which have a higher proportion of pioneer species with low wood density, will suffer more severe damage than old-growth forests, composed of less vulnerable high wood density species. This variability could affect forest succession in dynamic, fragmented landscapes, with forest patch and landscape characteristics influencing rates of biomass recovery via effects on exposure and vulnerability to wind disturbance.

Materials and Methods

Study area

The city of Pucallpa, the capital of the Ucayali region of Peru, is the largest Amazonian city connected to the national capital, Lima, by road. As a result, Pucallpa is an important transport center, and in recent years has been a hotspot of forest disturbance, deforestation, and fire in the Peruvian Amazon (Oliveira et al. 2007, Uriarte et al. 2012b, Schwartz et al. 2015). This research focuses on an area of 2,158 km^2 near Pucallpa, surrounding the highway from Lima to Pucallpa. The landscape is heterogeneous, with patches of old growth and second-growth forest surrounded by pastures, oil palm plantations, and smallholder farms (Gutiérrez-Vélez and DeFries 2013; Figure 1). Elevation ranges from 150 to 250 m a.s.l. and total annual precipitation ranges from about 1500-2500 mm, with a dry season from July to September.

On November 30, 2013, a mesoscale convective system (MCS) passed through the study area, resulting in widespread blowdowns and tree mortality. Though there is insufficient meteorological station data available from the study area to characterize the storm severity, data processed from the GOES-13 satellite using the method described in Bedka and Khlopenkov (2016) indicates high overshooting top probability during the November 30 storm in the study area (Appendix 3: Figure 1). Overshooting tops indicate regions where strong updrafts were present within the MCS. Strong downdrafts are often present near to these updrafts in regions of heavy precipitation. Storms with overshooting tops often generate winds that exceed 58 mph, the criterion for "damaging wind" by the U.S. NOAA National Weather Service (Dworak et al. 2012). Given the heterogeneity in land cover, forest age, and patch size, this landscape offers an ideal opportunity to study how impacts of damaging winds vary with fragmentation and landscape context.

Remote sensing of wind damage

We obtained Landsat 8 OLI scenes covering the study area (path-row 06-066 and 07-066) from 2013 (pre-storm) and 2014 (post-storm; Appendix 3: Table 1) at 30 m resolution. All scenes were acquired with atmospheric corrections from the Landsat CDR archive (LaSRC product; USGS 2016) via USGS Earth Explorer (http://earthexplorer.usgs.gov/). The LaSRC product includes a cloud mask band, generated with the FMASK algorithm (Zhu and Woodcock 2012). We used this band to mask pixels that were cloudy in 2013 or 2014. 1023 ha were masked out due to cloud cover, equal to 0.5% of the study area. Because the atmospheric composition between multi-temporal images differs, especially regarding water vapor and ozone, we applying a radiometric normalization (Hall et al., 1991) to normalize the 2014 scene to the 2013 scene, using the MAD algorithm (Canty and Nielsen 2008). All remote sensing data processing was conducted in ENVI (Exelis Visual Information Solutions, Boulder, Colorado) unless otherwise indicated.

To map wind damage we follow the approach outlined by Negron-Juarez et al. (2010, 2011), which uses spectral mixture analysis (SMA) to map the change in non-photosynthetic vegetation (NPV) fraction across pixels. SMA assumes that every pixel is a linear combination of some number of target endmember spectra, such as vegetation, shade, NPV, and/or bare soil, and quantifies the per-pixel fraction of each endmember (Adams and Gillespie 2006). Wind damage increases the amount of wood, dead vegetation, and litter exposed to the sensor, and so the change in NPV fraction is associated with the amount of wind damage.

We applied linear spectral unmixing to each image using endmembers for green vegetation (GV), NPV, and shade. Endmembers were identified from the 2013 scene using the

Pixel Purity Index algorithm (Boardman et al. 1995) available in ENVI (Appendix 3: Figure 2). Following unmixing, we normalized the fraction of NPV without shade as NPV/(GV+NPV) so that fractions reflected only relative proportions of NPV and GV, and not differences due to effects of shading (Adams and Gillespie 2006). Change in NPV (ΔNPV) was calculated by subtracting the normalized NPV fraction in 2013 from 2014.

Field data collection

Wind damage was measured in the field to assess whether ΔNPV provided an adequate approximation of damage. Because previous studies (Negron-Juarez et al. 2011, Rifai et al. 2016) had validated the relationship between ΔNPV and wind damage in old-growth forests, we focused our validation and field data collection on second-growth forest. During the months of July and August of 2014 and 2015, we established 30-0.1 ha forest plots (Figure 1). We used satellite images to identify forest patches, and from those, chose sites where we could locate and get permission from the landowners to access their property. Within these areas, plot locations were selected to encompass a range of ΔNPV. Because plots were slightly larger than a Landsat pixel, plot-level ΔNPV was calculated as the weighted mean of ΔNPV in pixels overlapped by the plot. We determined age of the forest plots from a 28-year land cover time series (see Chapter 1), as the number of years since the last year that the plot location was classified as non-forest. Though all forest plots were located within forest classified as second growth (see below), not all had been observed as having been clear-cut during the 30 year satellite record, and plot ages ranged from 3 years to >30 (i.e. never cleared). Plots were geolocated using a Garmin GPSMAP 62sc.

In each plot we measured diameter at breast height (dbh) of all trees greater than 5 cm, and coded each tree as damaged (uprooted, trunk snapped, or severe branch loss) or undamaged. Downed or damaged trees that were severely rotted were marked as such, since these trees were likely damaged prior to the 2013 storm. We conducted all analyses including and excluding these previously damaged individuals and it did not significantly affect our results; reported results exclude these trees. Measures of damage include both stems directly thrown by wind and trees that were damaged by other trees, because it is difficult to distinguish between these two types of damage in the field. We calculated aboveground biomass (AGB) using the following allometric equation developed for secondary forest species in the central Amazon (Nelson et al. 1999):

$$\ln(\text{biomass}) = -1.9968 + 2.4128 * \ln(\text{DBH})$$

We divided biomass by two so that estimates were in terms of kg C instead of kg biomass, under the assumption that C makes up 50% of biomass (Brown and Lugo 1982). To characterize plot-level damage, we calculated total damaged biomass, proportion biomass damaged, total stems damaged, and proportion of stems damaged for each plot. We assessed the relationship between ΔNPV and wind damage by calculating linear regressions of ΔNPV vs. field measurements of wind damage in the 30 forest plots. To estimate AGB loss across the study area, we used the parameters from the linear model of ΔNPV vs. total AGB lost in field plots (Appendix 3: Figure 6c), and applied it to each forest pixel to calculate lost biomass based on a pixel's NPV. Because allometries based on secondary forest species yield lower estimates of biomass, using an allometric equation designed for secondary forest species across the whole study area is likely to underestimate biomass lost in old-growth forest. Furthermore, wind damage tends to increase with age (Figure 3), and so old-growth forests likely experienced more severe damage than second-growth forests. However, because we measured wind damage in second-growth forests

only, we are extrapolating using parameters derived from the relationship between damage and AGB in second-growth forests. Therefore, our estimates represent a conservative estimate of biomass lost across in the study area's forests, particularly for old-growth forests.

Remote sensing of land cover

We developed a land cover classification at 30 m resolution for use in generating predictor variables related to fragmentation and masking analyses to forested areas. The classification expanded on the approach laid out in Gutierrez-Velez and DeFries (2013). Land use classes were old-growth forest, second-growth forest, mature oil palm (> 3 years old), and "other," which included young oil palm (< 3 years old), bare ground, burned non-forest areas, fallow, pasture, degraded pasture, and bodies of water. Training data were collected in the field, and for the training data, second-growth forests were identified as tree-dominated vegetation growing in areas that had previously been cleared, with significantly lower basal area than old-growth forests in the study area (Gutiérrez-Vélez et al. 2011). Old-growth forests were identified as predominantly residual forest from logging and extraction of non-timber resources, but they have significantly higher basal area and biomass than second-growth forests (Gutiérrez-Vélez et al. 2011). Ultimately, whether a pixel was classified as old-growth or second-growth depends on its spectral properties, which do not always coincide with its land-use history.

We classified Landsat 8 OLI images (Appendix 3: Table 1) with a random forest classification built with several spectral indices and spectral transformations: i) NDVI, ii) bare soil, vegetation, and shade fractions from SMA, iii) brightness, greenness, and third from a tasseled cap transformation, and iv) first- and second-order texture measures. Components i-iii were shown to be effective for classifying the non-oil palm land cover classes in a land cover

classification from the same study area (Gutiérrez-Vélez and DeFries 2013). Component iv, the texture measures, were useful for distinguishing oil palm plantations, which are spectrally similar to secondary forests but appear more uniform in satellite images due to even-aged planting. Training and testing data for land cover classes were collected during a 2015 field campaign and included 2198.52 ha total, divided among classes (Appendix 3: Table 2). For more details about the classification, see Appendix 3.

The land cover map from 2014 was used to mask analyses to forested areas (old growth and second growth). We also masked areas near known anthropogenic disturbance, since spillover disturbance from recent forest clearing might bias results along forest edges. To do so, we identified recently deforested areas – areas that were classified as forest in 2013 and as non-forest in 2014 – and masked all pixels within 60 m to prevent anthropogenic disturbance biasing results (Appendix 3: Figure 3).

Characterizing forest fragmentation

We used Fragstats (McGarigal et al. 2012) to characterize forest patch fragmentation. Old-growth and second-growth forests were all treated as a single forest category for the purpose of characterizing patches. Fragmentation has three key axes: area, edge, and isolation (Fahrig 2003, Haddad et al. 2015). We calculated one Fragstats metric to represent each of these axes (Figure 2). Patch area (ha) represents patch size. Edginess is quantified with the shape index, which is calculated as:

$$SHAPE = \frac{0.25p}{\sqrt{a}}$$

where p is the patch perimeter and a is the patch area. Shape index increases as the perimeter of a patch gets more complex, and equals 1 if a patch is a perfect square. We quantified isolation with

the proximity index. The proximity index takes into account the area and distance of forest within a particular radius around the focal patch, and increases from zero with the upper limit determined by the search radius. For a given patch *i*, proximity index is calculated as:

$$PROX = \left(\sum_{j=1}^{n} \frac{a_{ij}}{h_{ij}^2} \right)$$

where a_{ij} is the area (m^2) of patches $j=1...n$ within specified neighborhood radius (m) of focal patch i and h_{ij} is the distance (m) between patch i and patch j. Using this formulation assumes that larger and closer patches decrease patch isolation more than smaller or more distant ones, a reasonable assumption. We calculated proximity index with several radii (250 m, 500 m, 1000 m, 2000 m, 4000 m and 10000 m), but these indices were highly correlated and there was no significant different in model performance depending on the distance, so we used the 1000 m radius in our final models. So that higher values represented increasing isolation, we multiplied proximity index by -1.

Statistical analysis

We compared sizes of damaged vs. undamaged trees, and fragmentation variables in old- vs. second-growth forest using t-tests. To test the relationship between wind damage, forest fragmentation, and forest age (old vs second growth), we fit a generalized linear model to predict ΔNPV at the pixel scale (Table 1). Pixels with ΔNPV less than 0 were excluded from analysis, because a decline in NPV cannot represent negative damage and instead likely represents changes due to forest succession or recovery from prior disturbance. Both pixel characteristics and patch characteristics were included as predictors. Pixel level predictors were distance from forest edge and a binary predictor for second-growth forest (0 = old growth, 1 = second growth). Patch level predictors were area, edginess, and isolation of the patches in which pixels were

located. Because the total number of pixels was large (461,610) and ΔNPV was highly left skewed, we stratified pixels according to ΔNPV (0-0.05, 0.05-0.15, 0.15-0.25, >0.25) and randomly sampled 2000 pixels from each stratum for use in statistical analyses (Appendix 3: Figure 4). The sample was bootstrapped 200 times. ΔNPV was log-transformed to meet the assumption of normality. Distance from edge was also log-transformed because it was highly left-skewed. To facilitate interpretation, all predictors were scaled to unit standard deviation by subtracting the mean and dividing by the standard deviation (Gelman and Hill 2007). To test for collinearity among predictors we calculated variance inflation factors (VIF; Fox and Monette 1992) and condition indices (Belsley 1991). VIF values greater than ~5 indicate strong collinearity (Dormann et al. 2013), though values as low as 2 can have impacts on parameter estimates (Graham 2003). VIF for all predictors was < 4 with the exception of edginess (VIF = 5.2). To address this potential collinearity issue we ran the model with all predictors other than patch area, which was correlated with the other fragmentation predictors and was the predictor with the weakest effect in the full model. The maximum VIF in this partial model was 2.2, and the parameters for all remaining predictors were qualitatively the same as in the full model. We followed the same steps, removing edginess, which had the highest VIF at 2.2. In this partial model, the maximum VIF was 1.4 and still, parameters were qualitatively the same. Condition indices greater than 30 indicate substantial collinearity (Belsley 1991). All condition indices in our model were < 5. We tested for spatial autocorrelation among model residuals by calculating Moran's I and found no spatial autocorrelation in the model residuals (Moran's I = 0.0003, p = 0.45). Model parameters reported are the median estimates of the 200 bootstrapped models and 95% bootstrapped confidence intervals. Statistical analyses were conducted in R (R Development Core Team 2014).

Results

Overview: linking field and remote sensing data

Validation of ΔNPV with field observations: Mean pre-damage AGB in field plots was 62.04 Mg C ha^{-1} (s.d. = 13.31, Appendix 3: Table 4). Mean AGB damaged was 17.5 Mg C ha^{-1} (s.d. = 18.7), or 24.6% of pre-storm AGB (s.d. = 25.1%). Mean stem density in field plots was 1286 stems ha^{-1} (s.d. = 342.6), with an average 16.5% of stems damaged (s.d. = 15.7%). Damaged stems were significantly larger than undamaged stems (Appendix 3: Figure 5, $t = -9.73$, $p < 0.0001$).

ΔNPV was strongly related to damage as measured in the field plots. It was most strongly correlated with the proportion of stems damaged in field plots ($R^2 = 0.699$, Figure 3), but the relationship held when damage was quantified in terms of total number of stems damaged ($R^2 = 0.649$), total AGB damaged ($R^2 = 0.542$), or proportion of AGB damaged ($R^2 = 0.603$, Appendix 3: Figure 6). On average ΔNPV was low across the landscape: mean ΔNPV was 0.03, and standard deviation was 0.04 (Figure 4). Five percent of forest pixels, or 2058 ha, had ΔNPV higher than 0.1, corresponding to 20.7% stems damaged, or 31.5% of carbon lost (22.5 Mg C ha^{-1}, Table 2). ΔNPV was greater than 0.2 in 0.8% of forest pixels (348.5 ha), corresponding to 48.6% stems damaged, or 82.0% of carbon lost (59.1 Mg C ha^{-1}, Table 2). The total biomass lost as a result of the wind event in second-growth forests was 0.161 Tg C (95% CI = 0.026, 0.553, Table 2). When extrapolating across the whole study area, carbon lost was approximately 0.296 Tg C (95% CI = 0.05, 1.02), with 54 percent in second growth forest, and 46 percent in old growth (Table 2). Estimates for carbon lost in old-growth forest are based on extrapolation of

data from second-growth forest, and therefore they are conservative estimates of total carbon lost.

Characterizing land cover and fragmentation: The land cover classification accurately distinguished between oil palm, old-growth forest, second-growth forest, and other classes (Appendix 3: Table 3). Overall accuracy was 96.4%. Forty-four percent of the study area, 95,596 ha, was classified as forest. Forty percent of forest pixels were classified as old-growth forest, and 60% were classified as second-growth forest (Figure 1). There were 6110 forest patches in the study area, with a mean area of 42.1 ha (Appendix 3: Figure 7). Mean edginess (shape index) was 1.3, and mean isolation (-1*proximity index) was -19688 (Appendix 3: Figure 7).

Fragmentation in old- vs. second-growth forests

Degree of fragmentation varied across old-growth and second-growth forest pixels, with second-growth forests more fragmented along most measures (Figure 5). Second-growth forest pixels were closer to forest edges ($t = 237.15$, $p < 0.001$, Appendix 3: Table 5), but in less edgy patches ($t = 134.76$, $p < 0.0001$, Appendix 3: Table 5). Second-growth pixels were also located in smaller ($t = 141.28$, $p < 0.001$, Figure 5) and more isolated patches, ($t = 47.658$, $p < 0.0001$, Figure 5).

Wind damage model

Fragmentation and forest type were significantly associated with ΔNPV ($R^2 = 0.158$, 95% bootstrap CI = [0.143, 0.173]). Distance to edge had the strongest association with ΔNPV (Figure 6), which exponentially decreased with pixel distance from forest edge (Figure 7a). Patch edginess was positively associated with ΔNPV, with pixels in edgier patches suffering more

severe wind damage (Figure 6, Figure 7c). Isolation also influenced damage: ΔNPV was higher in more isolated patches (Figure 6, Figure 7d). Patch area was negatively associated with damage, though this effect was weaker than that of the other fragmentation predictors (Figure 6, Figure 7b). Predicted ΔNPV was slightly higher for old-growth forest pixels, though the difference between second growth and old growth was small compared to the predicted variation in Δ NPV associated with fragmentation (Figure 6, Figure 7).

Discussion

Effects of fragmentation on wind damage

This study provides the first unequivocal empirical evidence that fragmentation increases risk of damage from extreme wind events in tropical forests. The severe convection event that occurred in our study region caused an overall loss of approximately 0.3 Tg C in the study area (0.14 in second-growth forest and 0.16 in old-growth). When averaged across the total forested area in the study area (95,596 ha), this amounts to 3.09 Mg C ha^{-1} (2.79 Mg C ha^{-1} in second-growth, and 3.55 in old-growth), more than sixty percent greater per hectare than figures from a recent study that estimated annual carbon loss from natural disturbances in the entire Amazon forest (Espirito-Santo et al. 2014). That study estimated the total loss at 1.3 Pg C y^{-1}, an average of 1.9 Mg C ha^{-1} across the ~6.8 x 10^8 ha of Amazon forest.

A number of differences between their study and ours could explain the discrepancy. The Espírito-Santo et al. study mapped disturbances across a study area many times the size of ours, and developed a disturbance size-frequency distribution for the entire Amazon. The disturbances captured in our far smaller study are likely on the intermediate-to-large end of their disturbance size-frequency distribution. However, the discrepancy might also reflect differences in landscape

structure in the two studies. Espírito-Santo et al. focused on contiguous forest, where, based on our results, wind damage is likely to be less severe than in the fragmented landscapes of our study region. These findings illustrate the importance of considering fragmented landscapes when assessing disturbance regimes in tropical forests. Studies that do not consider the effects of landscape configuration may underestimate the importance of wind disturbance for quantifying the tropical forest carbon sink. Recent estimates suggest 70% of the world's forests are within 1 km of a forest edge (Haddad et al. 2015), and that 19% of tropical forests are less than 100 m from an edge (Brinck et al. 2017). Brinck et al. (2017) estimate that edge effects result in 0.34 Gt additional carbon emissions from tropical forests per year, though this estimate does not explicitly take into account effects of extreme winds. Considering the impacts of extreme winds in fragmented landscapes would likely affect estimates of the effects of fragmentation on forest carbon balance, and would influence our understanding of the importance of extreme wind events for driving carbon cycling in the Amazon.

Though many studies suggest that fragmented forests should have heightened vulnerability to wind damage (SAUNDERS et al. 1991, Laurance and Curran 2008), evidence for this phenomenon has been lacking. For example, a number of studies that set out to measure effects of fragmentation on wind damage after Cyclone Larry, a category 5 tropical cyclone, found little difference in wind damage between fragments and continuous forest (Catterall et al. 2008, Grimbacher et al. 2008, Pohlman et al. 2008). Our study may have detected an effect where former studies did not for several reasons. First, the storm we considered was not as intense as a Cyclone Larry, and continuous forest cover may provide a protective benefit only up to a certain degree of storm intensity (Catterall et al. 2008). We do not have precise wind speed measurements from the date of the storm, but the presence and intensity of overshooting tops

indicates that winds were probably ≥ 93 km/h (Bedka and Khlopenkov 2016). By contrast, Category 5 tropical storms are associated with sustained winds > 200 km/h. Lending support to this threshold hypothesis, a study after Hurricane Hugo in South Carolina found that in areas struck by the most intense part of the hurricane, species differences in wind resistance were not apparent (Hook et al. 1991). Differences in rates of damage across species were only observed in areas where wind speeds were lower. Variation in exposure and vulnerability to extreme winds due to species composition and landscape configuration may come into play only when winds are not so severe that they cause widespread damage regardless.

Second, previous studies of fragmentation and wind damage were based on field data from a relatively small number of plots. Heterogeneity in damage and wind speeds may have affected the statistical ability to detect underlying patterns related to fragmentation (Grimbacher et al. 2008). This patchiness and unmodeled variation in wind speeds is likely the reason for the substantial unexplained variance in our statistical models. However, because our remote sensing approach allows us to consider a broad landscape with a large sample size we are able to detect an effect of fragmentation despite the noise, demonstrating, as many other studies have, the usefulness of remote sensing for understanding ecosystems at landscape to regional scales (Chambers et al. 2007).

Fragmented forests may be more prone to wind damage via two main mechanisms: because they are exposed to stronger winds than continuous forest, or because they are more vulnerable to strong winds due to differences in species composition or forest structure (Laurance and Curran 2008). We found effects of all three axes of fragmentation – isolation, edge, and area – on wind damage, which suggest possible support for both mechanisms. The effects of isolation are probably due to exposure to stronger winds. Forest slows wind down;

rougher surfaces exert more drag leading to slower wind speeds (Davies-Colley et al. 2000). Wind picks up more speed over smoother vegetation types, like pasture. Because isolated fragments are surrounded by larger expanses of open areas and non-forest land cover types, they likely are subject to stronger winds. However, species composition may also differ depending on patch isolation. Because we do not have measurements of species composition in relation to isolation, we cannot rule out that differences in composition also contribute to the observed effect of isolation.

Edge and area effects on wind damage are more difficult to attribute to exposure versus vulnerability, and could be due to either or both mechanisms. We found that pixels close to forest edges and pixels in edgier patches were more likely to be severely damaged. We also found a weak effect of patch size, likely because pixels in smaller patches are closer to edges. Forest edges are exposed to stronger winds (Somerville 1980, Morse et al. 2002), but there are also well-documented edge effects on species composition that could increase vulnerability to wind damage (Oosterhoorn and Kappelle 2000, Laurance et al. 2006). The degree to which differences in exposure or vulnerability explain the relationship between fragmentation and wind damage has implications for management actions to minimize impacts of strong winds. Future research could focus on disentangling the mechanisms responsible for these patterns.

Wind damage in old- vs. second-growth forest

The results from the model predicting wind damage (ΔNPV) indicate that when controlling for fragmentation, second-growth forests suffer slightly lower damage (have lower ΔNPV) than old-growth forests, counter to our initial hypothesis. Because trees with lower wood density are more prone to wind damage and community mean wood density tends to increase

over succession in wet tropical forests (Bazzaz and Pickett 1980, Lohbeck et al. 2013), we hypothesized that wind damage would be more severe in second-growth forests. Our finding to the contrary may be due to differences in tree stature between old-growth and second-growth forests. Larger trees and more slender trees are more susceptible to wind damage, in particular to uprooting (Putz et al. 1983, Zimmerman et al. 1994, Everham and Brokaw 1996, Canham et al. 2010, Ribeiro et al. 2016), which translates into differences in damage across sites with different forest structure. For example, Uriarte et al. (2004) found that damage after Hurricane Georges in the Dominican Republic was higher in sites with higher basal area and that young forests with low basal area were not severely affected by hurricane. Similarly, McGroddy et al. (2013) found that forest stands in the southern Yucatan with taller canopies and higher basal area suffered more severe hurricane damage, and that these structural differences were associated with past land use. Furthermore, because of the high levels of anthropogenic disturbance in the study area, we do not necessarily expect the successional shifts in species composition that are predicted for relatively undisturbed forests. Old-growth forests in the study area have never been completely cleared, but they have still been subject to anthropogenic disturbance, such as selective logging and fire. Selective logging tends to target timber species with higher wood density (Verburg and van Eijk-Bos 2003), so the largest remaining trees in selectively logged forests may be species with low wood density. Large stature and low-density wood would make these forest fragments especially prone to wind damage, perhaps explaining the higher damage we observed in old-growth forests. Alternatively, it is possible that large, high wood-density trees are more vulnerable to wind, or that when they do fall, they result in larger blowdowns due to a domino effect of large, heavy trees causing more damage than trees with lighter wood. In future studies, additional field plot data, with information on forest stature, species identification and wood

density from damaged vs. undamaged trees could help further elucidate which of these mechanisms drives the observed pattern.

In our model, however, fragmentation had a much stronger influence on damage than forest type (Figure 6, 7). Second-growth forests in the study area are more fragmented than old-growth forests, which ultimately might result in more severe wind impacts in these forests. Elsewhere, studies have found that second growth tends to happen along forest margins and in small fragments surrounded by non-forest land use (Helmer 2000, Asner et al. 2009b, Sloan et al. 2016). Wind is not the only disturbance for which risk is higher along edges: fire in the Amazon tends to be concentrated along forest edges (Cochrane and Laurance 2002, Alencar et al. 2004, Armenteras et al. 2013). There is potential for wind and fire to interact and amplify the other's impacts: studies in temperate ecosystems have found that an earlier fire can increase the severity of subsequent blow downs, and wind damage can increase the risk of fire by adding fuels and opening up the forest canopy (Myers and Van Lear 1998, Kulakowski and Veblen 2002). These interactions might occur in the Amazon, and could exacerbate disturbance effects on forest carbon balance.

Wind and other disturbances can alter successional pathways in regrowing forests (Anderson-Teixeira et al. 2013, Uriarte et al. 2016b). Variability in disturbance risk should thus be taken into account in spatial planning, management, and carbon accounting in tropical second-growth forests where the goal is to promote carbon sequestration. Silviculture has long considered wind damage risk in site and species selection and planting configuration (Somerville 1980, Savill 1983, Talkkari et al. 2000). However, managing tropical second-growth forests for carbon is a relatively new endeavor and the way landscape configuration influences susceptibility to disturbance is not well understood for tropical forests (US DOE 2012).

However, where possible, and where risk of extreme winds is high, minimizing fragmentation and isolation could reduce risk of wind damage. Smallholders, too, get services such as timber or other forest products from forest fragments on their properties, and may wish to protect their forest fragments from the impacts of extreme winds. Promoting regrowth close to existing forests, maintaining less edgy patches, or planting wind-firm species in isolated fragments and close to forest edges are all steps that smallholders could take to reduce risk of wind damage in their forests.

Future research should attempt to disentangle the mechanisms behind the patterns observed in this study. Understanding the degree to which differences in vulnerability versus exposure underlie variation in wind impacts will clarify appropriate management actions to minimize risk of wind damage in second-growth or remnant forests. Fragmentation experiments such as the Biological Dynamics of Forest Fragments experiment in Brazil have shed light on how fragmentation affects forest composition, structure, and microclimate (Laurance et al. 2002). However, understanding what those changes mean for impacts of extreme winds is not straightforward, and doing so would require some "luck" in that a severe windstorm would have to strike the experiment. This limitation presents some challenges in studying mechanisms of wind damage in fragmented landscapes, but there are ways forward. Fragmentation experiments like the aforementioned, but located in landscapes that suffer frequent severe wind events, such as Caribbean forests, could be useful in that the likelihood of extreme winds striking an experiment would be higher. However, an experimental approach relying on random chance is not the only way to further investigate these mechanisms. Improvements in modeling and mapping wind speed and in our understanding of how wind interacts with complex landscapes will further shed light on how exposure varies with fragmentation. Advances in remote sensing

technology, which are beginning to provide a more detailed picture of forest structure and composition, will be useful in understanding ecological mechanisms responsible for variability in disturbance impacts (Chambers et al. 2007). Finally, much of what we already know about variation in species and stand susceptibility to wind comes from opportunistic field sampling after extreme winds (e.g. Zimmerman et al. 1994, Uriarte et al. 2004c, McGroddy et al. 2013), and there is a need for further opportunistic post-storm sampling in fragmented landscapes. Continued monitoring of forest disturbance in fragmented landscapes, such as with the remote sensing approach demonstrated in this paper, is essential so that such opportunities are not lost. An improved understanding of how and why fragmentation and landscape configuration influence disturbance regimes in tropical second-growth forests will help ensure that the carbon potential of tropical second-growth forests is better achieved.

Acknowledgements

We thank C. Gabriel Hidalgo, Luís Calderon Vasquez, Robert Piña, and Geancarlo Cohello for assistance with fieldwork. Thanks to the Uriarte and DeFries lab groups, and Bianca Lopez, for helpful feedback on early drafts of this manuscript. We acknowledge support from the Institute for Latin American Studies at Columbia University, and the Center for International Forestry Research (CIFOR).

Figures and Tables

Figure 1: Location of the study area, near Pucallpa, Ucayali, Peru. Inset depicts forest cover, and locations of field plots and roads.

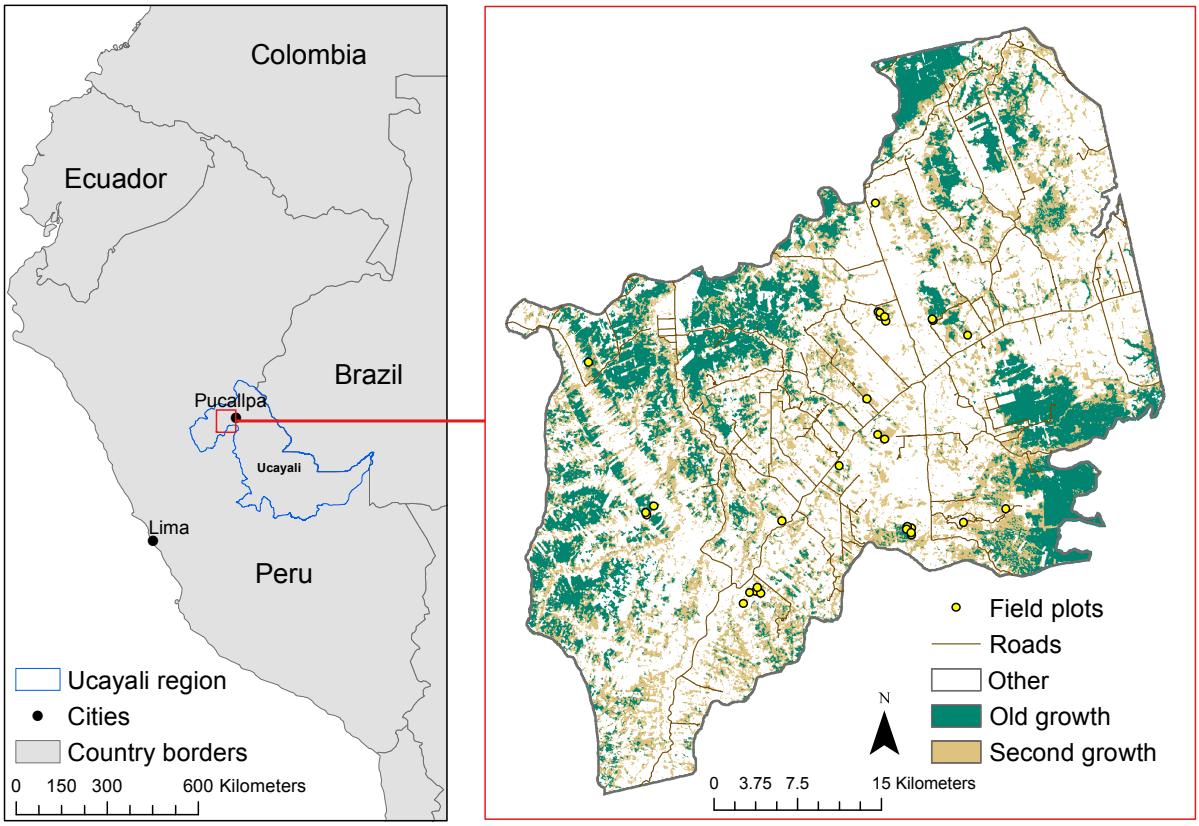

Figure 2: Conceptual figure illustrating axes of fragmentation, and variables associated with fragmentation included in analyses. Green squares represent forest pixels, and adjacent pixels represent a patch. Orange outline indicates focal pixel/patch for distance to edge and isolation measures.

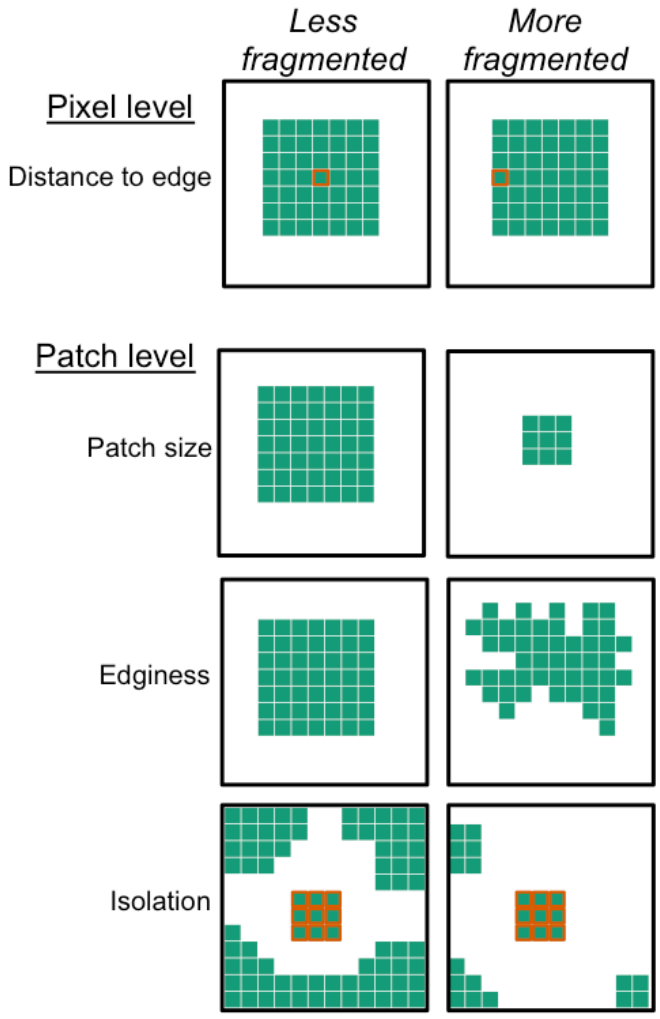

Figure 3: ΔNPV vs. proportion of stems > 5 cm DBH damaged in second growth forest field plots. Shaded areas indicate 95% confidence interval of regression line. Regression p-value < 0.001.

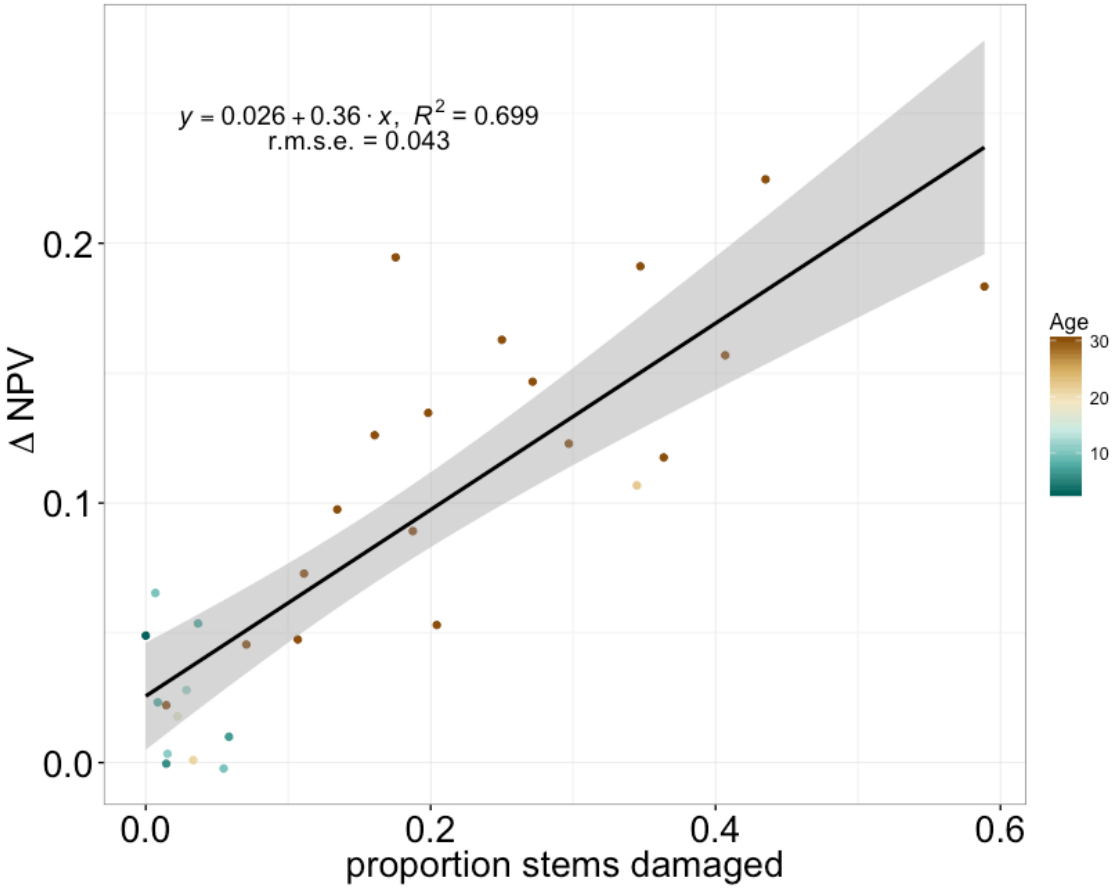

Figure 4: Map of wind damage (ΔNPV) in study area. Insets show two areas of interest where several field plots were located.

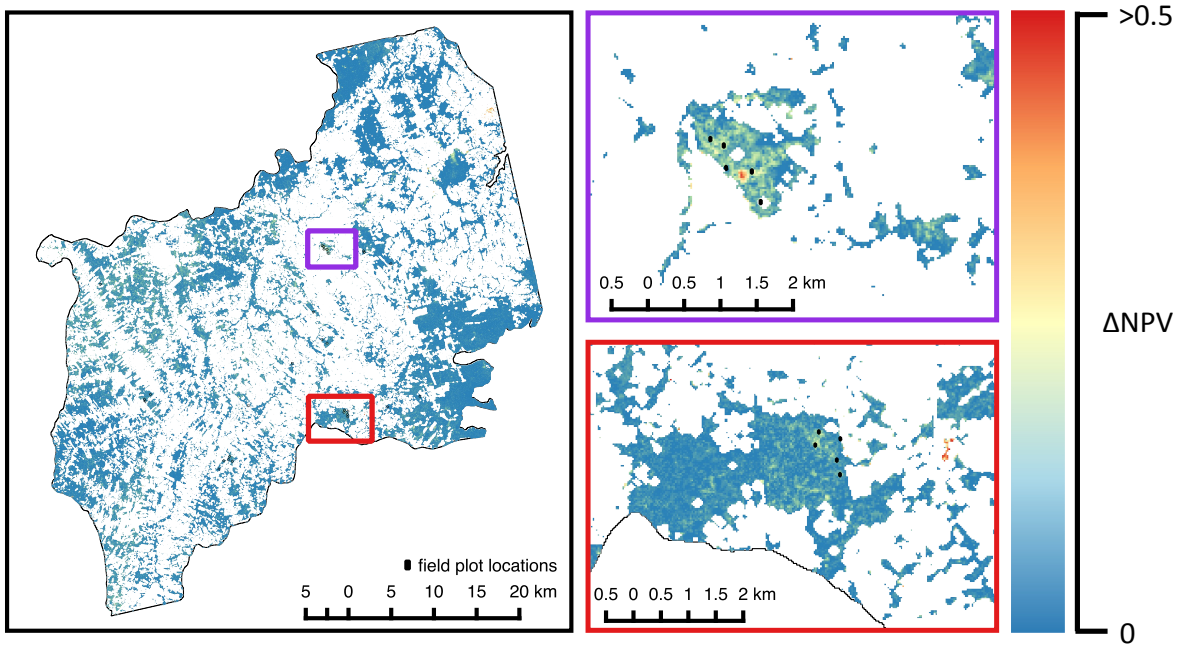

Figure 5: Comparison of the distribution of fragmentation variables between old-growth and second-growth forest pixels. Boxes show 25, 50, and 75% quantiles and whisker endpoints are 2.5 and 97.5% quantiles of observed data. Light grey points are outliers. Figures include data from all forest pixels in the study area. Fragmentation variables are a) distance to edge, b) area, c) edginess, and d) isolation.

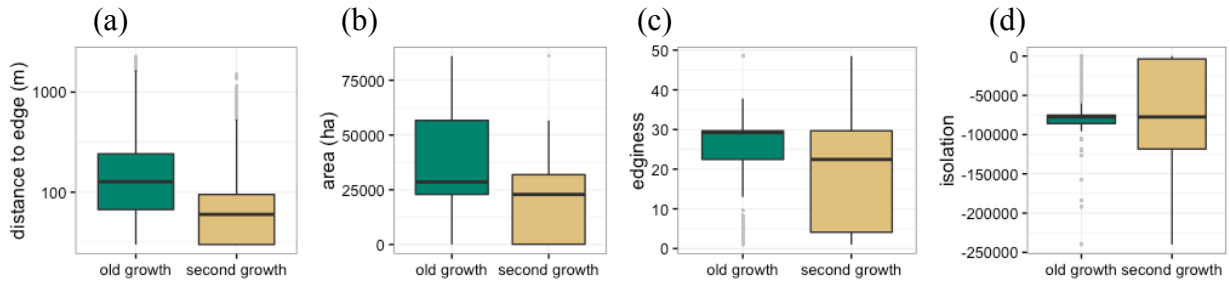

Figure 6: Parameter estimates from wind damage model. Points show the median coefficient estimates from the 200 bootstrapped model fits, whiskers show bootstrapped 95% confidence interval.

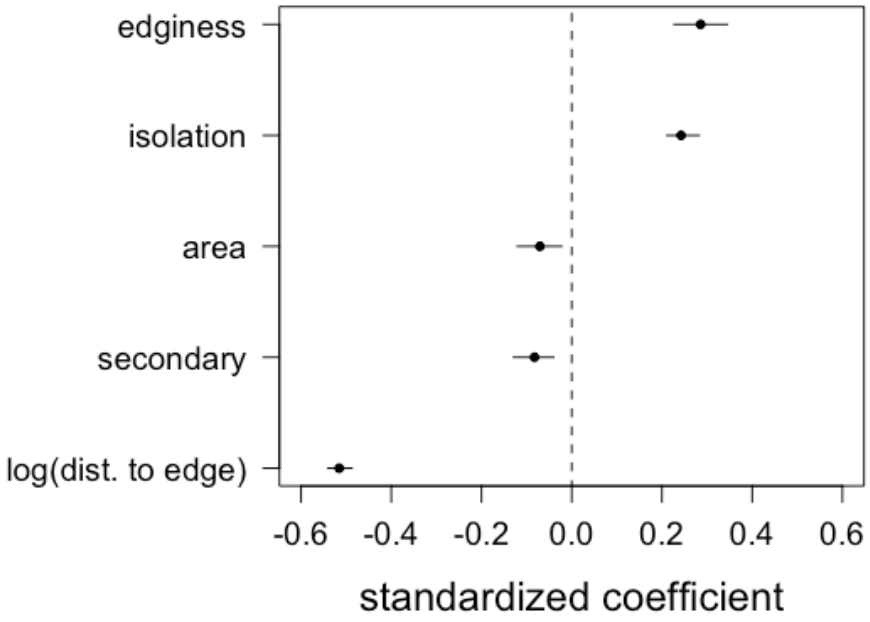

Figure 7: Model predictions of ΔNPV and fragmentation predictors. Solid lines depict predictions of the median coefficient estimates from bootstrapped model fits, dashed lines and shaded areas show predictions of 2.5 and 97.5% quantiles of coefficient estimates. A) distance from edge. B) patch area. C) edginess. D) isolation.

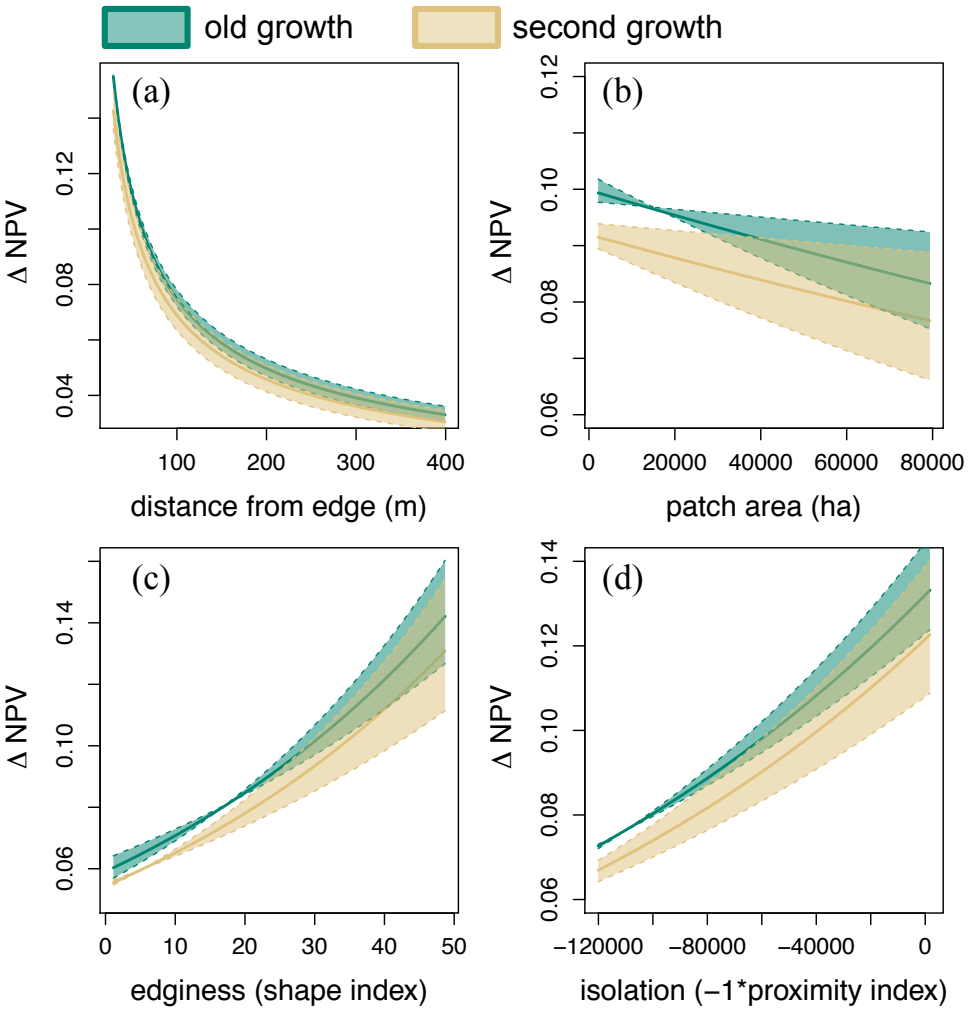

Table 1: Model covariates, descriptions, and summary statistics.

Variable name	*Description*	*Landscape mean (SD)*	*Bootstrap sample mean (95% bootstrapped CI)*	*Bootstrap sample SD (95% bootstrapped CI)*
Response				
ΔNPV	Change in non-photosynthetic vegetation fraction in pixel, i.e. wind damage (log transformed).	0.034 (0.039)	0.1560 [0.1556, 0.1565]	0.1318 [0.1312, 0.1322]
Predictors				
Distance to edge	Pixel distance to forest edge (meters)	102.5 (2.5)	69.4 [68.0, 70.8]	2.39 [2.36, 2.44]
Secondary	Binary variable for second growth. 0 = old growth, 1 = second growth	0.53 (0.50)	0.59 [0.58, 0.60]	0.491 [0.490, 0.493]
Area	Patch size in which pixel is located (hectares).	33247.5 (28869.9)	33035.4 [32503.2, 33605.0]	30899.6 [30592.6, 31200.1]
Edginess (shape index)	Shape index for patch in which pixel is located.	24.4 (14.6)	24.9 [24.6, 25.2]	15.9 [15.7, 16.0]
Isolation (-1* proximity index)	Proximity index for patch in which pixel is located.	75887.7 (50523.7)	-71336.3 [-72230.3, -70415.9]	48734.9 [47999.9, 49327.5]

Table 2: Summary of wind damage effects by forest type. 95% confidence intervals for lost carbon are in parenthesis.

	Old growth	**Second growth**	**All forest**
Total area (hectares)	38137	57459	95596
Mean ΔNPV	0.033	0.035	0.034
Proportion pixels with ΔNPV > 0.1	0.04	0.05	0.05
Proportion pixels with ΔNPV > 0.2	0.01	0.01	0.01
Carbon lost (Tg C)	0.135 (0.020, 0.470)	0.161 (0.026, 0.553)	0.296 (0.05, 1.02)
Biomass lost per ha (Mg C/ha)	3.55 (0.519, 12.32)	2.79 (0.460, 9.63)	3.09

CHAPTER 4: TRAITS AND TOPOGRAPHY MODULATE DROUGHT RESPONSE IN A TROPICAL SECOND-GROWTH FOREST

Naomi B. Schwartz, Maria Uriarte, Jess Zimmerman, Bob Muscarella, Nate Swenson

Abstract

Regional climate is filtered through elevation, topography, and vegetation to generate fine scale variation in moisture conditions. Thus, predicting individual drought responses in tropical forests remains challenging, in part because individual trees experience drought differently. We used a hierarchical Bayesian modeling framework to assess how tree performance and drought response vary with microtopography in a tropical second-growth forest. We integrated annual census data from the El Yunque Chronosequence plots with functional trait measures and LiDAR-derived microtopography measurements to ask how drought, topography, and crowding affect individual tree growth and survival, and how functional traits mediate species' responses to those drivers. Drought decreased growth and reduced survival, though effects on growth were much stronger than effects on survival. Tree performance and drought effects varied with topography, but often not in the directions we expected: trees on topographic positions we assumed to be wetter were more negatively affected by drought. Wood density and specific leaf area (SLA) affected species average performance and response to topography, and high wood density and low SLA were associated with reduced sensitivity to drought and topography. Fine-scale species sorting across topography may drive observed relationships between average performance, drought response, and topography. Our results highlight the complex interactions between climate, topography, crowding, and traits that underlie individual and species variation in drought response.

Introduction

Tropical rainfall regimes are predicted to change in future climate scenarios, with many parts of the tropics getting drier (Feng et al. 2013, Duffy et al. 2015, Chadwick et al. 2015). Drier conditions will likely have large impacts on tropical forests: drought influences forest ecosystem structure, composition, and function (Bonal et al. 2016, Uriarte et al. 2016b), and importantly, could decrease the size of the tropical forest carbon sink (Phillips et al. 2009, Pan et al. 2011, Gatti et al. 2014). However, large uncertainties about the impacts of drought on tropical forests remain, in part due to the difficulties of manipulating moisture conditions in tropical forests (but see Nepstad *et al.*, 2007; da Costa *et al.*, 2010). Observational studies of forest dynamics during natural droughts provide an opportunity to learn how drought affects tropical forests, especially where long-term data have been collected over multiple years. Understanding the impacts of recent droughts will help anticipate future changes in tropical forests caused by shifting frequency and intensity of drought.

Most studies of drought in tropical forests have aimed to quantify drought effects on carbon uptake and storage. Drought increases tree mortality and reduces tree growth (Chazdon et al. 2005, Feeley et al. 2007, Nepstad et al. 2007, Clark et al. 2010, da Costa et al. 2010, Phillips et al. 2010), which can result in large losses of stored carbon from tropical forests (Phillips et al. 2009, Lewis et al. 2011, Saatchi et al. 2013, Gatti et al. 2014). Other studies have focused on how sensitivity to drought varies across species and size classes. Species differences in their responses to drought can often be linked to their physiology or functional traits (O'Brien et al. 2017, Greenwood et al. 2017). For example, turgor loss point, wood density, stem hydraulic conductivity, and specific leaf area are all useful traits for predicting species-level variation in drought response (Bartlett et al. 2012, Maréchaux et al. 2015, Uriarte et al. 2016a, Greenwood et

al. 2017). Growth and mortality of larger trees tend to respond more strongly to drought, though this effect varies across sites (Chazdon et al. 2005, Nepstad et al. 2007, Phillips et al. 2010, Bennett et al. 2015, Uriarte et al. 2016a).

However, even within species and/or size classes, there can still be substantial unexplained variation in drought response. One hypothesis to explain these differences is fine-scale variation in the amount of water stress individual trees experience, due to differences in moisture availability linked to topography, soils, or competitive environment. Though the phenomenon has been little studied in the tropics, studies in other biomes have found drought effects can depend on topography. Variation in drainage and runoff means that slopes and ridges are drier than valleys (Burt and Butcher 1985, Western et al. 1999, Daws et al. 2002). Southwest facing slopes (northwest facing in the southern hemisphere) receive more solar radiation and have higher rates of evapotranspiration, and so water stress is typically higher (Stephenson 1990). Accordingly, drought-induced mortality is often higher in drier landscape positions (Fekedulegn et al. 2003, Guarín and Taylor 2005). Few studies have explicitly considered topographic variation in drought effects in tropical forests (but see Nakagawa *et al.*, 2000; Silva *et al.*, 2013), though several have demonstrated that topography influences species distributions both across and within sites (Ashton et al. 2006, Engelbrecht et al. 2007, Bartlett et al. 2016), and have linked topographic variation to observed differences in demographic rates (Silva et al. 2013). Drought could amplify these differences in performance, due to moisture stress being more severe at drier topographic positions. Furthermore, variation in performance across topography should depend on species and their functional traits, as some species are more sensitive to moisture stress and nutrient availability than others.

In the tropics and elsewhere, studies linking tree performance, moisture, and topography have typically focused on variation across sites or plots (Fekedulegn et al. 2003, Guarín and Taylor 2005, Ashton et al. 2006, Engelbrecht et al. 2007, Comita and Engelbrecht 2009). However, soil moisture and tree performance both vary with microtopographic relief (Famiglietti et al. 1998, Daws et al. 2002, Tenenbaum et al. 2006, Nishimua et al. 2007, Bartlett et al. 2016), at scales as small as 1 m (Tenenbaum et al. 2006). Ecological studies of the effects of microsite topography on tree performance have typically used categorical designations of topographic position (e.g. hummock vs. hollow, Nishimua et al. 2007; dry plateau vs. wet slopes, Englebrecht et al. 2007) but it is difficult to scale up these classifications across a landscape. New remote sensing techniques can generate digital elevation models (DEMs) at very fine scales (< 1 m), which can be used to quantify microtopographic relief and linked to variation in soil moisture (Tenenbaum et al. 2006, Buchanan et al. 2014). To our knowledge, no study has linked these quantitative characterizations of microsite topography with variation in tree performance during drought or otherwise.

Today, over 50% of tropical forests are classified as second growth (FAO 2010). Second-growth forests might be particularly sensitive to drought because of intense competition for resources and high proportion of drought-sensitive pioneer species in young forests (Uriarte et al. 2016b). Furthermore, land abandonment tends to happen in more remote, topographically complex, marginal locations (Helmer 2000, Asner et al. 2009b), which makes understanding how topography affects drought response particularly important in second growth forests. In this study, we link annual tree census data from second-growth forest in Puerto Rico with LiDAR-derived measures of microtopographic relief to assess how drought affects tree demography, and if and how traits, topography, and crowding mediate drought response. Specifically, we ask:

1) *How does drought affect tree growth and survival?* We expect growth and survival to be reduced during drought years.
2) *How does microtopographic relief affect tree growth and survival, and do its effects differ during drought years?* We expected that growth and survival would be lower on steeper slopes and on ridges (i.e. areas with more convex curvature). Because these topographic positions tend to be drier, we also expected the effects of drought on tree growth and mortality would be amplified on steeper slopes and more convex surfaces.
3) *How does crowding affect tree growth and survival, and do its effects vary during drought years?* We expected that crowding would reduce growth and survival, and further predicted that the effect of crowding would be amplified during drought years, due to more intense competition for water between neighbors.
4) *How does interspecific variation in functional traits mediate the effects of drought, topography, and crowding on tree demographics?* We expected that trees with traits representing more acquisitive strategies would have higher growth rates and lower rates of survival than trees with more conservative traits. Furthermore, we predicted that trees with acquisitive traits would be more strongly affected by stressful conditions, i.e. drought, dry topographic position, and crowding.

To address these questions, we used hierarchical Bayesian models, which allowed us to examine the importance of drought, topography, and crowding for tree performance. We focused on two topographic variables that are important for moisture conditions and flow of water across surfaces: slope and curvature (Burt and Butcher 1985). This approach also allows us to assess if and how functional traits drive intra-specific variation in response to environmental conditions. We considered two functional traits that have been found to be important for carbon metabolism

and plant hydraulics: specific leaf area (SLA) and wood density (WD). SLA represents the investment in photosynthetic machinery (leaf surface area) relative to total investment in leaf biomass. Leaves with high SLA tend to have higher photosynthetic rates and nutrient concentrations, and high SLA species typically have higher growth rates (Reich *et al.*, 1998). However, high SLA leaves tend to be shorter-lived, potentially leading to shorter full-plant life spans (Reich et al. 1992). Wood density represents the investment in wood biomass per volume of wood. Investing more in wood biomass means that trees with higher WD tend to have lower growth rates (King et al. 2005, Poorter et al. 2008). However, denser wood is more resistant to cavitation (Hacke et al. 2001) and structural damage (Everham and Brokaw 1996, Curran et al. 2008b), so species with higher wood density tend to have longer life spans, higher survival rates, and lower sensitivity to drought (Poorter *et al.*, 2008; Phillips *et al.*, 2010; Greenwood *et al.*, 2017). Better understanding the role of these widely measured traits in driving variation in tree species response to drought and other environmental conditions is an important step towards building a general predictive framework for species' responses to future environmental change.

Materials and methods

Study area and tree census data

This study was conducted with data from four forest plots, comprising the El Yunque Chronosequence Plots (Table 1). The land-use histories and ages of these plots were determined from aerial photographs taken between 1936 and 1977: three of the plots were previously cleared for agriculture, and represent a range of forest ages from 35 to 76 years since agricultural abandonment. The fourth plot is primary forest. The plots range in elevation from 100-500 m above sea level, and vary in size from ~0.5 to 1 hectare (Table 1). Annual rainfall in the region

ranges from 2700 mm to 3500 mm, with a 3,500mm average. Since 2013, All stems > 1 cm diameter at breast height (dbh) have been measured, mapped, and identified to species annually. We used these data to calculate absolute diameter growth and survival for each individual tree for each census interval.

In 2015, Puerto Rico experienced a severe drought: rainfall in El Yunque was only 2035 mm, the second lowest recorded. Rainfall was close to average in 2014 and 2016 (3193 and 3506 mm, respectively). For the purposes of assessing drought effects, we used growth and survival data from the 2014 (2013-2014), 2015 (2014-2015), and 2016 (2015-2016) censuses in our analyses, and considered drought as a binary variable. The 2015 census was coded as drought and the other two years as non-drought.

Functional trait data

Wood density and SLA measurements were collected using standard protocols (Cornelissen et al. 2003), with minor exceptions noted in Lasky et al. (2015). For all analyses, we used the mean trait value for each species. The two traits were weakly correlated ($r = -0.35$).

Topography data

Topography data were derived from airborne LiDAR data, collected by the National Center for Airborne Laser Mapping in May 2011. We followed standard procedures to generate a digital elevation model (DEM) at 1 m^2 resolution from LiDAR returns, using the minimum z-values of the last-return ground classified points to construct the DEM. Further details about the LiDAR data and DEM construction are in Wolf et al. (2016).

We used the DEM to derive topographic slope and hilltop curvature, following methods in Hurst et al. (2012). The method uses elevation data to approximate the land surface by fitting a six-term quadratic polynomial. We used a 99x99 m moving window to fit this regression, such that the surface is fitted for each 1 m^2 grid cell of the DEM, but taking into account a 99 m neighborhood. This scale best fits soil moisture data collected at a nearby site (Uriarte & Zimmerman, Data not shown). Slope and curvature were calculated from the fitted coefficients following the methods in Hurst et al. (2012). Hilltop curvature was calculated such that positive curvature indicates valley-like topography and negative curvature indicates ridge topography. We used the georeferenced stem locations from the plot data to extract slope and curvature at the stem location for each tree. Slope and curvature were not correlated (r = -0.004). Though the mean slope and curvature differ across plots, plots encompass large, overlapping ranges of values for slope and curvature (Appendix 4: Figure 1).

Modeling approach

We fit hierarchical Bayesian models of annual diameter growth and survival. Growth was normally distributed, as negative growth is common due to shrinkage. Our model of the expected value of growth took the form:

$$E(g_{tsi}) = \beta_{1s} + \beta_2 * \log(DBH_{tsi}) + \beta_{3s} * drought_t + \beta_{4s} \log(NCI_{tsi}) + \beta_{5s} * \log(slope_{si}) + \beta_{6s} * curvature_{si} + \beta_{7s} * \log(NCI_{tsi}) * drought_{tsi} + \beta_{8s} * \log(slope_{si}) * drought_{tsi} + \beta_{9s} * curvature_{si} * drought_{tsi} + \gamma_i$$

(Equation 1)

where g_{tsi} is absolute diameter growth of individual *i* of species *s* at time *t*. Covariates include stem diameter (DBH_{tsi}), a binary indicator for drought/non-drought year ($drought_t$ = 0 in 2014

and 2016, $drought_t = 1$ in 2015), slope and curvature for each stem ($slope_{si}$ and $curvature_{si}$), and NCI_{tsi}, a measure of neighborhood crowding. γ_i is an individual random effect for each stem. DBH, NCI, and slope were highly left-skewed and therefore log-transformed to facilitate analysis. Predictors were not strongly correlated (all $r < 0.16$, Table 2).

NCI is a dimensionless quantity calculated for each stem, taking into account the diameter and distance of all stems within a 10 m radius around the focal tree. Specifically, it is calculated as:

$$NCI_{tsi} = \sum_{j=1, i \neq j}^{J} \frac{DBH_j^2}{d_{ij}^2}$$

(equation 2)

where stem i has J neighbors within 10 m and d_{ij} is the distance from stem i to each neighbor j. We used a 10 m radius as prior studies have indicated that this radius is sufficient to capture effects of crowding (Uriarte et al. 2004a). Excluding trees less than 10 m from the edge of the plot would have resulted in exclusion of a large number of individuals. For those edge trees, we scaled their NCI by the ratio of a full-size neighborhood (i.e. a 10 m radius circle) to the size of the edge tree's partial neighborhood.

The model of survival took a similar form to the model of growth, but we used logistic regression and included a predictor term for each stem's previous year's growth ($g_{t-1,si}$). In the models of both growth and survival, we included data for all species with more than 20 individuals, and with available trait data (53 species; Appendix 4: Table 1), though all stems were included in calculations of neighborhood crowding. In the growth model, we excluded growth observations greater than two standard deviations from the mean, and in both models excluded observations with NCI greater than two standard deviations from the mean. This resulted in 26,833 growth observations and 28,828 survival observations across all years.

We incorporated functional traits into the second level of our model to assess how interspecific variation in functional traits mediates the effects of drought, topography, and crowding on tree demographics. If variation in functional traits represents variation in plant strategies, then species-level responses to stressful or high-resources conditions should vary predictably with their trait values. We expected that functional traits might influence average growth and survival rates (β_{1s}) along with species' sensitivities to drought (β_{3s}), crowding (β_{4s}), topography (β_{5s}, β_{6s}), and their interactions (β_{7s}, β_{8s}, β_{9s}). We did not model species-specific parameters for tree size (β_2). For each covariate (k) we modeled the species-specific β_{ks} as a normally distributed process deriving from a linear function of that species' traits:

$$\beta_{ks} \sim normal(b_k + b_{k1} * \log(SLA_s) + b_{k2} * WD_s,\ \sigma_k)$$

(equation 3)

σ_k is the variance in the covariate effects unexplained by trait variation. Because it was strongly left-skewed, we log-transformed SLA. We centered and scaled the traits so that b_k represents the mean species response to covariate k, and b_{k1} and b_{k2} represent the departure from the mean with an increase of one standard deviation of log(SLA) and WD, respectively.

We standardized all predictors to facilitate model convergence and ease interpretation (Gelman and Hill 2007). We standardized DBH and NCI on a species-by-species basis, to avoid confounding their effects with species-specific differences in size and crowding. Other predictors were standardized across the whole dataset. We specified uninformative priors for all parameters, and estimated posterior distributions using Markov chain Monte Carlo (MCMC) sampling implemented in JAGS (Plummer 2003). We verified convergence visually and by ensuring the potential scale reduction statistic ($\hat{R}$) was equal to 1 (Gelman and Rubin, 1992). Models generally converged after 30,000 iterations. We performed posterior predictive checks by

simulating predicted growth and survival for all observations and calculating the R^2 between predicted and observed values. All statistical analyses were conducted in R (R Development Core Team 2014) with the packages rjags and R2jags (Plummer et al. 2003, Su and Yajima 2015).

Results

Growth model

Across the study period, the average annual growth rate was 0.06 cm. Average growth was lowest during the drought year and highest in the year following the drought (Appendix 4: Figure 2). The model predicting tree growth was able to reproduce observed variation in growth ($R^2 = 0.32$), though it over/under predicted extreme high/low growth values (Appendix 4: Figure 3). Drought was the strongest predictor of growth, with lower growth during the drought year (Figure 1a). Diameter was also important, with larger trees having higher growth, on average (Figure 1a). Topography and crowding variables were significant predictors of tree growth. More crowded individuals (trees with higher NCI) had lower growth, as did trees on steeper slopes (Figure 1a, 2a, 2c). There was no significant interaction between crowding and drought, or between slope and drought, indicating that the effects of crowding and slope on growth were similar in drought vs. non-drought years (Figure 1a, 2a, 2c). The main effect for curvature was not significant, indicating that on average, curvature does not affect growth. However, there was a significant interaction between curvature and drought, indicating that trees located in areas with higher curvature were more negatively affected by drought (Figure 1a, 2b).

Though most trait effects were not significant, functional traits did influence growth via effects on species average growth, drought response, and response to topography (Table 3). High

wood density was associated with lower average growth rates (b_{12} in equation 3, Table 3). Trees with high wood density also had significantly less negative responses to drought (Figure 3). There were no significant trait associations with sensitivity of growth to crowding. SLA was negatively associated with slope response, such that the negative effect of growth was amplified for trees with high SLA (Figure 3). SLA also had a negative association with the curvature-drought interaction term, such that species with high SLA were more negatively affected by curvature during drought years (Table 3, Figure 4).

Survival model

The average survival rate across the whole dataset was 89%, with significant inter-annual variation (86% in 2014, 90% in 2015, 93% in 2016). The model of survival reproduced observed variation ($R^2 = 0.56$, Appendix 4: Figure 4). DBH and antecedent growth were the most important predictors of survival, with larger trees and trees that had experienced higher growth in the preceding year having a higher probability of survival. Drought also reduced survival, though it did not stand out relative to other predictors the way it did in the growth model (Figure 1b, Figure 2). Surprisingly, the effects of slope, curvature, and crowding were opposite to those in the growth model. More crowded trees and trees on steeper slopes had a higher probability of survival (Figure 1b, 2d, 2f). Higher curvature (i.e., valley habitats) reduced tree survival, contrary to expectations (Figure 1b, 2e). In the survival model none of the interaction terms were significant, indicating that the effects of topography and crowding on survival were similar, on average, across all three years of the study (Figure 2d-f).

There were a number of strong trait associations with survival (Table 3). Across the study period, trees with high SLA and high wood density had higher average survival, and responded

more positively to antecedent growth (Table 3). Wood density was not related to the effect of drought on survival. SLA, however, was significantly related to species' drought response, with trees with high SLA more likely to die during drought (Figure 3, Table 3). There were no significant trait associations with survival response to crowding.

However, we found complex interactions between the effects of topography, drought, and traits on survival. Both wood density and SLA were negatively associated with the slope effect on survival, meaning that trees with high SLA or high wood density had reduced survival on steep slopes. These traits were also significantly associated with the interaction between slope and drought. For SLA, there was a negative association with the drought-slope interaction, such that survival was further reduced for high-SLA trees on steep slopes (Figure 4). Wood density had a positive association with the interaction term, such that the negative relationship between wood density and the effect of slope on survival weakened during drought years. SLA was positively associated with response to curvature, such that trees with high SLA were more likely to survive in more valley-like sites (Figure 4). However, we found a significant relationship between SLA and the drought-curvature interaction, such that the relationship between SLA and the curvature effect flattened during drought years (Figure 4).

Discussion

Drought can have large effects on tropical forests, but impacts of drought vary across species and space (Bonal et al. 2016). Spatial variability in drought impacts is often driven by differences in the microclimates that individual trees experience, because of the way regional climate is filtered through topography, vegetation, and other environmental factors that vary on small scales (McLaughlin et al. 2017), and by species differences in physiology and drought

response. The 2015 drought in Puerto Rico provided a unique opportunity to leverage long-term data collected in a topographically complex tropical forest to examine the way that species differences and local filtering of climate affect drought response. Our study illustrates an integrative approach to predict demographic response to climate variation. We found evidence that drought affected tree performance, though effects on growth were stronger than survival. Topography and crowding influenced tree performance, but their effects and interactions with drought were not always in the direction we expected. Integrating functional traits into these models provided insight into the mechanisms by which drought, topography, and crowding affect tree performance.

Drought effects on tree performance

As expected, drought affected tree performance both directly and via interactions with topography. Though our models predicted greater mortality during drought years, the effect of drought on survival was relatively weak compared to the effects of topography and crowding on survival, and the effect of drought on survival was weaker than its effect on growth (Figure 1, Figure 2). In fact, survival was higher during the drought year than in the year preceding the drought, but it was lower than the year following the drought. This relatively weak effect of drought is consistent with other studies: in two drought experiments in the Amazon, 50-60% of rainfall was excluded, but mortality rates were low during the experiments' first years and major die-offs were only observed after about 3 years of prolonged drought (Nepstad et al. 2007, da Costa et al. 2010). In 2015, El Yunque rainfall was only 56% of the annual mean, but the drought only lasted for one year, perhaps not long enough to cause widespread mortality.

The effects of drought on growth were stronger than the effects on survival (Figure 1, 2). Tropical tree growth seems to respond to drought on more rapid time scales than survival: in the same throughfall experiments described above, growth impacts were apparent in the experiments' first years (Brando et al. 2008, da Costa et al. 2010). Tree-ring and long-term monitoring studies have found strong correlations between diameter growth and rainfall in tropical trees (Brienen et al. 2010, Clark et al. 2010). Reductions in radial growth may be driven by overall declines in productivity, and/or shifts in allocation from stem growth to leaves, branches, roots, or non-structural carbohydrates (Malhi et al. 2015). Trees can use non-structural carbohydrates to maintain NPP when photosynthetic rates are reduced during drought (Doughty et al. 2014), and shift allocation during and after drought (Metcalfe et al. 2010). The drivers of variation in tree allocation of carbon are poorly understood, though they are essential for understanding the mechanisms by which drought affects trees (Malhi et al. 2015).

Topography and crowding effects on tree performance

Steep slopes can be stressful environments, with lower soil moisture and shallower soil, so we expected that tree performance would be lower on steeper slopes. We found that growth was lower on steeper slopes, but surprisingly, survival was higher in steeper slopes, and the effect of slope did not vary between drought and non-drought years for both growth and survival. Though few studies have considered inter-specific variation in demographic rates along fine-scale topographical gradients in tropical forests, several studies have shown that local variation in water availability affects species distributions, with drought-tolerant species showing a stronger affinity for dry micro-sites where drought sensitive species may not persist (Ashton et al. 2006, Engelbrecht et al. 2007, Comita and Engelbrecht 2009). Such species sorting may occur

at our study sites, which would lead to a high abundance of trees with more conservative resource use strategies (i.e. lower growth but higher survival, Reich, 2014) on steep slopes. Lending some support to this hypothesis, we found a weak, but significant, negative correlation between slope and SLA, which is often assumed to be an acquisitive trait (Table 2). We also found growth and survival of trees with high SLA were more negatively affected by slope (Figure 3). Species sorting could also explain why the slope effect on growth was not stronger during drought years; if trees on steep slopes tend to be more drought-tolerant or conservative, they may not exhibit an elevated drought response despite experiencing more severe moisture stress.

The effect of species sorting may also help explain the results we observed with regards to curvature. Curvature represents how ridge-like or valley-like a surface is, and so we expected tree performance to be enhanced and drought effects to be minimized in valleys (positive curvature) relative to ridges. Our finding of lower survival at more positive curvature suggests that more acquisitive species—with higher growth rates but lower survival—are more abundant at valley-like positions. This possibility is further supported by the positive correlation between SLA and curvature and the negative correlation between wood density and curvature observed in our dataset (Table 2).

Our finding that growth did not vary with curvature during non-drought years suggests little advantage for trees in valleys (high curvature areas) during normal years, perhaps because consistently high rainfall means that soils are close to saturation regardless of their landscape position. Results from Panama support this hypothesis: seedling performance varied with microsite topography only in the dry season because all soils were at or near saturation during the wet season (Comita and Engelbrecht 2009). During drought years, however, there was a

negative growth response to curvature (Figure 2), despite our assumption that trees growing in areas with more positive curvature would experience less severe moisture deficits, and thus show less sensitivity to drought. The correlation between curvature and SLA may be driving this result: trees growing in valleys are more frequently of species that are more sensitive to drought and thus show a stronger growth response despite experiencing less severe moisture stress.

Somewhat contrary to our prediction that crowding would negatively impact tree performance, we found crowding reduced growth but, surprisingly, increased survival. While many studies have shown that competitive effects from crowding have a negative impact on tree performance (Uriarte et al. 2012a), others have shown no effect on growth and/or survival (Uriarte et al. 2016, Lasky et al. 2014) or even positive effects (Hurst et al. 2011). Furthermore, sensitivity to crowding varies across species (Uriarte et al. 2004b, 2004a, Canham et al. 2009). Variation in the effects of crowding across studies and our finding that crowding increased survival could have to do with the difficulty of disentangling the competitive impacts of crowding from the environmental drivers of crowding. Variation in number and size of stems within and across forest stands can be driven by variation in site favorability (Clark and Clark 2000, Malhi et al. 2006, Alves et al. 2010, Hernández-Stefanoni et al. 2011). If this is the case, our finding of enhanced survival in more crowded neighborhoods could reflect site quality. Trees in more crowded stands tend to allocate more carbon to height versus radial growth (Holbrook and Putz 1989, Weiner and Thomas 1992, Naidu et al. 1998, Poorter 2001), potentially explaining the observed negative effect of crowding on stem growth despite the positive effect of survival. This hypothesis is also consistent with our finding that crowding effects were not amplified during drought years. However, we found very low correlation between both of our topographic variables and crowding (Table 2). This lack of relationship suggests that if the

effects of crowding are driven by site favorability, soil nutrients or another factor and not topography, underlie variation in site favorability.

Interactions between functional traits, drought, topography, and tree performance

Variation in plant functional traits reflects differences in plant strategies, which span a tradeoff axis from "fast," acquisitive strategies that involve high growth and metabolic rates and strong competitive ability to quickly take up resources, to "slow," conservative strategies which entail lower metabolic rates, but enhanced ability to survive under low resource conditions (Wright et al. 2004, Reich 2014). These strategies can be manifested as a growth vs. survival trade-off, in which slow-growing conservative species have higher rates of survival while fast growing species have shorter lifespans (Sterck et al. 2006). The growth-survival tradeoff is partially reflected in our results: wood density is negatively related to average growth, but positively associated with average survival (b_{12}, Table 3). This supports many studies that have found that high wood density is a conservative strategy that entails low growth, but enhanced persistence under more stressful conditions (Chave et al. 2009, Poorter et al. 2010). Our results for SLA, however, are less consistent with expectations: we found that trees with high SLA had slightly above-average growth (non-significant, positive relationship with b_{11}), and above average survival. Though surprising, this fits in with the highly variable and poorly resolved relationships between SLA and performance in other studies. For example, Lasky et al. (2015) found the expected growth-survival tradeoff with SLA, while Poorter et al. (2008) found a negative association between SLA and growth, and no relationship between SLA and survival.

Differences in plant strategies are reflected in variation in performance across topography. For example, the reduced performance of high SLA species on slopes, and enhanced

growth at high curvature suggests that high SLA is associated with low stress tolerance, but enhanced performance in high-resource areas. Apart from a negative effect of wood density on the slope effect on survival, there was no relationship between wood density and variation in performance across topography. Many studies have linked variation in wood density to shade tolerance (Lawton 1984, Poorter et al. 2010, Markesteijn et al. 2011), and so it is possible that light, which is likely unrelated to microtopography, is a stronger filter on performance as it relates to wood density. These associations between traits, topography, and performance likely underlie some of the fine-scale species sorting discussed above.

By incorporating functional traits into models of tree performance across environmental gradients, we can begin to identify general mechanisms by which environmental variation affects trees and species differentially. For example, we found that trees with high SLA were more likely to die during drought. Trees with high SLA tend to have higher photosynthetic rates and accordingly, higher transpiration rates, which predisposes them to higher levels of water loss during drought (depending on stomatal regulation, Poorter *et al.*, 2009). Though there was no relationship between wood density and the drought effect on survival, growth rates of trees with high wood density were less sensitive to drought. During non-drought conditions, trees with high wood density typically have slower growth rates due to lower transpiration rates and the higher carbon cost of building denser wood (Chave et al. 2009). However, these trees can also maintain hydraulic conductivity under drier conditions (Chave et al. 2009, Reich 2014) and so may be able to maintain photosynthetic and growth rates closer to normal during drought.

Our findings that trees with high wood density were less sensitive to drought, while trees with high SLA were more sensitive to drought, are consistent with other studies (Metcalfe et al. 2010, Phillips et al. 2010, Uriarte et al. 2016a). A recent meta-analysis found that globally, these

two traits are associated with sensitivity to drought-induced mortality (Greenwood et al. 2017). However, the strength and direction of these relationships have differed across studies (Russo et al. 2010, Hoffmann et al. 2011, O'Brien et al. 2017). Though SLA and wood density are indirectly related to water use strategies, neither is a direct measurement of plant hydraulics. Measuring hydraulic traits such as turgor loss point, water potential at 50% loss of conductivity, or stem water potential may provide more power for predicting species' drought responses (Bartlett et al. 2012, Maréchaux et al. 2015, O'Brien et al. 2017). Though these measurements can be expensive and time consuming (O'Brien et al. 2017), new methods are making them easier (Maréchaux et al. 2015), providing a promising way forward to improving predictions of drought response. The modeling framework we demonstrate here, which incorporates functional traits, drought response, and environmental variability could easily be applied with hydraulic trait data, and could greatly improve our ability to predict drought responses.

Acknowledgements

This work was supported by US National Science Foundation (NSF) awards DEB-1050957 to MU and DEB-1546686 to the Institute for Tropical Ecosystem Studies, University of Puerto Rico, working with the International Institute of Tropical Forestry (USDA Forest Service), for the Luquillo Long-Term Ecological Research Program. We thank the census crews that collected the data.

Figures and Tables

Figure 1: Average parameters from growth and survival models. Open circles are not significant. Parameter values are bk (equation 3) i.e. effects at the mean trait values.

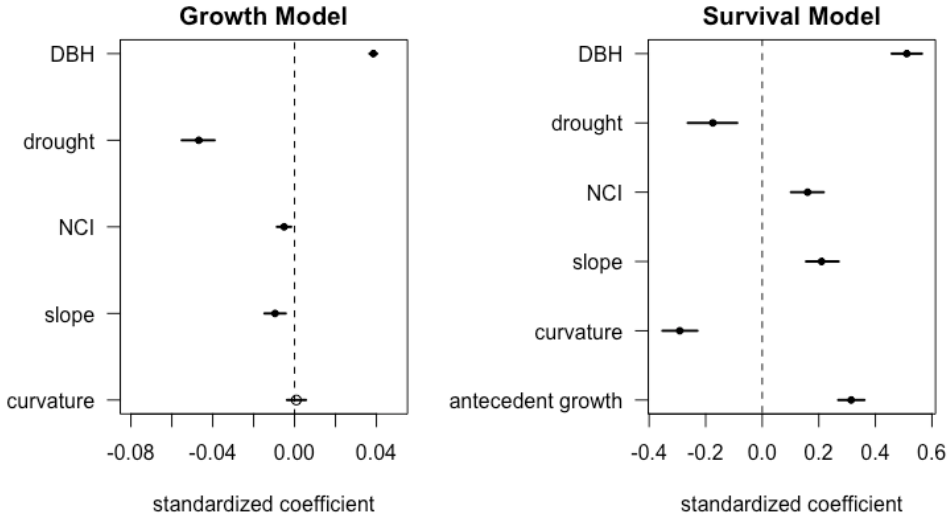

Figure 2: Predicted growth (a-c) and probability of survival (d-f) as a function of slope, curvature, and neighborhood crowding. Text in the lower left corner indicates whether main effects and interactions were significant* or not significant (n.s.).

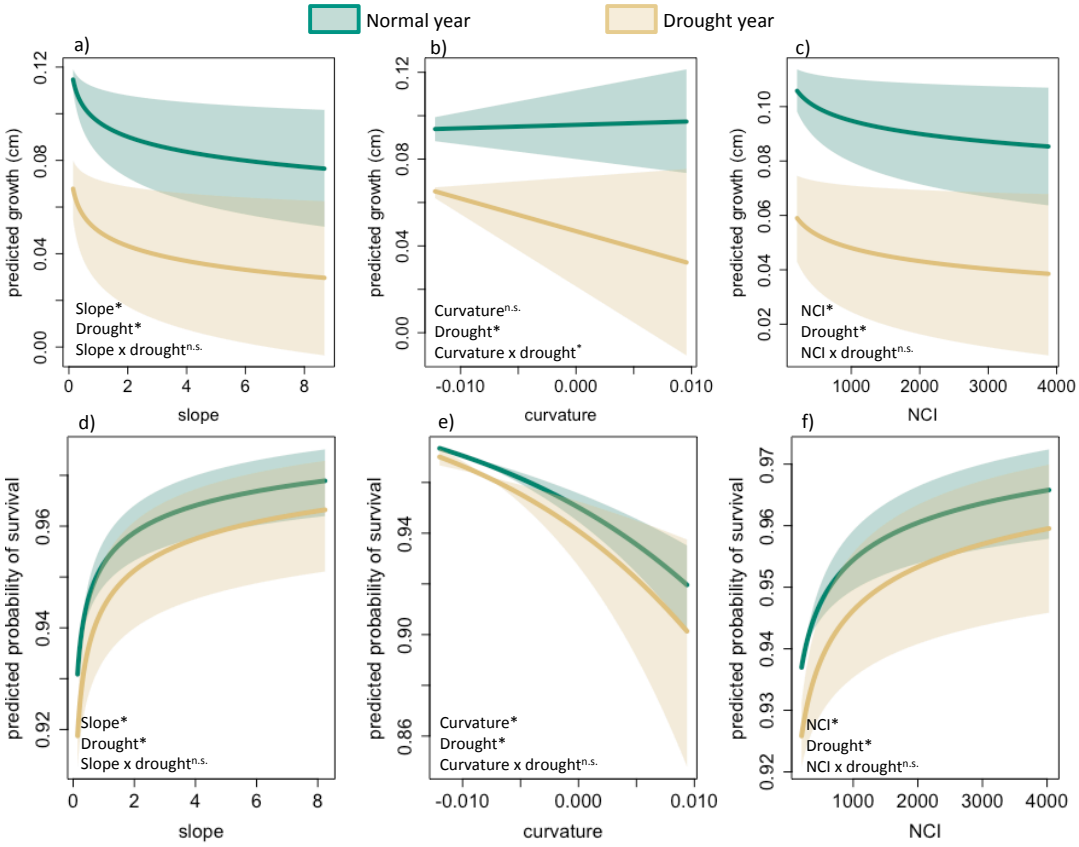

Figure 3: Relationships between traits (x-axis) and select species-specific estimates of model parameters (y-axis). All relationships shown were significantly different from zero. a) drought effect (growth model) vs. wood density. b) slope effect (growth model) vs. SLA. c) drought effect (survival model) vs. SLA. Note that SLA is log-transformed as we log-transformed it for our models.

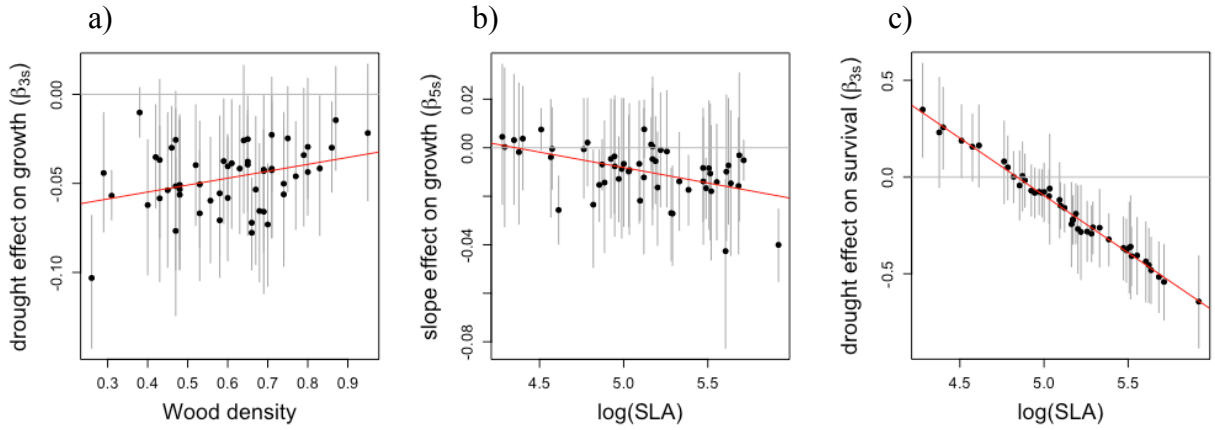

Figure 4: Relationships between traits (x-axis) and species-specific estimates of model parameters (y-axis) for variables which had a significant trait effect on the interaction term. Green points show variables' effects on performance during normal years, beige shows effects during drought years. a) Curvature effect (growth model) vs. SLA. b) Slope effect (survival model) vs. SLA. b) Curvature effect (growth model) vs. SLA.

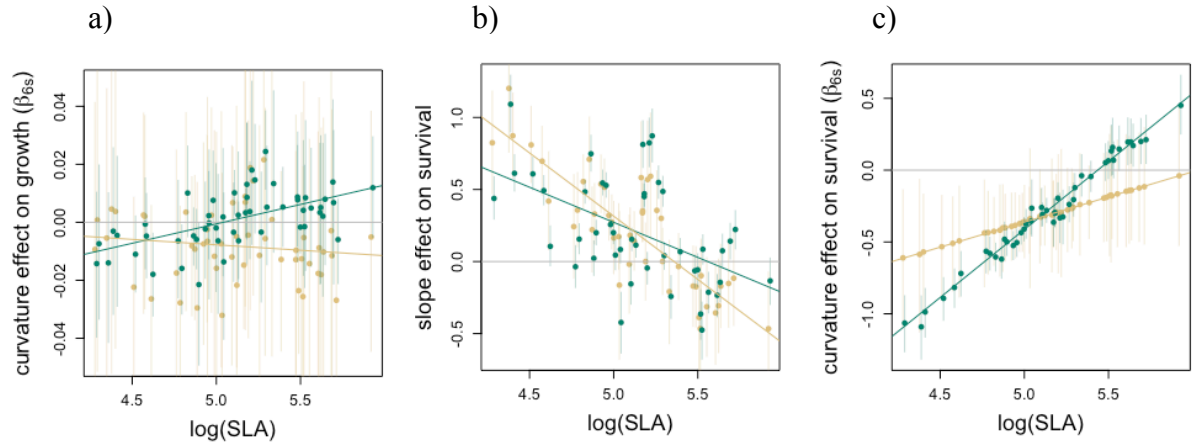

Table 1: Study site descriptions

Plot Name	Size (m^2)	Age, determined from aerial photos	Elevation	N stems in 2016
EV1	10,000	>62 yrs but < 76 yrs	~ 550m	2937
SB1	4,625	>35 yrs but < 62 yrs	~100-150m	2496
SB2	6,400	>62 yrs but not primary forest	~100-150m	4665
SB3	4,800	Primary forest	~100-150m	1756

Table 2: Correlations between variables and traits in the growth dataset. ** indicates $p < 0.01$, *** indicates $p < 0.001$.

	Diameter	NCI	Slope	Curvature	SLA	WD
Diameter	1					
NCI	-0.07***	1				
Slope	0.04***	0.07***	1			
Curvature	-0.02	-0.05***	0.02**	1		
SLA	0	0	-0.17***	0.12***	1	
WD	0	0	0.08***	-0.15***	-0.37**	1

Table 3: Trait results w 90% credible intervals. * indicates significant difference from 0. NA indicates parameter was not included in model.

Covariate	**SLA**	**Growth**	**Survival**
Intercept	b_{11}	0.008 (-0.008, 0.024)	0.41 (0.35, 0.48)*
Drought	b_{31}	0.008 (-0.001, 0.017)	-0.22 (-0.31, -0.10)*
NCI	b_{41}	-0.001 (-0.004, 0.003)	0.06 (-0.00, 0.12)
Slope	b_{51}	-0.005 (-0.012, -0.000)*	-0.31 (-0.38, -0.25)*
Curvature	b_{61}	0.004 (-0.002, 0.010)	0.39 (0.31, 0.47)*
NCI x drought	b_{71}	-0.002 (-0.008, 0.002)	-0.05 (-0.14, 0.03)
Slope x drought	b_{81}	0.004 (-0.002, 0.011)	-0.11 (-0.20, -0.02)*
Curvature x drought	b_{91}	-0.008 (-0.015, -0.002)*	-0.25 (-0.36, -0.13)*
Antecedent growth		NA	0.27 (0.22, 0.32)*
	WD	**Growth**	**Survival**
Intercept	b_{12}	-0.016 (-0.032, -0.000)*	0.12 (0.06, 0.20)*
Drought	b_{32}	0.010 (0.001, 0.018)*	0.03 (-0.07, 0.12)
NCI	b_{42}	-0.001 (-0.005, 0.002)	0.02 (-0.05, 0.09)
Slope	b_{52}	-0.001 (-0.007, 0.004)	-0.34 (-0.42, -0.26)*
Curvature	b_{62}	-0.004 (-0.009, 0.001)	0.06 (-0.02, 0.13)
NCI x drought	b_{72}	-0.001 (-0.005, 0.005)	0.02 (-0.08, 0.12)
Slope x drought	b_{82}	0.004 (-0.002, 0.010)	0.11 (0.001, 0.22)*
Curvature x drought	b_{92}	-0.003 (-0.010, 0.002)	-0.05 (-0.15, 0.05)
Antecedent growth		NA	0.06 (0.01, 0.10)*

CONCLUSION

Tropical second growth forests have the potential to provide a wide variety of benefits to people and nature on local and global scales (Locatelli et al. 2015, Chazdon et al. 2016), and many countries have set ambitious restoration targets under the Paris Climate Agreement and other mechanisms (see Chapter 1). However, the degree to which these targets are met and sustained will in part depend on forest exposure to disturbance and extreme events, which can be high due to second-growth forests' location in fragmented, human-dominated landscapes and their high proportion of vulnerable species (Uriarte et al. 2016). This dissertation examined how landscape context influences vulnerability to disturbance and extreme events in tropical second-growth forests. By integrating a variety of types of data and taking a long-term perspective, I hope that my dissertation has improved our understanding of the causes of disturbance in second-growth forests and the consequences for ecology, carbon sequestration, and management.

Second-growth forests are, by definition, subject to human influences whether through the residual effects of prior land-use or through human activities in and around second-growth forests (Guariguata and Ostertag 2001). This dissertation shows that understanding the ecological dynamics of second growth forests requires considering them in the context of the human-dominated landscapes in which they tend to be located. For example, Chapter 1 illustrates that where forest is most likely to regrow is strongly influenced by spatial location in the landscape, and linked to anthropogenic features such as roads and villages. The results in Chapter 2 highlight the importance of anthropogenic factors in driving fire activity; forest exposure to fire in the study landscape is largely subject to controls linked to human activities and forest position on the landscape, and characteristics of the forest itself may be less important. In a similar vein, Chapter 3 illustrates how vulnerability to wind damage varies with fragmentation, again

emphasizing how important a forest's location in a landscape matrix is. Finally, Chapter 4 highlights the importance of non-anthropogenic landscape factors, specifically topography, in shaping forest demographics and vulnerability to drought. Considering the role of topography in second-growth forest ecology may be particularly important since most land abandonment occurs on steep and marginal terrain (Helmer 2000, Asner et al. 2009b).

The strong influence of landscape context on second-growth forest ecology means that a landscape perspective is also highly important for carbon accounting and predicting future carbon fluxes. In Chapter 1, I show that estimates of future carbon sequestration in second-growth forests differ significantly depending on assumptions made about landscape context and exposure to clearing. Chapters 2 and 3 show how exposure to disturbance, which can have a major impact on rates and quantities of carbon sequestration, varies with land cover and fragmentation. Chapter 3 also demonstrates how ignoring the effects of fragmentation can result in underestimating the role of extreme winds in driving carbon loss in tropical forests. Finally, the results from Chapter 4 highlight the importance of considering topography when modeling tree performance and forest dynamics. Currently, most dynamic global vegetation models such as the Ecosystem Demography model (Medvigy et al. 2009) and LPJ (Smith et al. 2001) do not incorporate topographic indices or lateral movement of water (but see Tang et al. 2014), though, as our results illustrate, small-scale topography and hydrologic variation can affect tree performance and carbon fluxes (Sjögersten et al. 2006, Pacific et al. 2008, Lecki and Creed 2016). Incorporating landscape context and topography into these models could affect outputs and estimates of future carbon fluxes and other ecosystem properties.

I hope that the results of this dissertation are useful for people making decisions about forest management and landscape planning. Many countries have recently developed plans for

large-scale forest restoration and natural regeneration and other countries will likely follow suit in upcoming years (Chazdon and Guariguata 2016). Such plans require prioritizing and protecting areas where natural regeneration and restoration are likely to be most successful (Chazdon and Guariguata 2016). The results from this dissertation could be useful for such efforts: for example, forest protection, tree planting, and fire prevention programs could be spatially targeted at the most fragmented and vulnerable locations. Furthermore, the interdisciplinary approaches demonstrated in this dissertation could be useful for studying other landscapes where anthropogenic influences and their impacts on forest ecology may differ.

Finally, this dissertation illustrates the insight that can be gained by taking a long-term, observational approach to understanding ecological processes at a landscape scale. Experimental manipulations of tropical forests are logistically difficult and all but impossible to conduct at the requisite scale to understand the influence of spatial configuration and landscape context (but see Laurance et al. 2002). Satellite remote sensing and long-term data give researchers the ability to take a broad-scale perspective, to look back in time, and to "be in the right place all the time" in order to observe the impacts of large-scale disturbances and extreme events when they occur. However, these approaches, while powerful for detecting spatial and temporal patterns across landscapes, may be limited in their ability to observe the processes and mechanisms that generate observed patterns. Future research could delve into the biological and social mechanisms behind the patterns detected in this study. For example, field measurements of forest structure, composition, and wind speed could help disentangle the mechanisms responsible for increasing wind damage in fragmented forests. Studying differences in soil moisture and other soil characteristics with microtopography could help explain the plant demographic patterns observed in Chapter 4. Surveys of people's land-use practices in the study area could shed light on what

drives people's decisions to clear or protect second-growth forest and help explain the spatial patterns in Chapter 1.

Disturbance, extreme events, and human influences are important and unavoidable parts of most ecosystems, especially tropical forests. Better understanding how the biophysical and social aspects of landscapes influence vulnerability to disturbance and extreme events allows us to anticipate, manage, and/or minimize their negative impacts. I hope that this dissertation broadens and deepens our understanding of the landscape and disturbance ecology of tropical forests, and that it contributes to future efforts to conserve and promote tropical second-growth forests to benefit humans and nature.

REFERENCES CITED

Adams, J., and A. R. Gillespie. 2006. Remote sensing of landscapes with spectral images. Cambridge University Press, Cambridge, UK.

Aide, T. M., M. L. Clark, H. R. Grau, D. López-Carr, M. A. Levy, D. Redo, M. Bonilla-Moheno, G. Riner, M. J. Andrade-Núñez, and M. Muñiz. 2013. Deforestation and Reforestation of Latin America and the Caribbean (2001-2010). Biotropica 45:262–271.

Alencar, A. A. C., L. A. Solórzano, and D. C. Nepstad. 2004. Modeling forest understory fires in an eastern amazonian landscape. Ecological Applications 14:139–149.

Alencar, A., G. P. Asner, D. Knapp, and D. Zarin. 2011. Temporal variability of forest fires in eastern Amazonia. Ecological Applications 21:2397–412.

Alencar, A., C. Vera, D. Nepstad, and M. Del Carmen Vera Diaz. 2006. Forest understory fire in the Brazilian Amazon in ENSO and non-ENSO years: Area burned and committed carbon emissions. Earth Interactions 10:1–17.

Alves, L. F., S. A. Vieira, M. A. Scaranello, P. B. Camargo, F. A. M. Santos, C. A. Joly, and L. A. Martinelli. 2010. Forest structure and live aboveground biomass variation along an elevational gradient of tropical Atlantic moist forest (Brazil). Forest Ecology and Management 260:679–691.

Anderson-Teixeira, K. J., A. D. Miller, J. E. Mohan, T. W. Hudiburg, B. D. Duval, and E. H. DeLucia. 2013. Altered dynamics of forest recovery under a changing climate. Global Change Biology 19:2001–2021.

Aragão, L. E. O. C., Y. Malhi, N. Barbier, A. A. Lima, Y. Shimabukuro, L. Anderson, and S. Saatchi. 2008. Interactions between rainfall, deforestation and fires during recent years in the Brazilian Amazonia. Philosophical Transactions of the Royal Society of London. Series B, Biological Sciences 363:1779–85.

Aragão, L. E. O. C., Y. Malhi, R. M. Roman-Cuesta, S. Saatchi, L. O. Anderson, and Y. E. Shimabukuro. 2007. Spatial patterns and fire response of recent Amazonian droughts. Geophysical Research Letters 34:L07701.

Aragão, L. E. O. C., and Y. E. Shimabukuro. 2010. The incidence of fire in Amazonian forests with implications for REDD. Science 328:1275–8.

Archibald, S., D. P. Roy, B. W. van Wilgen, and R. J. Scholes. 2009. What limits fire? An examination of drivers of burnt area in Southern Africa. Global Change Biology 15:613–630.

Armenteras, D., T. M. González, and J. Retana. 2013. Forest fragmentation and edge influence on fire occurrence and intensity under different management types in Amazon forests. Biological Conservation 159:73–79.

Armenteras, D., and J. Retana. 2012. Dynamics, patterns and causes of fires in Northwestern Amazonia. PloS one 7:e35288.

Ashton, M. S., B. M. P. Singhakumara, and H. K. Gamage. 2006. Interaction between light and drought affect performance of Asian tropical tree species that have differing topographic affinities. Forest Ecology and Management 221:42–51.

Asner, G. P., and A. Alencar. 2010. Drought impacts on the Amazon forest: the remote sensing perspective. The New phytologist 187:569–78.

Asner, G. P., R. E. Martin, A. J. Ford, D. J. Metcalfe, and M. J. Liddell. 2009a. Leaf chemical and spectral diversity in Australian tropical forests. Ecological Applications 19:236–253.

Asner, G. P., T. K. Rudel, T. M. Aide, R. Defries, and R. Emerson. 2009b. A contemporary

assessment of change in humid tropical forests. Conservation Biology 23:1386–1395.
Balch, J. K., D. C. Nepstad, P. M. Brando, L. M. Curran, O. Portela, O. de Carvalho, and P. Lefebvre. 2008. Negative fire feedback in a transitional forest of southeastern Amazonia. Global Change Biology 14:2276–2287.
Balch, J. K., D. C. Nepstad, L. M. Curran, P. M. Brando, O. Portela, P. Guilherme, J. D. Reuning-Scherer, and O. de Carvalho. 2011. Size, species, and fire behavior predict tree and liana mortality from experimental burns in the Brazilian Amazon. Forest Ecology and Management 261:68–77.
Barlow, J., T. a Gardner, I. S. Araujo, T. C. Avila-Pires, a B. Bonaldo, J. E. Costa, M. C. Esposito, L. V Ferreira, J. Hawes, M. I. M. Hernandez, M. S. Hoogmoed, R. N. Leite, N. F. Lo-Man-Hung, J. R. Malcolm, M. B. Martins, L. a M. Mestre, R. Miranda-Santos, a L. Nunes-Gutjahr, W. L. Overal, L. Parry, S. L. Peters, M. a Ribeiro-Junior, M. N. F. da Silva, C. da Silva Motta, and C. a Peres. 2007. Quantifying the biodiversity value of tropical primary, secondary, and plantation forests. Proceedings of the National Academy of Sciences 104:18555–60.
Barlow, J., B. O. Lagan, and C. A. Peres. 2003. Morphological correlates of fire-induced tree mortality in a central Amazonian forest. Journal of Tropical Ecology 19:291–299.
Bartlett, M. K., C. Scoffoni, and L. Sack. 2012. The determinants of leaf turgor loss point and prediction of drought tolerance of species and biomes: A global meta-analysis. Ecology Letters 15:393–405.
Bartlett, M. K., Y. Zhang, J. Yang, N. Kreidler, S. W. Sun, L. Lin, Y. H. Hu, K. F. Cao, and L. Sack. 2016. Drought tolerance as a driver of tropical forest assembly: Resolving Spatial signatures for multiple processes. Ecology 97:503–514.
Bazzaz, F. A., and S. T. A. Pickett. 1980. Physiological Ecology of Tropical Succession : A comparative review. Annual Review of Ecology and Systematics 11:287–310.
Bedka, K. M., and K. Khlopenkov. 2016. A Probabilistic Multispectral Pattern Recognition Method for Detection of Overshooting Cloud Tops Using Passive Satellite Imager Observations. Journal of Applied Meteorology and Climatology 55:1983–2005.
Bellingham, P. J., V. Kapos, N. Varty, J. R. Healey, E. V. J. Tanner, D. L. Kelly, J. W. Dalling, L. S. Burns, D. Lee, and G. Sidrak. 1992. Hurricanes Need Not Cause High Mortality: The Effects of Hurricane Gilbert on Forests in Jamaica. Journal of Tropical Ecology 8:217–223.
Belsley, D. A. 1991. A Guide to using the collinearity diagnostics. Computer Science in Economics and Management 4:33–50.
Bennett, A. C., N. G. McDowell, C. D. Allen, and K. J. Anderson-Teixeira. 2015. Larger trees suffer most during drought in forests worldwide. Nature Plants 1:15139.
Boardman, J. W., F. a. Kruse, and R. O. Green. 1995. Mapping target signatures via partial unmixing of AVIRIS data. Summaries of JPL Airborne Earth Science Workshop:3–6.
Bonal, D., B. Burban, C. Stahl, F. Wagner, and B. Hérault. 2016. The response of tropical rainforests to drought - lessons from recent research and future prospects. Annals of Forest Science 73:27–44.
Bowman, D. M. J. S., J. Balch, P. Artaxo, W. J. Bond, M. A. Cochrane, C. M. D'Antonio, R. Defries, F. H. Johnston, J. E. Keeley, M. A. Krawchuk, C. A. Kull, M. Mack, M. A. Moritz, S. Pyne, C. I. Roos, A. C. Scott, N. S. Sodhi, and T. W. Swetnam. 2011. The human dimension of fire regimes on Earth. Journal of Biogeography 38:2223–2236.
Bowman, D. M. J. S., J. K. Balch, P. Artaxo, W. J. Bond, J. M. Carlson, M. A. Cochrane, C. M. DíAntonio, R. S. DeFries, J. C. Doyle, and S. P. Harrison. 2009. Fire in the Earth system.

Science 324:481.
Bowman, M. S., G. S. Amacher, and F. D. Merry. 2008. Fire use and prevention by traditional households in the Brazilian Amazon. Ecological Economics 67:117–130.
Bradstock, R. A., K. A. Hammill, L. Collins, and O. Price. 2010. Effects of weather, fuel and terrain on fire severity in topographically diverse landscapes of south-eastern Australia. Landscape Ecology 25:607–619.
Brando, P. M., D. C. Nepstad, J. K. Balch, B. Bolker, M. C. Christman, M. Coe, and F. E. Putz. 2012. Fire-induced tree mortality in a neotropical forest: the roles of bark traits, tree size, wood density and fire behavior. Global Change Biology 18:630–641.
Brando, P. M., D. C. Nepstad, E. A. Davidson, S. E. Trumbore, D. Ray, and P. Camargo. 2008. Drought effects on litterfall, wood production and belowground carbon cycling in an Amazon forest: results of a throughfall reduction experiment. Philosophical Transactions of the Royal Society B: Biological Sciences 363:1839–1848.
Brienen, R. J. W., E. Lebrija-Trejos, P. A. Zuidema, and M. Martínez-Ramos. 2010. Climate-growth analysis for a Mexican dry forest tree shows strong impact of sea surface temperatures and predicts future growth declines. Global Change Biology 16:2001–2012.
Brinck, K., R. Fischer, J. Groeneveld, S. Lehmann, M. Dantas De Paula, S. Pütz, J. O. Sexton, D. Song, and A. Huth. 2017. High resolution analysis of tropical forest fragmentation and its impact on the global carbon cycle. Nature Communications 8:14855.
Broadbent, E. N., G. P. Asner, M. Keller, D. E. Knapp, P. J. C. Oliveira, and J. N. Silva. 2008. Forest fragmentation and edge effects from deforestation and selective logging in the Brazilian Amazon. Biological Conservation 141:1745–1757.
Brondizio, E. S., and E. F. Moran. 2008. Human dimensions of climate change: the vulnerability of small farmers in the Amazon. Philosophical Transactions of the Royal Society B: Biological Sciences 363:1803–1809.
Brooks, S., and A. Gelman. 1998. General methods for monitoring convergence of iterative simulations. Journal of computational and graphical Statistics 7:434–455.
Brown, F., G. Santos, F. Pires, and C. da costa. 2011. World Resources Report Case Study. Brazil: Drought and Fire Response in the Amazon. Page World Resources Report. Washington, DC.
Brown, S., and A. E. Lugo. 1982. The Storage and Production of Organic Matter in Tropical Forests and Their Role in the Global Carbon Cycle. Biotropica 14:161.
Brown, S., and A. E. Lugo. 1990. Tropical secondary forests. Journal of Tropical Ecology 6:1–32.
Buchanan, B. P., M. Fleming, R. L. Schneider, B. K. Richards, J. Archibald, Z. Qiu, and M. T. Walter. 2014. Evaluating topographic wetness indices across central New York agricultural landscapes. Hydrology and Earth System Sciences 18:3279–3299.
Burt, T. P., and D. P. Butcher. 1985. Topographic Controls of Soil-Moisture Distributions. Journal of Soil Science 36:469–486.
Bush, M. ., M. . Silman, C. McMichael, and S. Saatchi. 2008. Fire, climate change and biodiversity in Amazonia: a Late-Holocene perspective. Philosophical Transactions of the Royal Society B: Biological Sciences 363:1795–1802.
Canham, C. D., M. J. Papaik, M. Uriarte, W. H. Mcwilliams, J. C. Jenkins, and M. J. Twery. 2009. Neighborhood analyse of canopy tree competition along environmental gradients in New England forests. Ecological Applications 16:540–554.
Canham, C. D., J. Thompson, J. K. Zimmerman, and M. Uriarte. 2010. Variation in susceptibility

to hurricane damage as a function of storm intensity in puerto Rican tree species. Biotropica 42:87–94.
Canty, M. J., and A. A. Nielsen. 2008. Automatic radiometric normalization of multitemporal satellite imagery with the iteratively re-weighted MAD transformation. Remote Sensing of Environment 112:1025–1036.
Cardille, J. a, and S. J. Ventura. 2001. Environmental and Social Factors Influencing Wildfires in the Upper Midwest, United States. Ecological Applications 11:111–127.
Carmenta, R., S. Vermeylen, L. Parry, and J. Barlow. 2013. Shifting Cultivation and Fire Policy: Insights from the Brazilian Amazon. Human Ecology 41:603–614.
de Casenave, J. L., J. P. Pelotto, and J. Protomastro. 1995. Edge-interior differences in vegetation structure and composition in a Chaco semi-arid forest, Argentina. Forest Ecology and Management 72:61–69.
Catterall, C. P., S. McKenna, J. Kanowski, and S. D. Piper. 2008. Do cyclones and forest fragmentation have synergistic effects? A before-after study of rainforest vegetation structure at multiple sites. Austral Ecology 33:471–484.
Chadwick, R., P. Good, G. Martin, and D. P. Rowell. 2015. Large rainfall changes consistently projected over substantial areas of tropical land. Nature Climate Change 6:177–182.
Chambers, J. Q., G. P. Asner, D. C. Morton, L. O. Anderson, S. S. Saatchi, F. D. B. Espírito-Santo, M. Palace, and C. Souza. 2007. Regional ecosystem structure and function: ecological insights from remote sensing of tropical forests. Trends in Ecology and Evolution 22:414–423.
Chambers, J. Q., R. I. Negrón-Juárez, G. C. Hurtt, D. M. Marra, and N. Higuchi. 2009. Lack of intermediate-scale disturbance data prevents robust extrapolation of plot-level tree mortality rates for old-growth tropical forests. Ecology Letters 12:22–25.
Chambers, J. Q., R. I. Negron-Juarez, D. M. Marra, A. Di Vittorio, J. Tews, D. Roberts, G. H. P. M. Ribeiro, S. E. Trumbore, and N. Higuchi. 2013. The steady-state mosaic of disturbance and succession across an old-growth Central Amazon forest landscape. Proceedings of the National Academy of Sciences 110:3949–3954.
Chave, J., D. Coomes, S. Jansen, S. L. Lewis, N. G. Swenson, and A. E. Zanne. 2009. Towards a worldwide wood economics spectrum. Ecology Letters 12:351–366.
Chazdon, R. L., A. R. Brenes, and B. V. Alvarado. 2005. Effects of climate and stand age on annual tree dynamics in tropical second-growth rain forests. Ecology 86:1808–1815.
Chazdon, R. L., E. N. Broadbent, D. M. A. Rozendaal, F. Bongers, A. M. A. Zambrano, T. M. Aide, P. Balvanera, J. M. Becknell, V. Boukili, P. H. S. Brancalion, D. Craven, J. S. Almeida-Cortez, G. A. L. Cabral, B. de Jong, J. S. Denslow, D. H. Dent, S. J. DeWalt, J. M. Dupuy, S. M. Duran, M. M. Espirito-Santo, M. C. Fandino, R. G. Cesar, J. S. Hall, J. L. Hernandez-Stefanoni, C. C. Jakovac, A. B. Junqueira, D. Kennard, S. G. Letcher, M. Lohbeck, M. Martinez-Ramos, P. Massoca, J. A. Meave, R. Mesquita, F. Mora, R. Munoz, R. Muscarella, Y. R. F. Nunes, S. Ochoa-Gaona, E. Orihuela-Belmonte, M. Pena-Claros, E. A. Perez-Garcia, D. Piotto, J. S. Powers, J. Rodriguez-Velazquez, I. E. Romero-Perez, J. Ruiz, J. G. Saldarriaga, A. Sanchez-Azofeifa, N. B. Schwartz, M. K. Steininger, N. G. Swenson, M. Uriarte, M. van Breugel, H. van der Wal, M. D. M. Veloso, H. Vester, I. C. G. Vieira, T. V. Bentos, G. B. Williamson, and L. Poorter. 2016. Carbon sequestration potential of second-growth forest regeneration in the Latin American tropics. Science Advances 2:e1501639–e1501639.
Chazdon, R. L., and M. R. Guariguata. 2016. Natural regeneration as a tool for large-scale forest

restoration in the tropics: prospects and challenges. Biotropica 48:716–730.
Chazdon, R. L., C. A. Peres, D. Dent, D. Shiel, A. E. Lugo, D. Lamb, N. E. Stork, and S. E. Miller. 2009. The Potential for Species Conservation in Tropical Secondary Forests. Conservation Biology 23:1406–1417.
Chen, Y., J. T. Randerson, D. C. Morton, R. S. DeFries, G. J. Collatz, P. S. Kasibhatla, L. Giglio, Y. Jin, and M. E. Marlier. 2011. Forecasting Fire Season Severity in South America Using Sea Surface Temperature Anomalies. Science 334:787–791.
Clark, D. ., and D. . Clark. 2000. Landscape-scale variation in forest structure and biomass in a tropical rain forest. Forest Ecology and Management 137:185–198.
Clark, D. B., D. A. Clark, and S. F. Oberbauer. 2010. Annual wood production in a tropical rain forest in NE Costa Rica linked to climatic variation but not to increasing CO2. Global Change Biology 16:747–759.
Cochrane, M. A., and W. F. Laurance. 2002. Fire as a large-scale edge effect in Amazonian forests. Journal of Tropical Ecology 18:311–325.
Cochrane, M. A., and W. F. Laurance. 2008. Synergisms among Fire, Land Use, and Climate Change in the Amazon. AMBIO: A Journal of the Human Environment 37:522–527.
Cochrane, M. A., and M. D. Schulze. 1999. Fire as a Recurrent Event in Tropical Forests of the Eastern Amazon: Effects on Forest Structure, Biomass, and Species Composition1. Biotropica 31:2–16.
Comita, L. S., and B. M. J. Engelbrecht. 2009. Seasonal and spatial variation in water availability drive habitat associations in a tropical forest. Ecology 90:2755–2765.
Coomes, O. T., F. Grimard, and G. J. Burt. 2000. Tropical forests and shifting cultivation: Secondary forest fallow dynamics among traditional farmers of the Peruvian Amazon. Ecological Economics 32:109–124.
da Costa, A. C. L., D. Galbraith, S. Almeida, B. T. T. Portela, M. da Costa, J. de Athaydes Silva Junior, A. P. Braga, P. H. L. de Gonçalves, A. A. de Oliveira, R. Fisher, O. L. Phillips, D. B. Metcalfe, P. Levy, and P. Meir. 2010. Effect of 7 yr of experimental drought on vegetation dynamics and biomass storage of an eastern Amazonian rainforest. New Phytologist 187:579–591.
Cressman, G. P. 1959. An Operational Objective Analysis System. Monthly Weather Review 87:367–374.
Crk, T., M. Uriarte, F. Corsi, and D. Flynn. 2009. Forest recovery in a tropical landscape: What is the relative importance of biophysical, socioeconomic, and landscape variables? Landscape Ecology 24:629–642.
Curran, T. J., R. L. Brown, E. Edwards, K. Hopkins, C. Kelley, E. McCarthy, E. Pounds, R. Solan, and J. Wolf. 2008a. Plant functional traits explain interspecific differences in immediate cyclone damage to trees of an endangered rainforest community in north Queensland. Austral Ecology 33:451–461.
Curran, T. J., L. N. Gersbach, W. Edwards, and A. K. Krockenberger. 2008b. Wood density predicts plant damage and vegetative recovery rates caused by cyclone disturbance in tropical rainforest tree species of North Queensland, Australia. Austral Ecology 33:442–450.
Davies-Colley, R. J., G. W. Payne, and M. van Elswijk. 2000. Microforest gradients across a forest edge. New Zealand Journal of Ecology 24:111–121.
Daws, M. I., C. E. Mullins, D. F. R. P. Burslem, S. R. Paton, and J. W. Dalling. 2002. Topographic position affects the water regime in a semideciduous tropical forest in

Panam'a. Plant and Soil 238:79–90.
DeFries, R. S., J. A. Foley, and G. P. Asner. 2004. Land-use choices: balancing human needs and ecosystem function. Frontiers in Ecology and the Environment 2:249–257.
DeFries, R. S., R. A. Houghton, M. C. Hansen, C. B. Field, D. Skole, and J. Townshend. 2002. Carbon emissions from tropical deforestation and regrowth based on satellite observations for the 1980s and 1990s. Proceedings of the National Academy of Sciences 99:14256–14261.
DeFries, R. S., D. C. Morton, G. R. van der Werf, L. Giglio, G. J. Collatz, J. T. Randerson, R. a. Houghton, P. K. Kasibhatla, and Y. Shimabukuro. 2008. Fire-related carbon emissions from land use transitions in southern Amazonia. Geophysical Research Letters 35:L22705.
Dormann, C. F., J. Elith, S. Bacher, C. Buchmann, G. Carl, G. Carré, J. R. G. Marquéz, B. Gruber, B. Lafourcade, P. J. Leitão, T. Münkemüller, C. Mcclean, P. E. Osborne, B. Reineking, B. Schröder, A. K. Skidmore, D. Zurell, and S. Lautenbach. 2013. Collinearity: A review of methods to deal with it and a simulation study evaluating their performance. Ecography 36:027–046.
Doughty, C. E., Y. Malhi, A. Araujo-Murakami, D. B. Metcalfe, J. E. Silva-Espejo, L. Arroyo, J. P. Heredia, E. Pardo-Toledo, L. M. Mendizabal, V. D. Rojas-Landivar, M. Vega-Martinez, M. Flores-Valencia, R. Sibler-Rivero, L. Moreno-Vare, L. J. Viscarra, T. Chuviru-Castro, M. Osinaga-Becerra, and R. Ledezma. 2014. Allocation trade-offs dominate the response of tropical forest growth to seasonal and interannual drought. Ecology 95:2192–2201.
Duffy, P. B., P. Brando, G. P. Asner, and C. B. Field. 2015. Projections of future meteorological drought and wet periods in the Amazon. Proceedings of the National Academy of Sciences 112:13172–13177.
Dworak, R., K. M. Bedka, J. C. Brunner, and W. F. Feltz. 2012. Comparison between GOES-12 Overshooting-Top Detections, WSR-88D Radar Reflectivity, and Severe Storm Reports. Weather and Forecasting 27:684–699.
Engelbrecht, B. M. J., L. S. Comita, R. Condit, T. Kursar, M. T. Tyree, B. L. Turner, and S. P. Hubbell. 2007. Drought sensitivity shapes species distribution patterns in tropical forests. Nature 447:80–82.
Espirito-Santo, F. D., M. Gloor, M. Keller, Y. Malhi, S. Saatchi, B. Nelson, R. C. Junior, C. Pereira, J. Lloyd, S. Frolking, M. Palace, Y. E. Shimabukuro, V. Duarte, A. M. Mendoza, G. Lopez-Gonzalez, T. R. Baker, T. R. Feldpausch, R. J. Brienen, G. P. Asner, D. S. Boyd, and O. L. Phillips. 2014. Size and frequency of natural forest disturbances and the Amazon forest carbon balance. Nature Communications 5:3434.
Esprito-Santo, F. D. B., M. Keller, B. Braswell, B. W. Nelson, S. Frolking, and G. Vicente. 2010. Storm intensity and old-growth forest disturbances in the Amazon region. Geophysical Research Letters 37:1–6.
Etter, A., C. McAlpine, D. Pullar, and H. Possingham. 2005. Modeling the age of tropical moist forest fragments in heavily-cleared lowland landscapes of Colombia. Forest Ecology and Management 208:249–260.
Everham, E. M., and N. V. L. Brokaw. 1996. Forest damage and recovery from catastrophic wind. The Botanical Review 62:113–185.
Fahrig, L. 2003. Effects of Habitat Fragmentation on Biodiversity. Annual Review of Ecology Evolution and Systematics 34:487–515.
Famiglietti, J. S., J. W. Rudnicki, and M. Rodell. 1998. Variability in surface moisture content along a hillslope transect: Rattlesnake Hill, Texas. Journal of Hydrology 210:259–281.

FAO. 2010. Global Forest Resources Assessment 2010. America 147:350 pp.
Feeley, K. J., S. Joseph Wright, M. N. Nur Supardi, A. R. Kassim, and S. J. Davies. 2007. Decelerating growth in tropical forest trees. Ecology Letters 10:461–469.
Fekedulegn, D., R. R. Hicks, and J. J. Colbert. 2003. Influence of topographic aspect, precipitation and drought on radial growth of four major tree species in an Appalachian watershed. Forest Ecology and Management 177:409–425.
Feng, X., A. Porporato, and I. Rodriguez-Iturbe. 2013. Changes in rainfall seasonality in the tropics. Nature Climate Change 3:811–815.
Fernandes, K., W. Baethgen, S. Bernardes, R. DeFries, D. G. DeWitt, L. Goddard, W. Lavado, D. E. Lee, C. Padoch, M. Pinedo-Vasquez, and M. Uriarte. 2011. North Tropical Atlantic influence on western Amazon fire season variability. Geophysical Research Letters 38:1–5.
Ferreira, L. V., and W. F. Laurance. 1997. Effects of Forest Fragmentation on Mortality and Damage of Selected Trees in Central Amazonia. Conservation Biology 11:797–801.
Fisher, J. I., G. C. Hurtt, R. Q. Thomas, and J. Q. Chambers. 2008. Clustered disturbances lead to bias in large-scale estimates based on forest sample plots. Ecology Letters 11:554–563.
Flatley, W. T., C. W. Lafon, and H. D. Grissino-Mayer. 2011. Climatic and topographic controls on patterns of fire in the southern and central Appalachian Mountains, USA. Landscape Ecology 26:195–209.
Flynn, D. F. B., M. Uriarte, T. Crk, J. B. Pascarella, J. K. Zimmerman, T. M. Aide, and M. A. Caraballo Ortiz. 2010. Hurricane disturbance alters secondary forest recovery in Puerto Rico. Biotropica 42:149–157.
Fons, W. 1940. Influence of forest cover on wind velocity. Journal of Forestry 38:481–486.
Fox, J., and G. Monette. 1992. Generalized Collinearity Diagnostics. Journal of the American Statistical Association 87:178–183.
Fujisaka, S., and D. White. 1998. Pasture or permanent crops after slash-and-burn cultivation? Land-use choice in three Amazon colonies. Agroforestry Systems 42:45–59.
Fuss, S., J. G. Canadell, G. P. Peters, M. Tavoni, R. M. Andrew, P. Ciais, R. B. Jackson, C. D. Jones, F. Kraxner, N. Nakicenovic, C. Le Quéré, M. R. Raupach, A. Sharifi, P. Smith, and Y. Yamagata. 2014. Betting on negative emissions. Nature Climate Change 4:850–853.
Garstang, M., H. L. Massie, J. Halverson, S. Greco, and J. Scala. 1994. Amazon Coastal Squall Lines. Part I: Structure and Kinematics. Monthly Weather Review 122:608–622.
Garstang, M., S. White, H. H. Shugart, and J. Halverson. 1998. Convective cloud downdrafts as the cause of large blowdowns in the Amazon rainforest. Meteorology and Atmospheric Physics 67:199–212.
Gatti, L. V, M. Gloor, J. B. Miller, C. E. Doughty, Y. Malhi, L. G. Domingues, L. S. Basso, A. Martinewski, C. S. C. Correia, V. F. Borges, S. Freitas, R. Braz, L. O. Anderson, H. Rocha, J. Grace, O. L. Phillips, and J. Lloyd. 2014. Drought sensitivity of Amazonian carbon balance revealed by atmospheric measurements. Nature 506:76–80.
Gelman, A., and J. Hill. 2007. Data analysis using regression and multilevel/hierarchical models. Cambridge University Press, Cambridge, UK.
Del Genio, A. D., M. S. Yao, and J. Jonas. 2007. Will moist convection be stronger in a warmer climate? Geophysical Research Letters 34:1–5.
Gerwing, J. J. 2002. Degradation of forests through logging and fire in the eastern Brazilian Amazon. Forest Ecology and Management 157:131–141.
Gobierno regional de Ucayali. 2006. Evaluación de impactos ambientales de quema e incendios forestales en la provincial de Coronel Portillo. Pucallpa, Peru.

Goldammer, J. 1998. Early warning systems for the prediction of an appropriate response to wildfires and related environmental hazards. Pages 6–9Health Guidelines for Vegetation Fire Events. Lima, Peru.
Goodman, L. 1961. Snowball Sampling. The Annals of Mathematical Statistics 32:148–170.
Graham, M. H. 2003. Confronting Multicollinearity in Ecological Multiple Regression 84:2809–2815.
Grau, H. R., and M. Aide. 2008. Globalization and Land-Use Transitions in Latin America 13.
Greenwood, S., P. Ruiz-Benito, J. Martínez-Vilalta, F. Lloret, T. Kitzberger, C. D. Allen, R. Fensham, D. C. Laughlin, J. Kattge, G. Bönisch, N. J. B. Kraft, and A. S. Jump. 2017. Tree mortality across biomes is promoted by drought intensity, lower wood density and higher specific leaf area. Ecology Letters 20:539–553.
Grimbacher, P. S., C. P. Catterall, and N. E. Stork. 2008. Do edge effects increase the susceptibility of rainforest fragments to structural damage resulting from a severe tropical cyclone? Austral Ecology 33:525–531.
Grove, S., S. Turton, and D. Siegenthaler. 2000. Mosaics of Canopy Openness Induced by Tropical Cyclones in Lowland Rain Forests with Contrasting Management Histories in Northeastern Australia. Journal of Tropical Ecology 16:883–894.
Guariguata, M. R., and R. Ostertag. 2001. Neotropical secondary forest succession: changes in structural and functional characteristics. Forest Ecology and Management 148:185–206.
Guarín, A., and A. H. Taylor. 2005. Drought triggered tree mortality in mixed conifer forests in Yosemite National Park, California, USA. Forest Ecology and Management 218:229–244.
Gutiérrez-Vélez, V. H., and R. DeFries. 2013. Annual multi-resolution detection of land cover conversion to oil palm in the Peruvian Amazon. Remote Sensing of Environment 129:154–167.
Gutiérrez-Vélez, V. H., R. DeFries, M. Pinedo-Vásquez, M. Uriarte, C. Padoch, W. Baethgen, K. Fernandes, and Y. Lim. 2011. High-yield oil palm expansion spares land at the expense of forests in the Peruvian Amazon. Environmental Research Letters 6:44029.
Gutiérrez-Velez, V. H., M. Uriarte, R. Defries, M. Pinedo-Vasquez, K. Fernandes, P. Ceccato, W. Baethgen, and C. Padoch. 2014. Land cover change interacts with drought severity to change fire regimes in Western Amazonia. Ecological Applications 24:1323–1340.
Hacke, U. G., J. S. Sperry, W. T. Pockman, S. D. Davis, and K. A. McCulloh. 2001. Trends in wood density and structure are linked to prevention of xylem implosion by negative pressure. Oecologia 126:457–461.
Haddad, N. M., L. a. Brudvig, J. Clobert, K. F. Davies, A. Gonzalez, R. D. Holt, T. E. Lovejoy, J. O. Sexton, M. P. Austin, C. D. Collins, W. M. Cook, E. I. Damschen, R. M. Ewers, B. L. Foster, C. N. Jenkins, a. J. King, W. F. Laurance, D. J. Levey, C. R. Margules, B. a. Melbourne, a. O. Nicholls, J. L. Orrock, D.-X. Song, and J. R. Townshend. 2015. Habitat fragmentation and its lasting impact on Earth's ecosystems. Science Advances 1:1–9.
Harper, K. A., S. E. MacDonald, P. J. Burton, J. Chen, K. D. Brosofske, Sa. C. Saunder, E. S. Euskirchen, D. Roberts, M. S. Jaiteh, and P.-A. Esseen. 2005. Edge Influence on Forest Structure and Composition in Fragmented Landscapes. Conservation Biology 19:768–782.
Harrod, J. C., M. E. Harmon, and P. S. White. 2000. Post-fire succession and 20th century reduction in fire frequency on xeric southern Appalachian sites. Journal of Vegetation Science 11:465–472.
Hawbaker, T. J., V. C. Radeloff, S. I. Stewart, R. B. Hammer, N. S. Keuler, and M. K. Clayton. 2013. Human and biophysical influences on fire occurrence in the United States. Ecological

Applications 23:565–582.
Hecht, S. B., S. Kandel, I. Gomes, N. Cuellar, and H. Rosa. 2006. Globalization, forest resurgence, and environmental politics in El Salvador. World Development 34:308–323.
Heinimann, A., P. Messerli, D. Schmidt-Vogt, and U. Wiesmann. 2007. The Dynamics of Secondary Forest Landscapes in the Lower Mekong Basin. Mountain Research and Development 27:232–241.
Helmer, E. H. 2000. The Landscape Ecology of Tropical Secondary Forest in Montane Costa Rica. Ecosystems 3:98–114.
Helmer, E. H., T. J. Brandeis, A. E. Lugo, and T. Kennaway. 2008. Factors influencing spatial pattern in tropical forest clearance and stand age: Implications for carbon storage and species diversity. Journal of Geophysical Research 113:G02S04.
Hernández-Stefanoni, J. L., J. M. Dupuy, F. Tun-Dzul, and F. May-Pat. 2011. Influence of landscape structure and stand age on species density and biomass of a tropical dry forest across spatial scales. Landscape Ecology 26:355–370.
Hoffmann, W. A., R. M. Marchin, P. Abit, and O. L. Lau. 2011. Hydraulic failure and tree dieback are associated with high wood density in a temperate forest under extreme drought. Global Change Biology 17:2731–2742.
Holbrook, N. M., and F. E. Putz. 1989. Influence of Neighbors on Tree Form : Effects of Lateral Shade and Prevention of Sway on the Allometry of Liquidambar styraciflua (Sweet Gum). American Journal of Botany 76:1740–1749.
Hook, D. D., M. A. Buford, T. M. Williams, F. Lauderdale, D. Hook, M. Williams, and B. W. Baruch. 1991. Impact of Hurricane Plain Forest. Journal of Coastal Research 8:291–300.
Hurst, J. M., R. B. Allen, D. A. Coomes, and R. P. Duncan. 2011. Size-specific tree mortality varies with neighbourhood crowding and disturbance in a montane Nothofagus forest. PLoS ONE 6.
Imbert, D., P. Labbet, and A. Rousteau. 1996. Hurricane Damage and Forest Structure in Guadeloupe, French West Indies. Journal of Tropical Ecology 12:663–680.
Instituto Nacional de Estadistica e Informatica. 2009. Migraciones Internas 1993-2007 Peru.
IPCC. 2013. Climate Change 2013: The Physical Science Basis. Contribution of Working Group I to the Fifth Assessment Report of the Intergovernmental Panel on Climate Change. Page (T. F. Stocker, D. Qin, G.-K. Plattner, M. Tignor, S. K. Allen, J. Boschung, A. Nauels, Y. Xia, V. Bex, and P. M. Midgley, Eds.). Cambridge University Press, London, U.K.
Jacobson, M. Z. 2014. Effects of biomass burning on climate, accounting for heat and moisture fluxes, black and brown carbon, and cloud absorption effects. Journal of Geophysical Research: Atmospheres 119:8980–9002.
Jakovac, C. C., F. Bongers, T. W. Kuyper, R. C. G. Mesquita, M. Peña-Claros, and T. Nakashizuka. 2016. Land use as a filter for species composition in Amazonian secondary forests. Journal of Vegetation Science 27:1104–1116.
Jeon, S. B., P. Olofsson, and C. E. Woodcock. 2014. Land use change in New England: a reversal of the forest transition. Journal of Land Use Science 9:105–130.
De Jong, W., L. Freitas, J. Baluarte, P. Van de Kop, A. Salazar, E. Inga, W. Melendez, and C. Germaná. 2001. Secondary forest dynamics in the Amazon floodplain in Peru. Forest Ecology and Management 150:135–146.
Juárez, R. I. N., J. Q. Chambers, H. Zeng, and D. B. Baker. 2008. Hurricane driven changes in land cover create biogeophysical climate feedbacks. Geophysical Research Letters 35:3–7.
Kanowski, J., C. P. Catterall, S. G. Mckenna, and R. Jensen. 2008. Impacts of cyclone Larry on

the vegetation structure of timber plantations, restoration plantings and rainforest on the Atherton Tableland, Australia. Austral Ecology 33:485–494.
King, D. A., S. J. Davies, M. N. Nur Supardi, and S. Tan. 2005. Tree growth is related to light interception and wood density in two mixed dipterocarp forests of Malaysia. Functional Ecology 19:445–453.
Knutson, T. R., J. L. McBride, J. Chan, K. A. Emanuel, G. Holland, C. Landsea, I. Held, J. P. Kossin, A. Srivastava, and M. Sugi. 2010. Tropical cyclones and climate change. Nature Geoscience 3:157–163.
Krawchuk, M. A., and M. A. Moritz. 2011. Constraints on global fire activity vary across a resource gradient. Ecology 92:121–132.
Krawchuk, M. a, M. a Moritz, M.-A. Parisien, J. Van Dorn, and K. Hayhoe. 2009. Global pyrogeography: the current and future distribution of wildfire. PloS one 4:e5102.
Kulakowski, D., and T. T. Veblen. 2002. Influences of fire history and topography on the pattern of a severe wind blowdown in a Colorado subalpine forest. Journal of Ecology 90:806–819.
Lambin, E. F., and P. Meyfroidt. 2011. Global land use change, economic globalization, and the looming land scarcity. Proceedings of the National Academy of Sciences 108:3465–3472.
Lasky, J. R., B. Bachelot, R. Muscarella, N. Schwartz, J. Forero-Montaña, C. J. Nytch, N. G. Swenson, J. Thompson, J. K. Zimmerman, and M. Uriarte. 2015. Ontogenetic shifts in trait-mediated mechanisms of plant community assembly. Ecology 96:2157–2169.
Laurance, W. F., and T. J. Curran. 2008. Impacts of wind disturbance on fragmented tropical forests: A review and synthesis. Austral Ecology 33:399–408.
Laurance, W. F., S. G. Laurece, V. Ferreira, Leandro, M. R. Merona, Judy, C. Gascon, and T. E. Lovejoy. 1997. Biomass Collapse in Amazonian Forest Fragments. Science 278:1117–1118.
Laurance, W. F., T. E. Lovejoy, H. L. Vasconcelos, E. M. Bruna, R. K. Didham, P. C. Stouffer, C. Gascon, R. O. Bierregaard, S. G. Laurance, and E. Sampaio. 2002. Ecosystem decay of Amazonian forest fragments : a 22-years investigation. Conservation Biology 16:605–618.
Laurance, W. F., H. E. M. Nascimento, S. G. Laurance, A. C. Andrade, P. M. Fearnside, J. E. L. Ribeiro, and R. L. Capretz. 2006. Rain forest fragmentation and the proliferation of successional trees. Ecology 87:469–482.
Lawton, R. O. 1984. Ecological Constraints on Wood Density in a Tropical Montane Rain Forest. American Journal of Botany 71:261–267.
Lecki, N. A., and I. F. Creed. 2016. Forest soil CO2 efflux models improved by incorporating topographic controls on carbon content and sorption capacity of soils. Biogeochemistry 129:307–323.
Lewis, S. L., P. M. Brando, O. L. Phillips, G. M. F. van der Heijden, and D. Nepstad. 2011. The 2010 Amazon Drought. Science 331:554–554.
Liebsch, D., M. C. M. Marques, and R. Goldenberg. 2008. How long does the Atlantic Rain Forest take to recover after a disturbance? Changes in species composition and ecological features during secondary succession. Biological Conservation 141:1717–1725.
Locatelli, B., C. P. Catterall, P. Imbach, C. Kumar, R. Lasco, E. Marín-Spiotta, B. Mercer, J. S. Powers, N. Schwartz, and M. Uriarte. 2015. Tropical reforestation and climate change: Beyond carbon. Restoration Ecology 23:337–343.
Loehle, C. 1991. Managing and monitoring ecosystems in the face of heterogeneity. Page *in* J. Kolasa and S. T. A. Pickett, editors. Ecological Heterogeneity. Springer Verlag, New York, NY.

Lohbeck, M., L. Poorter, E. Lebrija-Trejos, M. Martínez-Ramos, J. A. Meave, H. Paz, E. A. Pérez-García, I. E. Romero-Pérez, A. Tauro, and F. Bongers. 2013. Successional changes in functional composition contrast for dry and wet tropical forest. Ecology 94:1211–1216.

Lohman, D. J., D. Bickford, and N. S. Sodhi. 2007. Environment: The Burning Issue. Science 316:376–376.

Lugo, A. E. 2008. Visible and invisible effects of hurricanes on forest ecosystems: An international review. Austral Ecology 33:368–398.

Magnabosco Marra, D., N. Higuchi, S. E. Trumbore, G. H. P. M. Ribeiro, J. Dos Santos, V. M. C. Carneiro, A. J. N. Lima, J. Q. Chambers, R. I. Negrón-Juárez, F. Holzwarth, B. Reu, and C. Wirth. 2016. Predicting biomass of hyperdiverse and structurally complex central Amazonian forests - A virtual approach using extensive field data. Biogeosciences 13:1553–1570.

Malhi, Y., L. E. O. C. Aragao, D. Galbraith, C. Huntingford, R. Fisher, P. Zelazowski, S. Sitch, C. McSweeney, and P. Meir. 2009. Exploring the likelihood and mechanism of a climate-change-induced dieback of the Amazon rainforest. Proceedings of the National Academy of Sciences 106:20610–20615.

Malhi, Y., C. E. Doughty, G. R. Goldsmith, D. B. Metcalfe, C. A. J. Girardin, T. R. Marthews, J. del Aguila-Pasquel, L. E. O. C. Aragão, A. Araujo-Murakami, P. Brando, A. C. L. da Costa, J. E. Silva-Espejo, F. Farfán Amézquita, D. R. Galbraith, C. A. Quesada, W. Rocha, N. Salinas-Revilla, D. Silvério, P. Meir, and O. L. Phillips. 2015. The linkages between photosynthesis, productivity, growth and biomass in lowland Amazonian forests. Global Change Biology 21:2283–2295.

Malhi, Y., D. Wood, T. R. Baker, J. Wright, O. L. Phillips, T. Cochrane, P. Meir, J. Chave, S. Almeida, L. Arroyo, N. Higuchi, T. J. Killeen, S. G. Laurance, W. F. Laurance, S. L. Lewis, A. Monteagudo, D. A. Neill, P. N. Vargas, N. C. A. Pitman, C. A. Quesada, R. Salomão, J. N. M. Silva, A. T. Lezama, J. Terborgh, R. V. Martínez, and B. Vinceti. 2006. The regional variation of aboveground live biomass in old-growth Amazonian forests. Global Change Biology 12:1107–1138.

Maréchaux, I., M. K. Bartlett, L. Sack, C. Baraloto, J. Engel, E. Joetzjer, and J. Chave. 2015. Drought tolerance as predicted by leaf water potential at turgor loss point varies strongly across species within an Amazonian forest. Functional Ecology 29:1268–1277.

Markesteijn, L., L. Poorter, F. Bongers, H. Paz, and L. Sack. 2011. Hydraulics and life history of tropical dry forest tree species: Coordination of species' drought and shade tolerance. New Phytologist 191:480–495.

Marlier, M. E., R. S. DeFries, A. Voulgarakis, P. L. Kinney, J. T. Randerson, D. T. Shindell, Y. Chen, and G. Faluvegi. 2012. El Niño and health risks from landscape fire emissions in southeast Asia. Nature Climate Change 3:131–136.

Mather, A. 1992. The forest transition. Area 24:367–379.

McGarigal, K., S. A. Cushman, M. C. Neel, and E. Ene. 2012. FRAGSTATS v4: Spatial Pattern Analysis Program for Categorical and Continuous Maps. University of Massachusettes, Amherst, MA. URL http://www.umass.edu/landeco/research/fragstats/fragstats.html.

McGroddy, M., D. Lawrence, L. Schneider, J. Rogan, I. Zager, and B. Schmook. 2013. Damage patterns after Hurricane Dean in the southern Yucatán: Has human activity resulted in more resilient forests? Forest Ecology and Management 310:812–820.

McLaughlin, B. C., D. D. Ackerly, P. Z. Klos, J. Natali, T. E. Dawson, and S. E. Thompson. 2017. Hydrologic refugia, plants, and climate change. Global Change Biology 23:000–000.

Medvigy, D., S. C. Wofsy, J. W. Munger, D. Y. Hollinger, and P. R. Moorcroft. 2009. Mechanistic scaling of ecosystem function and dynamics in space and time: Ecosystem Demography model version 2. Journal of Geophysical Research: Biogeosciences 114:1–21.

de Mendonça, M. J. C., M. D. C. Vera Diaz, D. Nepstad, R. Seroa da Motta, A. Alencar, J. C. Gomes, and R. A. Ortiz. 2004. The economic cost of the use of fire in the Amazon. Ecological Economics 49:89–105.

Mesquita, R. C. G., P. Delamônica, and W. F. Laurance. 1999. Effect of surrounding vegetation on edge-related tree mortality in Amazonian forest fragments. Biological Conservation 91:129–134.

Metcalfe, D. B., P. Meir, L. E. O. C. Aragão, R. Lobo-do-Vale, D. Galbraith, R. A. Fisher, M. M. Chaves, J. P. Maroco, A. C. L. da Costa, S. S. de Almeida, A. P. Braga, P. H. L. Gonçalves, J. de Athaydes, M. da Costa, T. T. B. Portela, A. A. R. de Oliveira, Y. Malhi, and M. Williams. 2010. Shifts in plant respiration and carbon use efficiency at a large-scale drought experiment in the eastern Amazon. New Phytologist 187:608–621.

Meyfroidt, P., and E. F. Lambin. 2011. Global Forest Transition: Prospects for an End to Deforestation. Annual Review of Environment and Resources 36:343–371.

Meyfroidt, P., T. K. Rudel, and E. F. Lambin. 2010. Forest transitions, trade, and the global displacement of land use. Proceedings of the National Academy of Sciences 107:20917–20922.

Moritz, M. A., M.-A. Parisien, E. Batllori, M. A. Krawchuk, J. Van Dorn, D. J. Ganz, and K. Hayhoe. 2012. Climate change and disruptions to global fire activity. Ecosphere 3:art49.

Moritz, M. a, M. E. Morais, L. a Summerell, J. M. Carlson, and J. Doyle. 2005. Wildfires, complexity, and highly optimized tolerance. Proceedings of the National Academy of Sciences of the United States of America 102:17912–7.

Morse, A. P., B. A. Gardiner, and B. J. Marshall. 2002. Mechanisms Controlling Turbulence Development Across A Forest Edge. Boundary-Layer Meteorology 103:227–251.

Morton, D. C., Y. Le Page, R. DeFries, G. J. Collatz, and G. C. Hurtt. 2013. Understorey fire frequency and the fate of burned forests in southern Amazonia. Philosophical Transactions of the Royal Society B: Biological Sciences 368:20120163–20120163.

Myers, R. K., and D. H. Van Lear. 1998. Hurricane-fire interactions in coastal forests of the south: A review and hypothesis. Forest Ecology and Management 103:265–276.

Naidu, S. L., E. H. DeLucia, and R. B. Thomas. 1998. Contrasting patterns of biomass allocation in dominant and suppressed loblolly pine. Canadian Journal of Forest Research 28:1116–1124.

Nakagawa, M., K. Tanaka, T. Nakashizuka, T. Ohkubo, T. Kato, T. Maeda, K. Sato, H. Miguchi, H. Nagamasu, K. Ogino, S. Teo, A. A. Hamid, and L. H. Seng. 2000. Impact of severe drought associated with the 1997–1998 El Niño in a tropical forest in Sarawak. Journal of Tropical Ecology 16:355–367.

Negrón-Juárez, R. I., J. Q. Chambers, G. Guimaraes, H. Zeng, C. F. M. Raupp, D. M. Marra, G. H. P. M. Ribeiro, S. S. Saatchi, B. W. Nelson, and N. Higuchi. 2010. Widespread Amazon forest tree mortality from a single cross-basin squall line event. Geophysical Research Letters 37:1–5.

Negrón-Juárez, R. I., J. Q. Chambers, D. M. Marra, G. H. P. M. Ribeiro, S. W. Rifai, N. Higuchi, and D. Roberts. 2011. Detection of subpixel treefall gaps with Landsat imagery in Central Amazon forests. Remote Sensing of Environment 115:3322–3328.

Nelson, B. W. 1994. Natural forest disturbance and change in the Brazilian Amazon. Remote

Sensing Reviews 10:105–125.
Nelson, B. W., R. Mesquita, J. L. G. Pereira, S. G. a Souza, G. T. Batista, and L. B. Couto. 1999. Allometric Regressions for Improved of Secondary Forest Biomass in the Central Amazon. Forest Ecology and Management 117:149–167.
Nepstad, D. C., C. M. Stickler, B. S.- Filho, and F. Merry. 2008. Interactions among Amazon land use, forests and climate: prospects for a near-term forest tipping point. Philosophical Transactions of the Royal Society B: Biological Sciences 363:1737–1746.
Nepstad, D. C., I. M. Tohver, R. David, P. Moutinho, and G. Cardinot. 2007. Mortality of large trees and lianas following experimental drought in an amazon forest. Ecology 88:2259–2269.
Nepstad, D. C., A. Verissimo, A. Alencar, C. Nobre, E. Lima, P. Lefebvre, P. Schlesinger, C. Potter, P. Moutinho, E. Mendoza, M. Cochrane, and V. Brooks. 1999. Large-scale impoverishment of Amazonian forests by logging and fire. Nature 398:505–508.
Nepstad, D., G. Carvalho, A. Cristina, A. Alencar, Ä. Paulo, J. Bishop, P. Moutinho, P. Lefebvre, U. Lopes, S. Jr, and E. Prins. 2001. Road paving, fire regime feedbacks, and the future of Amazon forests. Forest Ecology and Management 154:395–407.
Nepstad, D., P. Lefebvre, U. Lopes da Silva, J. Tomasella, P. Schlesinger, L. Solorzano, P. Moutinho, D. Ray, and J. Guerreira Benito. 2004. Amazon drought and its implications for forest flammability and tree growth: a basin-wide analysis. Global Change Biology 10:704–717.
Nishimua, T. B., E. Suzuki, T. Kohyama, and S. Tsuyuzaki. 2007. Mortality and growth of trees in peat-swamp and heath forests in Central Kalimantan after severe drought. Plant Ecology 188:165–177.
O'Brien, M. J., B. M. J. Engelbrecht, J. Joswig, G. Pereyra, B. Schuldt, S. Jansen, J. Kattge, S. M. Landhäusser, S. R. Levick, Y. Preisler, P. Väänänen, and C. Macinnis-Ng. 2017. A synthesis of tree functional traits related to drought-induced mortality in forests across climatic zones. Journal of Applied Ecology:Accepted.
Oliveira, P., G. Asner, and D. Knapp. 2007. Land-use allocation protects the Peruvian Amazon. Science.
Oliver, H. R. 1971. Wind profiles in and above a forest canopy. Quarterly Journal of the Royal Meteorological Society 97:548–553.
Oosterhoorn, M., and M. Kappelle. 2000. Vegetation structure and composition along an interior-edge-exterior gradient in a Costa Rican montane cloud forest. Forest Ecology and Management 126:291–307.
Orlowsky, B., and S. I. Seneviratne. 2012. Global changes in extreme events: Regional and seasonal dimension. Climatic Change 110:669–696.
Ouédraogo, D. Y., F. Mortier, S. Gourlet-Fleury, V. Freycon, and N. Picard. 2013. Slow-growing species cope best with drought: Evidence from long-term measurements in a tropical semi-deciduous moist forest of Central Africa. Journal of Ecology 101:1459–1470.
Pacific, V. J., B. L. McGlynn, D. A. Riveros-Iregui, D. L. Welsch, and H. E. Epstein. 2008. Variability in soil respiration across riparian-hillslope transitions. Biogeochemistry 91:51–70.
Padoch, C., E. Brondizio, S. Costa, M. Pinedo-Vasquez, R. R. Sears, and A. Siqueira. 2008. Urban Forest and Rural Cities: Multi-sited Households, Consumption Patterns, and Forest Resources in Amazonia. Ecology and Society 13:2.
Pan, Y., R. A. Birdsey, J. Fang, R. Houghton, P. E. Kauppi, W. A. Kurz, O. L. Phillips, A.

Shvidenko, S. L. Lewis, J. G. Canadell, P. Ciais, R. B. Jackson, S. W. Pacala, A. D. McGuire, S. Piao, A. Rautiainen, S. Sitch, and D. Hayes. 2011. A Large and Persistent Carbon Sink in the World's Forests. Science 333:988–993.

Parisien, M.-A., and M. A. Moritz. 2009. Environmental controls on the distribution of wildfire at multiple spatial scales. Ecological Monographs 79:127–154.

Parks, S. a, M.-A. Parisien, and C. Miller. 2012. Spatial bottom-up controls on fire likelihood vary across western North America. Ecosphere 3:art12.

Pechony, O., and D. T. Shindell. 2010. Driving forces of global wildfires over the past millennium and the forthcoming century. Proceedings of the National Academy of Sciences 107:19167–19170.

Peltola, H. 1996. Model computations on wind flow and turning moment by wind for Scots pines along the margins of clear-cut areas. Forest Ecology and Management 83:203–215.

Phillips, O. L., L. E. O. C. Aragao, S. L. Lewis, J. B. Fisher, J. Lloyd, G. Lopez-Gonzalez, Y. Malhi, A. Monteagudo, J. Peacock, C. a Quesada, G. van der Heijden, S. Almeida, I. Amaral, L. Arroyo, G. Aymard, T. R. Baker, O. Banki, L. Blanc, D. Bonal, P. Brando, J. Chave, A. C. A. de Oliveira, N. D. Cardozo, C. I. Czimczik, T. R. Feldpausch, M. A. Freitas, E. Gloor, N. Higuchi, E. Jimenez, G. Lloyd, P. Meir, C. Mendoza, A. Morel, D. a Neill, D. Nepstad, S. Patino, M. C. Penuela, A. Prieto, F. Ramirez, M. Schwarz, J. Silva, M. Silveira, A. S. Thomas, H. Ter Steege, J. Stropp, R. Vasquez, P. Zelazowski, E. A. Davila, S. Andelman, A. Andrade, K.-J. Chao, T. Erwin, A. Di Fiore, E. H. C., H. Keeling, T. J. Killeen, W. F. Laurance, A. P. Cruz, N. C. a Pitman, P. N. Vargas, H. Ramirez-Angulo, A. Rudas, R. Salamao, N. Silva, J. Terborgh, and A. Torres-Lezama. 2009. Drought Sensitivity of the Amazon Rainforest. Science 323:1344–1347.

Phillips, O. L., G. van der Heijden, S. L. Lewis, G. López-González, L. E. O. C. Aragão, J. Lloyd, Y. Malhi, A. Monteagudo, S. Almeida, E. A. Dávila, I. Amaral, S. Andelman, A. Andrade, L. Arroyo, G. Aymard, T. R. Baker, L. Blanc, D. Bonal, Á. C. A. de Oliveira, K.-J. Chao, N. D. Cardozo, L. da Costa, T. R. Feldpausch, J. B. Fisher, N. M. Fyllas, M. A. Freitas, D. Galbraith, E. Gloor, N. Higuchi, E. Honorio, E. Jiménez, H. Keeling, T. J. Killeen, J. C. Lovett, P. Meir, C. Mendoza, A. Morel, P. N. Vargas, S. Patiño, K. S.-H. Peh, A. P. Cruz, A. Prieto, C. a Quesada, F. Ramírez, H. Ramírez, A. Rudas, R. Salamão, M. Schwarz, J. Silva, M. Silveira, J. W. Ferry Slik, B. Sonké, A. S. Thomas, J. Stropp, J. R. D. Taplin, R. Vásquez, and E. Vilanova. 2010. Drought-mortality relationships for tropical forests. New Phytologist 187:631–646.

Pinard, M. A., and J. Huffman. 1997. Fire resistance and bark properties of trees in a seasonally dry forest in eastern Bolivia. Journal of Tropical Ecology 13:727–740.

Pinedo-Vasquez, M., D. Zarin, and P. Jipp. 1992. Economic returns from forest conversion in the Peruvian Amazon. Ecological Economics 6:163–173.

Plummer, M. 2003. JAGS: A program for analysis of Bayesian graphical models using Gibbs sampling. Proceedings of the 3rd international workshop on distributed statistical computing 124:125.

Pohlman, C. L., M. Goosem, and S. M. Turton. 2008. Effects of Severe Tropical Cyclone Larry on rainforest vegetation and understorey microclimate near a road, powerline and stream. Austral Ecology 33:503–515.

Poorter, H., Ü. Niinemets, L. Poorter, I. J. Wright, and R. Villar. 2009. Causes and consequences of variation in leaf mass per area (LMA): a meta-analysis. New Phytologist 182:565–588.

Poorter, L. 2001. Light dependent changes in biomass allocation and their importance for growth

of rain forest tree species. Functional Ecology 15:113–123.
Poorter, L., F. Bongers, T. M. Aide, A. M. Almeyda Zambrano, P. Balvanera, J. M. Becknell, V. Boukili, P. H. S. Brancalion, E. N. Broadbent, R. L. Chazdon, D. Craven, J. S. de Almeida-Cortez, G. A. L. Cabral, B. H. J. de Jong, J. S. Denslow, D. H. Dent, S. J. DeWalt, J. M. Dupuy, S. M. Durán, M. M. Espírito-Santo, M. C. Fandino, R. G. César, J. S. Hall, J. L. Hernandez-Stefanoni, C. C. Jakovac, A. B. Junqueira, D. Kennard, S. G. Letcher, J.-C. Licona, M. Lohbeck, E. Marín-Spiotta, M. Martínez-Ramos, P. Massoca, J. A. Meave, R. Mesquita, F. Mora, R. Muñoz, R. Muscarella, Y. R. F. Nunes, S. Ochoa-Gaona, A. A. de Oliveira, E. Orihuela-Belmonte, M. Peña-Claros, E. A. Pérez-García, D. Piotto, J. S. Powers, J. Rodríguez-Velázquez, I. E. Romero-Pérez, J. Ruíz, J. G. Saldarriaga, A. Sanchez-Azofeifa, N. B. Schwartz, M. K. Steininger, N. G. Swenson, M. Toledo, M. Uriarte, M. van Breugel, H. van der Wal, M. D. M. Veloso, H. F. M. Vester, A. Vicentini, I. C. G. Vieira, T. V. Bentos, G. B. Williamson, and D. M. A. Rozendaal. 2016. Biomass resilience of Neotropical secondary forests. Nature 530:211–214.
Poorter, L., I. McDonald, A. Alarcón, E. Fichtler, J. C. Licona, M. Peña-Claros, F. Sterck, Z. Villegas, and U. Sass-Klaassen. 2010. The importance of wood traits and hydraulic conductance for the performance and life history strategies of 42 rainforest tree species. New Phytologist 185:481–492.
Poorter, L., S. J. Wright, H. Paz, D. D. Ackerly, R. Condit, G. Ibarra-Manríquez, K. E. Harms, J. C. Licona, M. Martínez-Ramos, S. J. Mazer, H. C. Muller-Landau, M. Peña-Claros, C. O. Webb, and I. J. Wright. 2008. Are Functional Traits Good Predictors of Demographic Rates? Evidence From Five Neotropical Forests. Ecology 89:1908–1920.
Potter, L. 2015. Managing oil palm landscapes: A seven-country survey of the modern palm oil industry in Southeast Asia, Latin America and West Africa. CIFOR.
Putz, F. E., P. D. Coley, K. Lu, A. Montalvo, and A. Aiello. 1983. Uprooting and snapping of trees: structural determinants and ecological consequences. Canadian Journal of Forest Research 13:1011–1020.
R Development Core Team. 2014. R: A Language and Environment for Statistical Computing.
Ray, D., D. Nepstad, and P. Brando. 2010. Predicting moisture dynamics of fine understory fuels in a moist tropical rainforest system: Results of a pilot study undertaken to identify proxy variables useful for rating fire danger. New Phytologist 187:720–732.
Ray, D., D. Nepstad, and P. Moutinho. 2005. Micrometeorological and canopy controls of fire susceptibility in a forested Amazon landscape. Ecological Applications 15:1664–1678.
Reich, P. B. 2014. The world-wide "fast-slow" plant economics spectrum: A traits manifesto. Journal of Ecology 102:275–301.
Reich, P. B., D. S. Ellsworth, and M. B. Walters. 1998. Leaf structure (specific leaf area) modulates photosynthesis-nitrogen relations: evidence from within and across species and functional groups. Functional Ecology 12:948–958.
Reich, P. B., M. B. Walters, and D. S. Ellsworth. 1992. Leaf Life-Span in Relation to Leaf, Plant, and Stand Characteristics among Diverse Ecosystems. Ecological Monographs 62:365–392.
Rhodes, J. S., and D. W. Keith. 2008. Biomass with capture: Negative emissions within social and environmental constraints: An editorial comment. Climatic Change 87:321–328.
Ribeiro, G. H. P. M., J. Q. Chambers, C. J. Peterson, S. E. Trumbore, D. Magnabosco Marra, C. Wirth, J. B. Cannon, R. I. Négron-Juárez, A. J. N. Lima, E. V. C. M. de Paula, J. Santos, and N. Higuchi. 2016. Mechanical vulnerability and resistance to snapping and uprooting for Central Amazon tree species. Forest Ecology and Management 380:1–10.

Rifai, S. W., J. D. Urquiza Muñoz, R. I. Negrón-Juárez, F. R. Ramírez Arévalo, R. Tello-Espinoza, M. C. Vanderwel, J. W. Lichstein, J. Q. Chambers, and S. A. Bohlman. 2016. Landscape-scale consequences of differential tree mortality from catastrophic wind disturbance in the Amazon. Ecological Applications 26:2225–2237.

Rudel, T. K., D. Bates, and R. Machinguiashi. 2002. A Tropical Forest Transition? Agricultural change, out-migration, and secondary forests in the Ecuadorian Amazon. Annals of the Association of American Geographers 92:87–102.

Rudel, T. K., O. T. Coomes, E. Moran, F. Achard, A. Angelsen, J. Xu, and E. Lambin. 2005. Forest transitions: towards a global understanding of land use change. Global Environmental Change 15:23–31.

Rudel, T. K., M. Perez-Lugo, and H. Zichal. 2000. When fields revert to forest: Development and spontaneous reforestation in post-war Puerto Rico. The Professional Geographer 52:386–397.

Russo, S. E., K. L. Jenkins, S. K. Wiser, M. Uriarte, R. P. Duncan, and D. A. Coomes. 2010. Interspecific relationships among growth, mortality and xylem traits of woody species from New Zealand. Functional Ecology 24:253–262.

Saatchi, S., S. Asefi-Najafabady, Y. Malhi, L. E. O. C. Aragao, L. O. Anderson, R. B. Myneni, and R. Nemani. 2013. Persistent effects of a severe drought on Amazonian forest canopy. Proceedings of the National Academy of Sciences 110:565–570.

SAUNDERS, D. A., R. J. HOBBS, and C. R. MARGULES. 1991. Biological Consequences of Ecosystem Fragmentation: A Review. Conservation Biology 5:18–32.

Savill, P. 1983. Silviculture in Windy Climates. Forestry Abstracts 44:473–488.

Schwartz, N. B., M. Uriarte, V. H. Gutiérrez-Vélez, W. Baethgen, R. DeFries, K. Fernandes, and M. A. Pinedo-Vasquez. 2015. Climate, landowner residency, and land cover predict local scale fire activity in the Western Amazon. Global Environmental Change 31:144–153.

Silva, C. E., J. R. Kellner, D. B. Clark, and D. A. Clark. 2013. Response of an old-growth tropical rainforest to transient high temperature and drought. Global Change Biology 19:3423–3434.

da Silva, R. R., D. Werth, and R. Avissar. 2008. Regional impacts of future land-cover changes on the Amazon basin wet-season climate. Journal of Climate 21:1153–1170.

Silvestrini, R. A., B. S. Soares-Filho, D. Nepstad, M. Coe, H. Rodrigues, and R. Assunção. 2011. Simulating fire regimes in the Amazon in response to climate change and deforestation. Ecological Applications 21:1573–1590.

Sjögersten, S., R. Van Der Wal, and S. J. Woodin. 2006. Small-scale hydrological variation determines landscape CO2 fluxes in the high Arctic. Biogeochemistry 80:205–216.

Sloan, S., M. Goosem, and S. G. Laurance. 2016. Tropical forest regeneration following land abandonment is driven by primary rainforest distribution in an old pastoral region. Landscape Ecology 31:601–618.

Smith, B., I. C. Prentice, and M. T. Sykes. 2001. Representation of vegetation dynamics in the modelling of terrestrial ecosystems: Comparing two contrasting approaches within European climate space. Global Ecology and Biogeography 10:621–637.

Somerville, A. 1980. Wind stability: Forest layout and silviculture. New Zealand Journal of Forestry Science 10:476–501.

Sorrensen, C. 2009. Potential hazards of land policy: Conservation, rural development and fire use in the Brazilian Amazon. Land Use Policy 26:782–791.

Stephenson, N. L. 1990. Climatic Control of Vegetation Distribution: The Role of the Water

Balance. The American Naturalist 135:649–670.
Sterck, F. J., L. Poorter, and F. Schieving. 2006. Leaf Traits Determine the Growth-Survival Trade-Off across Rain Forest Tree Species. The American Naturalist 167:758–765.
Talkkari, A., H. Peltola, S. Kellomäki, and H. Strandman. 2000. Integration of component models from the tree, stand and regional levels to assess the risk of wind damage at forest margins. Forest Ecology and Management 135:303–313.
Tang, J., P. Pilesjö, P. A. Miller, A. Persson, Z. Yang, E. Hanna, and T. V. Callaghan. 2014. Incorporating topographic indices into dynamic ecosystem modelling using LPJ-GUESS. Ecohydrology 7:1147–1162.
Taylor, A. H., and C. N. Skinner. 2003. Spatial Patterns and Controls on Historical Fire Regimes and Forest Structure in the Klamath Mountains. Ecological Applications 13:704–719.
Tenenbaum, D. E., L. E. Band, S. T. Kenworthy, and C. L. Tague. 2006. Analysis of soil moisture patterns in forested and suburban catchments in Baltimore, Maryland, using high-resolution photogrammetric and LIDAR digital elevation datasets. Hydrological Processes 20:219–240.
Tilly, C. 2011. The impact of the economic crisis on international migration: a review. Work, employment and society 25:675–692.
Turner, M. G. 2010. Disturbance and landscape dynamics in a changing world. Ecology 91:2833–2849.
Uriarte, M., C. D. Canham, J. Thompson, and J. K. Zimmerman. 2004a. A neighborhood nalysis of tree growth and survival in a hurricane-driven tropical forest. Ecological Monographs 74:591–614.
Uriarte, M., J. S. Clark, J. K. Zimmerman, L. S. Comita, J. Forero-Montaña, and J. Thompson. 2012a. Multidimensional trade-offs in species responses to disturbance: Implications for diversity in a subtropical forest. Ecology 93:191–205.
Uriarte, M., R. Condit, C. D. Canham, and S. P. Hubbell. 2004b. A spatially explicit model of sapling growth in a tropical forest: does the identity of neighbours matter? Journal of Ecology 92:348–360.
Uriarte, M., J. R. Lasky, V. K. Boukili, and R. L. Chazdon. 2016a. A trait-mediated, neighbourhood approach to quantify climate impacts on successional dynamics of tropical rainforests. Functional Ecology 30:157–167.
Uriarte, M., M. Pinedo-Vasquez, R. S. DeFries, K. Fernandes, V. Gutierrez-Velez, W. E. Baethgen, and C. Padoch. 2012b. Depopulation of rural landscapes exacerbates fire activity in the western Amazon. Proceedings of the National Academy of Sciences 109:21546–21550.
Uriarte, M., L. W. Rivera, J. K. Zimmerman, T. M. Aide, A. G. Power, and A. S. Flecker. 2004c. Effects of land use history on hurricane damage and recovery in a neotropical forest. Plant Ecology formerly `Vegetatio' 174:49–58.
Uriarte, M., N. Schwartz, J. S. Powers, E. Marín-Spiotta, W. Liao, and L. K. Werden. 2016b. Impacts of climate variability on tree demography in second growth tropical forests: the importance of regional context for predicting successional trajectories. Biotropica 48:780–797.
US DOE. 2012. Research priorities for tropical ecosystems under climate change workshop report. US Department of Energy Office of Science.
Verburg, R., and C. van Eijk-Bos. 2003. Effects of selective logging on tree diversity, composition and plant functional type patterns in a Bornean rain forest. Journal of

Vegetation Science 14:99–110.
Vermote, E. F., N. Z. El Saleous, and C. O. Justice. 2002. Atmospheric correction of MODIS data in the visible to middle infrared: First results. Remote Sensing of Environment 83:97–111.
Di Vittorio, A. V, R. I. Negrón-Juárez, N. Higuchi, and J. Q. Chambers. 2014. Tropical forest carbon balance: effects of field- and satellite-based mortality regimes on the dynamics and the spatial structure of Central Amazon forest biomass. Environmental Research Letters 9:34010.
van Vuuren, D. P., S. Deetman, J. van Vliet, M. van den Berg, B. J. van Ruijven, and B. Koelbl. 2013. The role of negative CO2 emissions for reaching 2 °C—insights from integrated assessment modelling. Climatic Change 118:15–27.
Weiner, J., and S. C. Thomas. 1992. Competition and Allometry in Three Species of Annual Plants. Ecology 73:648–656.
van der Werf, G. R., D. C. Morton, R. S. DeFries, L. Giglio, J. T. Randerson, G. J. Collatz, and P. S. Kasibhatla. 2009. Estimates of fire emissions from an active deforestation region in the southern Amazon based on satellite data and biogeochemical modelling. Biogeosciences 6:235–249.
Van Der Werf, G. R., J. T. Randerson, L. Giglio, N. Gobron, and A. J. Dolman. 2008. Climate controls on the variability of fires in the tropics and subtropics. Global Biogeochemical Cycles 22:1–13.
Western, A. W., R. B. Grayson, G. Bschl, and G. R. Willgoose. 1999. Observed spatial organization of soil moisture indices. Water Resources Research 35:797–810.
Wright, I. J., M. Westoby, P. B. Reich, J. Oleksyn, D. D. Ackerly, Z. Baruch, F. Bongers, J. Cavender-Bares, T. Chapin, J. H. C. Cornellissen, M. Diemer, J. Flexas, J. Gulias, E. Garnier, M. L. Navas, C. Roumet, P. K. Groom, B. B. Lamont, K. Hikosaka, T. Lee, W. Lee, C. Lusk, J. J. Midgley, Ü. Niinemets, H. Osada, H. Poorter, P. Pool, E. J. Veneklaas, L. Prior, V. I. Pyankov, S. C. Thomas, M. G. Tjoelker, and R. Villar. 2004. The worldwide leaf economics spectrum. Nature 428:821–827.
Yackulic, C. B., M. Fagan, M. Jain, A. Jina, Y. Lim, M. Marlier, R. Muscarella, P. Adame, R. DeFries, and M. Uriarte. 2011. Biophysical and Socioeconomic Factors Associated with Forest Transitions at Multiple Spatial and Temporal Scales. Ecology and Society 16:art15.
Zarin, D. J., E. a. Davidson, E. Brondizio, I. C. Vieira, T. Sá, T. Feldpausch, E. A. Schuur, R. Mesquita, E. Moran, P. Delamonica, M. J. Ducey, G. C. Hurtt, C. Salimon, and M. Denich. 2005. Legacy of fire slows carbon accumulation in Amazonian forest regrowth. Frontiers in Ecology and the Environment 3:365–369.
Zeng, H., H. Peltola, A. Talkkari, A. Venäläinen, H. Strandman, S. Kellomäki, and K. Wang. 2004. Influence of clear-cutting on the risk of wind damage at forest edges. Forest Ecology and Management 203:77–88.
Zhu, Z., and C. E. Woodcock. 2012. Object-based cloud and cloud shadow detection in Landsat imagery. Remote Sensing of Environment 118:83–94.
Zimmerman, J. K., E. M. Everham, R. B. Waide, D. J. Lodge, C. M. Taylor, and N. V. L. Brokaw. 1994. Responses of Tree Species to Hurricane Winds in Subtropical Wet Forest in Puerto-Rico - Implications for Tropical Tree Life- Histories. Journal of Ecology 82:911–922.

Appendix 1: Supplementary information for Chapter 1

Land cover classification

This study employed a land cover classification developed and validated in a previous study in our study area (Gutiérrez-Vélez and DeFries 2013). The original classification spanned 10 years (2000-2010). It differentiates between high-biomass forest, low-biomass forest, and other land cover types, including oil palm, deforested, fallow, pasture, bare soil, and water, with overall accuracy of 93%. We applied the same procedure and classification tree to additional images to complete a 30 year time series with 30x30 m pixel resolution. Specifically, we identified Landsat TM/ETM+ scenes from 1984-1999, and 2011-2013 (Table 1). All scenes were acquired as surface reflectance with atmospheric corrections from the Landsat CDR archive (USGS 2017) via USGS Earth Explorer (http://earthexplorer.usgs.gov). Scenes were radiometrically normalized to a reference image from the year 2000 using the iMAD algorithm (Canty and Nielsen 2008) and clouds and cloud shadows were masked using the Fmask band included in the surface reflectance product (Zhu and Woodcock 2012, Zhu et al. 2015, USGS 2017). We calculated the following band transformations for each image, for use in the classification procedure: 1) tasseled cap band transformations (brightness, greenness, third), 2) bare, vegetation, and shade fractions from spectral mixture analysis, and 3) NDVI. Finally, we applied the previously developed random forest classifier to the transformed bands and masked oil palm plantations with a previously developed map of oil palm in the study area (Gutierrez-Velez and DeFries 2013). To improve accuracy and predict land cover in data gaps or areas covered by clouds when possible, we applied a temporal filter to disallowed trajectories (cite). Remote sensing analyses were conducted in ENVI 4.8 (Exelis Visual Information Solutions).

Field data collection and calculation of forest biomass

To establish the relationship between forest age and biomass accumulation, we used data from 30 field plots. In each plot, we measured all stems > 5 cm diameter at breast heigh (dbh). To determine plot level biomass, we used the following allometric equation developed for secondary forest species in the central Amazon (Nelson et al. 1999):

$$\ln(\text{biomass}) = -1.9968 + 2.4128 * \ln(\text{DBH})$$

We scaled plot-level values to units of Mg/ha, and divided values by two so that estimates were in terms of kg C instead of kg biomass, under the assumption that C makes up 50% of biomass (Brown and Lugo, 1982). We found a highly significant relationship between biomass and forest age ($R^2 = 0.517$, $p > 0.001$, Figure 1).

References

Brown S and Lugo A E 1982 The Storage and Production of Organic Matter in Tropical Forests and Their Role in the Global Carbon Cycle Biotropica 14 161 Online: http://www.jstor.org/stable/2388024?origin=crossref

Canty M J and Nielsen A A 2008 Automatic radiometric normalization of multitemporal satellite imagery with the iteratively re-weighted MAD transformation Remote Sens. Environ. 112 1025–36

Gutiérrez-Vélez V H and DeFries R 2013 Annual multi-resolution detection of land cover conversion to oil palm in the Peruvian Amazon Remote Sens. Environ. 129 154–67 Online: http://dx.doi.org/10.1016/j.rse.2012.10.033

Nelson B W, Mesquita R, Pereira J L G, Souza S G a, Batista G T and Couto L B 1999 Allometric Regressions for Improved of Secondary Forest Biomass in the Central Amazon For. Ecol. Manage. 117 149–67

USGS 2017. Landsat 4-7 climate data record (CDR) surface reflectance. Available at: https://landsat.usgs.gov/sites/default/files/documents/ledaps_product_guide.pdf

Zhu Z and Woodcock C E 2012 Object-based cloud and cloud shadow detection in Landsat imagery Remote Sens. Environ. 118 83–94 Online: http://dx.doi.org/10.1016/j.rse.2011.10.028

Zhu Z, Wang S and Woodcock C E 2015 Improvement and expansion of the Fmask algorithm: Cloud, cloud shadow, and snow detection for Landsats 4-7, 8, and Sentinel 2 images Remote Sens. Environ. 159 269–77 Online: http://dx.doi.org/10.1016/j.rse.2014.12.014

Table 1: Landsat images used for classification (images for 2000-2010 are listed in Gutierrez Velez and DeFries 2013).

Year	Julian date	Satellite	Path/row
1985	195	Landsat TM	06-066
1985	218	Landsat TM	07-066
1987	185	Landsat TM	06-066
1987	96	Landsat TM	07-066
1988	204	Landsat TM	06-066
1988	211	Landsat TM	07-066
1989	190	Landsat TM	06-066
1989	221	Landsat TM	07-066
1990	225	Landsat TM	06-066
1990	216	Landsat TM	07-066
1991	164	Landsat TM	06-066
1991	219	Landsat TM	07-066
1993	192	Landsat TM	07-066
1993	217	Landsat TM	06-066
1995	207	Landsat TM	06-066
1995	262	Landsat TM	07-066
1996	265	Landsat TM	07-066
1996	114	Landsat TM	06-066
1997	180	Landsat TM	06-066
1997	251	Landsat TM	07-066
1998	247	Landsat TM	06-066
1998	142	Landsat TM	07-066
1999	218	Landsat TM	06-066
1999	233	Landsat ETM+	07-066
2011	203	Landsat TM	06-066
2011	226	Landsat TM	07-066
2013	208	Landsat OLI	06-066
2013	231	Landsat OLI	07-066

Figure 1: Relationship between AGB and age in 30 field plots.

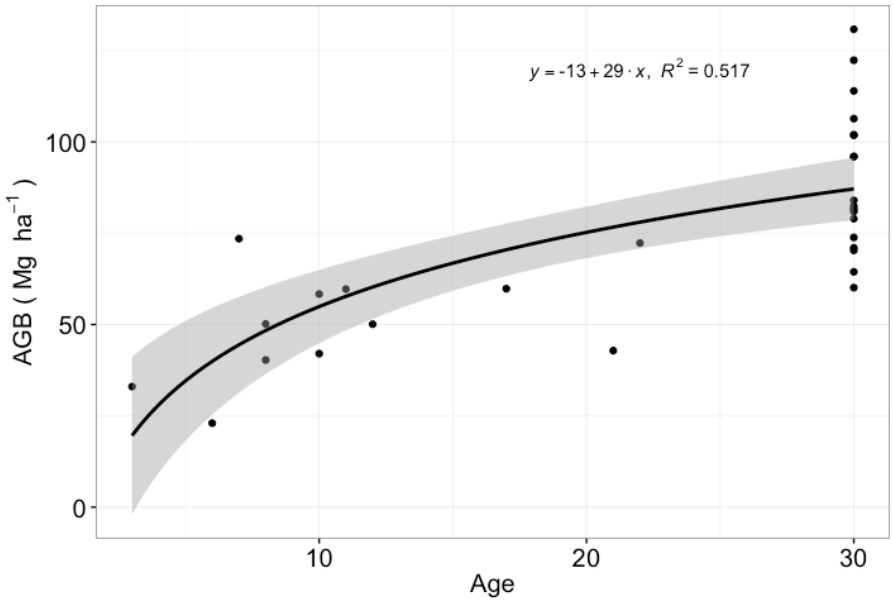

Figure 2: Plot of proportion of pixels with predicted probability of regrowth that actually re-grew. The solid 1:1 line indicates the expected value for a model that perfect predicts probability of regrowth. Our model somewhat over-predicts regrowth.

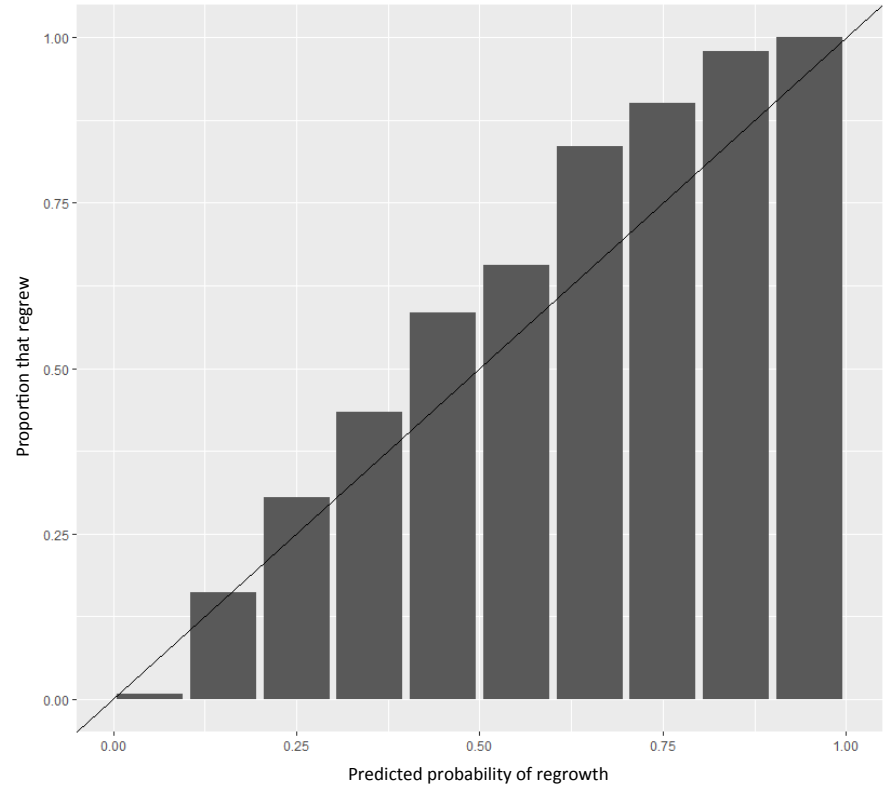

Figure 3: Plot of proportion of second-growth forest pixels with predicted probability of clearing that were actually cleared. The solid 1:1 line indicates the expected value for a model that perfect predicts probability of clearing. Our model somewhat under-predicts clearing.

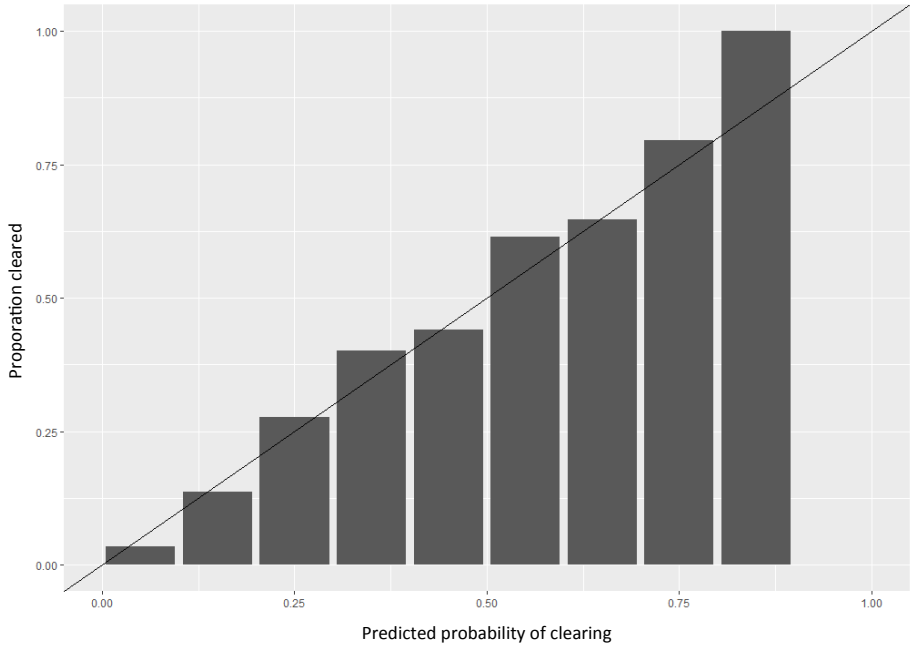

Figure 4: Distribution of forest ages in 2013.

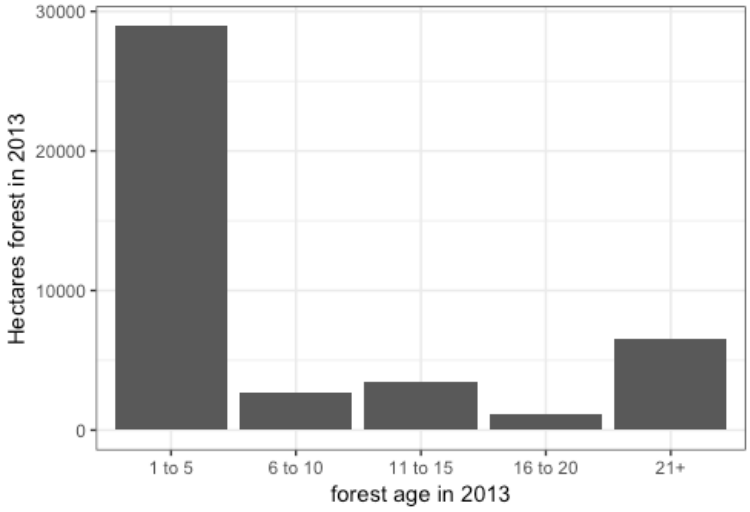

Figure 5: Inter-annual variability in probability of clearing and regrowth. Y-axis is the year-specific intercept from the mixed-effects models, i.e. the probability of event (forest regrowth, or second-growth forest clearing) at mean values for all predictors.

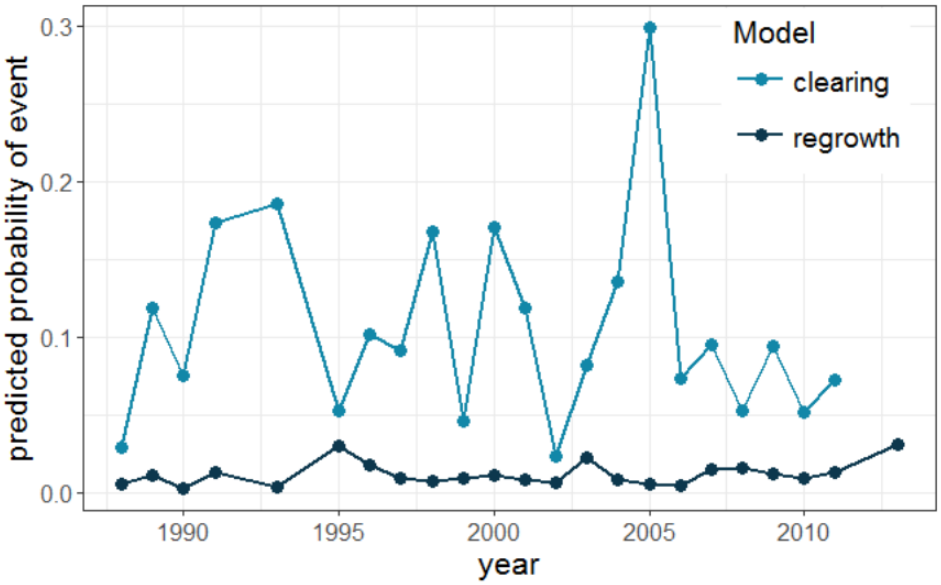

Appendix 2: Supplementary information for Chapter 2

Table 1: Correlation matrix between predictors used in analyses

	SPI	fallow (farm)	pasture (farm)	land owner present?	fallow (village)	pasture (village)	% landowners living in village	farm area
SPI	1							
fallow (farm)	0.043	1						
pasture (farm)	0.072	-0.098	1					
Land owner present?	0.002	0.090	0.034	1				
fallow (village)	0.031	0.278	-0.105	0.081	1			
pasture (village)	-0.002	0.053	0.386	-0.0359	0.169	1		
% landowners living in village	0.019	0.170	0.017	0.359	0.211	-0.087	1	
farm area	-0.010	-0.072	-0.042	-0.139	0.027	0.096	-0.105	1

Figure 1: Plot of proportion of parcels with predicted probability of fire that actually burned. The red dashed line indicates the expected value for a model that perfect predicts probability of fire.

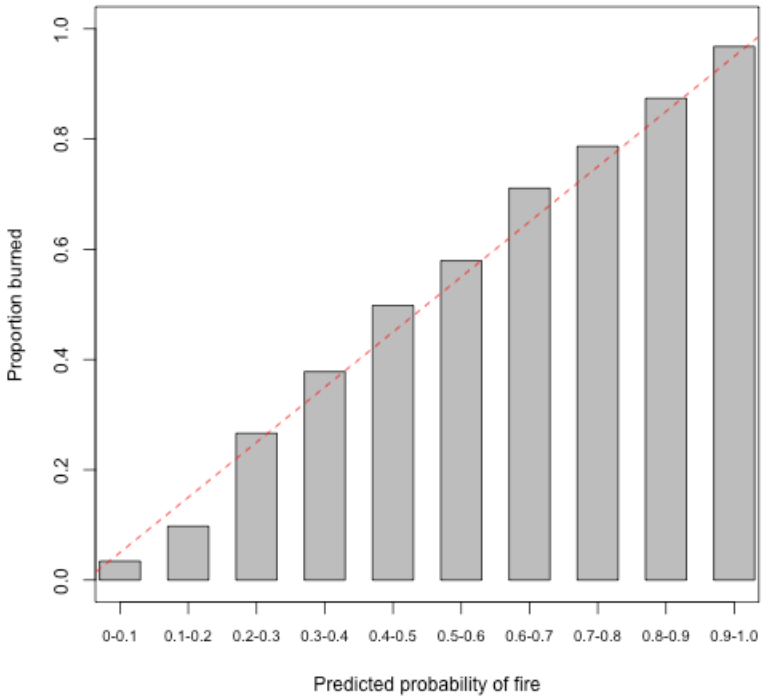

Figure 2: Observed fire size vs. predicted fire size. Our model underpredicts large fires.

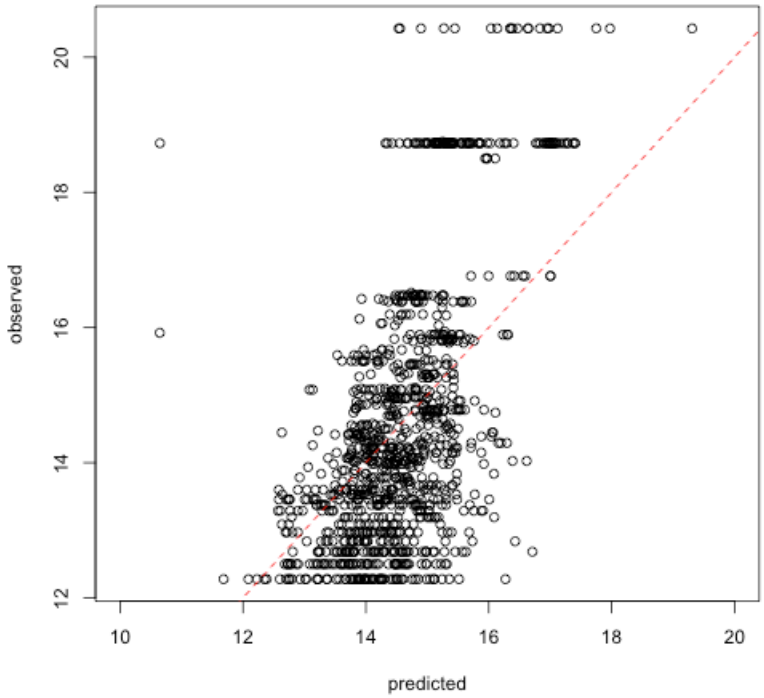

Appendix 3: Supplementary information for Chapter 3

Additional methods: Land cover classification

Field reference data for landcover classes were collected during a 2015 field campaign. These data were used for training and testing the classification. GPS points were taken at the center of uniform areas of the reference land cover categories using a Garmin GPSMAP 62sc. These points were later digitized into polygons covering the extent of the uniform area. This resulted in 152 polygons, or 2198.52 ha total, divided among classes (Table 2). Each polygon was divided into training and testing data, with 60% of pixels used for training and 30% used for testing. The middle 10% of pixels were excluded from each polygon so that training and testing areas were non-adjacent, to avoid inflating the accuracy of the classification due to spatial autocorrelation between training and testing data.

Landsat OLI images from 2014 and 2015 were used for the classification (Table 1). The 2013 land cover layer was obtained from a previous study (Gutiérrez-Vélez & DeFries, 2013). Images were calibrated and converted to surface reflectance prior to download, and pre-processed in the same manner as described for the wind damage mapping. Because field data were collected in 2015, we built the classification using the 2015 image and then applied the classification tree to the 2014 images. The classification was built using several spectral indices and spectral transformations: i) NDVI, ii) bare soil, vegetation, and shade fractions from SMA, iii) brightness, greenness, and third from a tasseled cap transformation, and iv) first- and second-order texture measures. Components i-iii were shown to be effective at classifying the non-oil palm land cover types in a land cover classification from the same study area (Gutiérrez-Vélez & DeFries, 2013). We used spectral libraries for bare, vegetation, and shade developed for the earlier classification for the SMA (Gutiérrez-Vélez & DeFries, 2013).

Texture measures were included to improve separation of oil palm plantations, which are spectrally similar to secondary forests but appear more uniform in satellite images due to even aged planting. Two measures were calculated: variance and homogeneity. Variance is the statistical variance in the pixel brightness value in the 3x3 neighborhood. Homogeneity is a second-order texture measure, based on a co-occurrence matrix, which characterizes relative frequencies between brightness levels (Haralick & Shanmugam, 1973; Rodriguez-Galiano *et al.*, 2012). Both measures were calculated over 3x3 pixel windows on bare, vegetation, and shade fractions from the SMA.

We used a random forest classifier to classify the images. Random forest is a supervised machine-learning algorithm that builds a series of decision trees, each one using a different random subset of the training data, and then assigns final classes based on the "votes" of each tree (Breiman, 2001). We fit our classification from 1000 decision trees, trying 6 variables at each split. Though the classification predicts error internally (Breiman, 2001), we further assessed the accuracy of the classification using the 30% of each polygon set aside as testing data, to avoid inflating the accuracy assessment of our classification. Because the goals of this classification were to accurately map forested areas, we lumped the non-forest and young oil palm categories into one "other" category for accuracy assessment. Because mature oil palm is common in the study area (Gutiérrez-Vélez *et al.*, 2011) and is easily confused with forest, it was not included in the *other* category to ensure that it was being accurately and effectively distinguished from forest. Random forest models were fit using the randomForest package in R. After classification, we applied a 3x3 majority filter to reduce speckle and noise. This filter also improved classification of edges of oil palm plantations, where texture measures may differ from interior pixels of oil palm plantations.

We applied a temporal filter for disallowed transitions to the 2014 land cover map (Roberts, 2002). This approach looks at three-year periods for every pixel and replaces "unreasonable" trajectories with the likely land cover given information from the other years. For example, a pixel classified as forest-pasture-forest in a three-year period would be reclassified as forest in the second year (Gutiérrez-Vélez & DeFries, 2013). This approach is also useful for predicting land cover in masked areas such as clouds or cloud shadows.

Figure 1: Maximum observed overshooting top probability on November 30, 2013 between 19:45 and 23:45 GMT. Center polygon indicates study area. Only values greater than 0.7 are shown to coincide with the greatest separation between overshooting top probability of detection and false alarm rate. Data derived from GOES-13 satellite following the methods of Bedka and Khlopenkov (2016). OT probability is derived from satellite observations made every 30 minutes, so high OT probability was not necessary confined observed locations. Rather, these data indicate high probability severe winds throughout the region on the indicated dates.

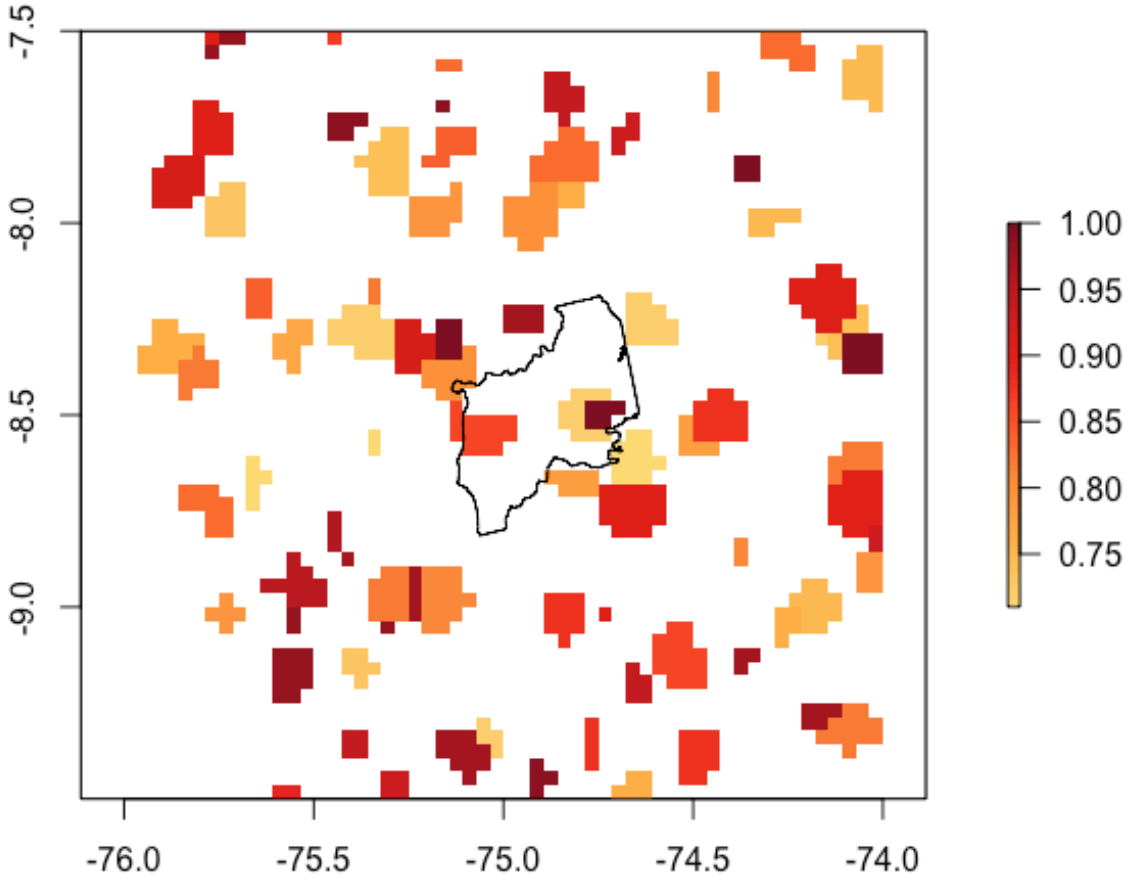

Figure 2: Endmembers used in spectral unmixing.

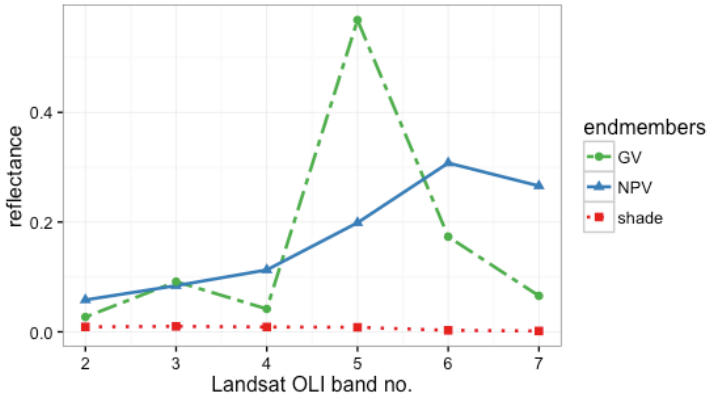

Figure 3: Schematic illustrating how spillover effects from anthropogenic disturbance were masked. A) ΔNPV before masking, with newly deforested areas shown in dark purple. Note high ΔNPV on forest edges near locations of recent deforestation. B) ΔNPV after masking 60 m buffer around deforested areas. Note that areas with high ΔNPV next to recent anthropogenic clearing have been masked.

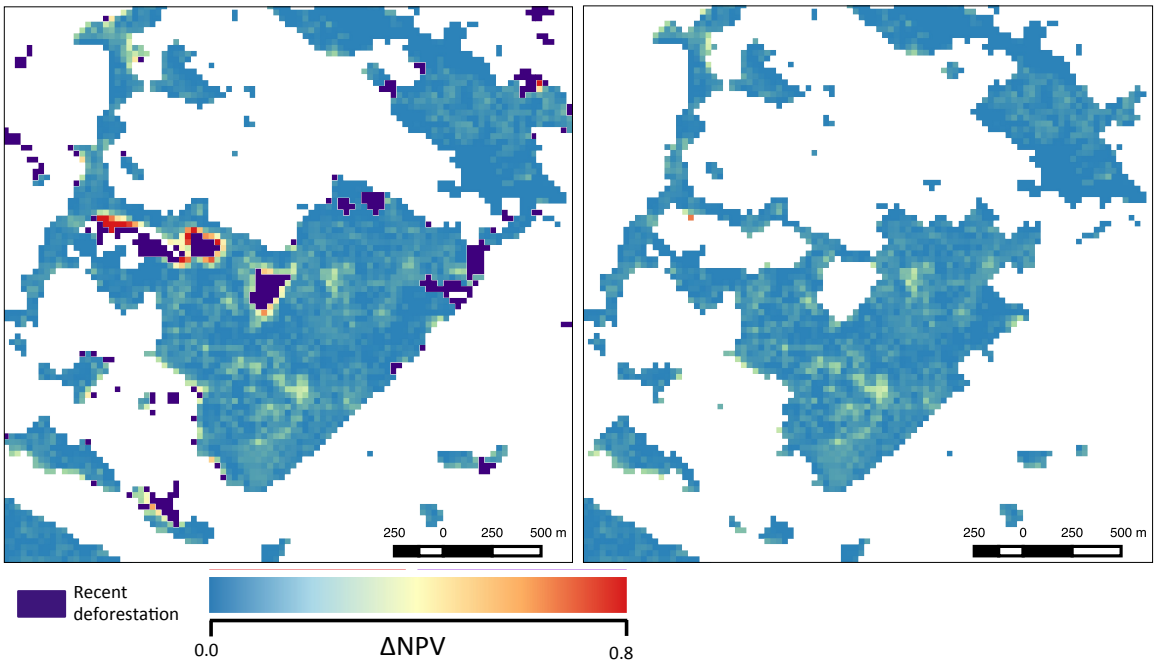

Figure 4: Histograms of ΔNPV. a) Histogram of ΔNPV of all pixels. b) Distribution of ΔNPV in a stratified random sample.

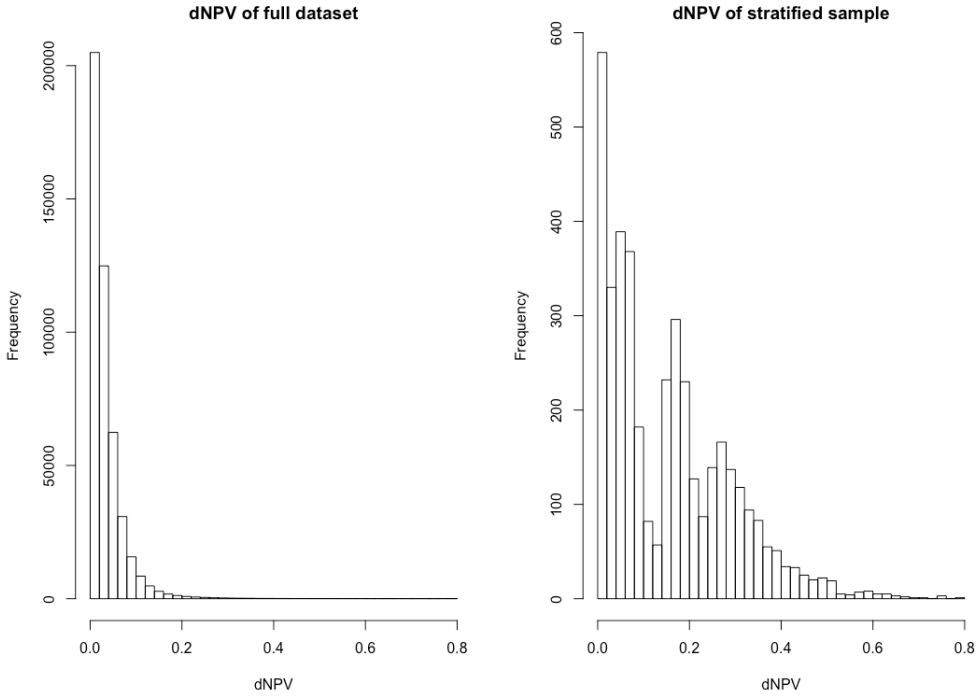

Figure 5: Frequency distributions and box plots of tree sizes for undamaged vs. damaged trees. Boxes show 25, 50, and 75% quantiles and whisker endpoints are 2.5 and 97.5% quantiles.

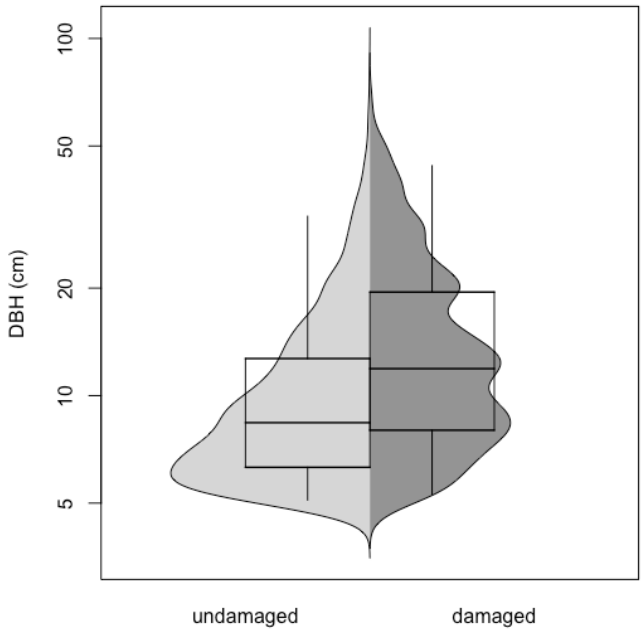

Figure 6: Relationships between ΔNPV and field measurements of damage. P-values for all regressions are < 0.001. a) ΔNPV vs. number of stems damaged in field plots. b) ΔNPV vs. total damaged basal area c) ΔNPV vs. proportion basal area damaged.

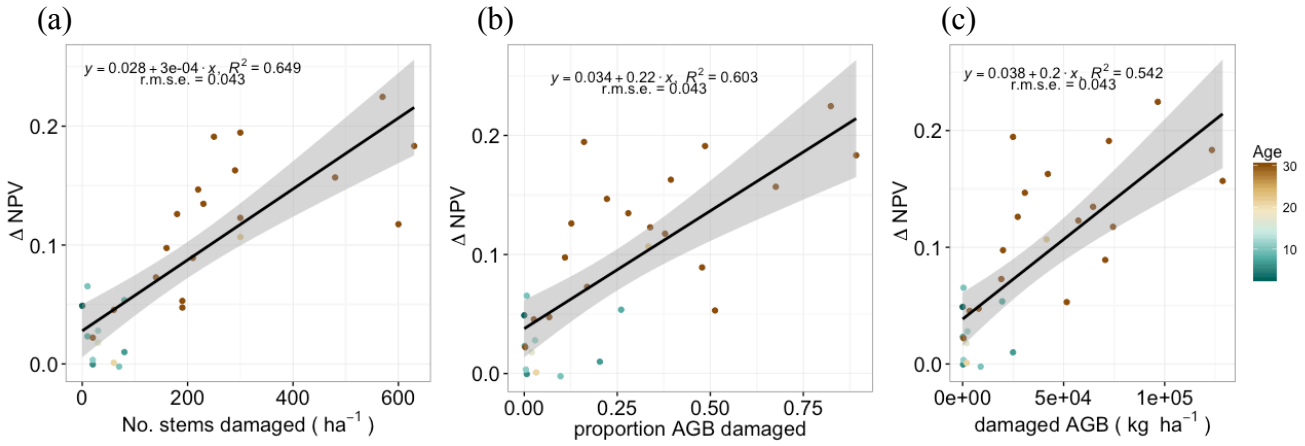

Figure 7: Distribution of patch-level fragmentation variables across the study area. Note that these distributions are different from the pixel level distributions of these variables, as each patch is comprised of many pixels. a) Distribution of patch sizes (ha), b) Patch edginess, c) Patch isolation.

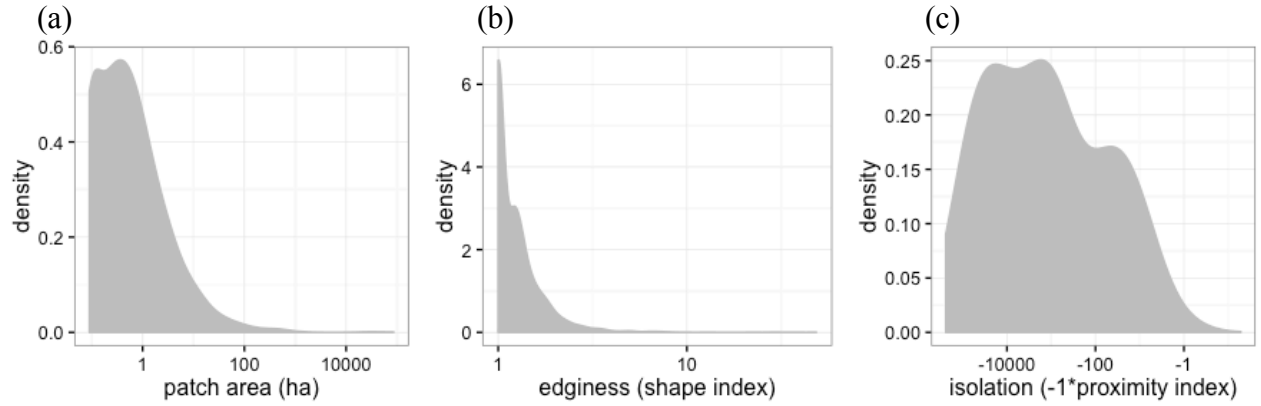

Table 1: List of all Landsat scenes used in analysis. All scenes were downloaded from the Landsat CDR archive via USGS Earth Explorer (http://earthexplorer.usgs.gov/).

Sensor	Path-row	Year	Julian day
Wind damage mapping			
Landsat OLI	06-066	2013	208
Landsat OLI	07-066	2013	247
Landsat OLI	06-066	2014	195
Landsat OLI	07-066	2014	250
Land cover mapping			
Landsat OLI	06-066	2015	230
Landsat OLI	07-066	2015	253
Landsat OLI	06-066	2014	227
Landsat OLI	07-066	2014	234
Landsat OLI	06-066	2013	208
Landsat OLI	07-066	2013	231

Table 2: Number and area of polygons for each LC class.

Class	No. Polygons	Training area (ha)	Validation area (ha)
Old-growth forest	8	216.54	108.90
Second-growth forest	30	129.78	67.05
Oil palm	25	109.62	57.15
Other	89	863.46	438.39

Table 3: Accuracy for LC classification. Rows are predicted class, columns are observed class. Producer's, user's and overall accuracy are presented as proportions, other values as pixel counts.

	Predicted class						
Observed class		**Old growth**	**oil palm**	**Second growth**	**other**	**total pixels**	**producer's accuracy**
	Old growth	1104	0	39	0	1143	0.97
	oil palm	2	554	43	36	635	0.87
	second growth	77	20	629	19	745	0.84
	other	0	20	10	4841	4871	0.99
	total pixels	1183	594	721	4896	7394	
	user's accuracy	0.93	0.93	0.87	0.99	**overall accuracy =**	**0.96**

Table 4: Summary data from the 30 field plots.

Plot No.	Plot age (years)	Stem density (No. stems ha^{-1})	ABG (Mg ha^{-1})	Damaged stems (No. stems ha^{-1})	Damaged AGB (Mg ha^{-1})
1	3	1900	36.31	0	0.00
2	6	1390	25.30	20	0.19
3	7	1370	80.86	80	14.91
4	8	1180	44.31	10	0.07
5	8	2180	55.19	80	11.56
6	10	1280	64.17	70	5.99
7	10	1480	46.23	10	0.33
8	11	1310	65.65	20	0.35
9	12	1050	55.10	30	1.71
10	17	1350	65.78	30	1.40
11	21	1800	47.14	60	1.56
12	22	870	79.53	300	26.91
13	30	1120	134.59	180	18.04
14	30	1710	105.57	300	17.52
15	30	1160	70.88	290	27.88
16	30	1120	92.39	210	41.07
17	30	850	86.88	60	2.56
18	30	1390	112.13	20	0.37
19	30	1190	112.01	160	13.38
20	30	1260	78.11	140	13.02
21	30	1160	143.90	230	39.94
22	30	810	89.03	220	20.86
23	30	720	90.64	250	46.09
24	30	1010	105.60	300	35.68
25	30	930	66.10	190	31.88
26	30	1780	81.24	190	5.86
27	30	1650	125.36	600	47.99
28	30	1310	77.34	570	61.40
29	30	1180	117.01	480	77.09
30	30	1070	89.77	630	78.82

Appendix 4: Supplementary information for Chapter 4

Table 1: Species included in models

Species	N. individuals in 2016	SLA	WD	Present in plots:
ALCFLO	13	295.00	0.43	EV1, SB3
ALCLAT	38	191.83	0.40	All
ANDINE	37	258.06	0.65	SB1, SB2, SB3
BUCTET	19	271.87	0.64	EV1, SB3
BYRSPI	36	237.99	0.61	All
CASARB	382	218.19	0.58	All
CASSYL	33	152.93	0.71	All
CECSCH	61	184.78	0.26	All
COCPYR	23	79.64	0.48	EV1, SB3
COCSWA	39	77.35	0.68	EV1
CORBOR	83	179.35	0.71	EV1, SB1, SB3
DACEXC	82	137.59	0.53	All
DENARB	18	293.76	0.43	SB1, SB2
DRYGLA	21	146.75	0.67	SB3
EUGSTA	259	97.00	0.69	EV1, SB3
FAROCC	537	242.06	0.60	All
GUAGLA	13	176.29	0.47	EV1, SB3
GUAGUI	60	276.74	0.59	SB1, SB2
HENFAS	17	280.41	0.48	EV1, SB1, SB3
HIRRUG	156	117.10	0.87	EV1, SB3
HOMRAC	39	248.28	0.79	EV1, SB1, SB3
ILESID	21	148.46	0.74	EV1, SB3
INGLAU	52	198.41	0.63	All
IXOFER	111	144.19	0.65	All
MANBID	191	100.83	0.86	All
MATDOM	12	73.17	0.69	EV1
MELHER	9	167.37	0.45	SB3
MICIMP	168	206.54	0.75	EV1, SB1, SB2
MICMIR	51	123.89	0.60	All
MICPRA	939	163.62	0.65	All
MICTET	22	132.45	0.71	EV1, SB2, SB3
MIRCHR	83	81.50	0.70	EV1
MYRDEF	641	130.61	0.80	All
MYRFAL	48	153.54	0.95	EV1, SB1
MYRLEP	44	162.81	0.80	SB1, SB3
MYRSPL	37	246.40	0.74	SB1, SB2, SB3
OCOLEU	258	128.38	0.46	All

OCOSIN	5	140.74	0.58	SB2
ORMKRU	60	176.16	0.48	EV1, SB3
PALRIP	12	273.31	0.47	EV1, SB1, SB2
PREMON	772	174.79	0.31	All
PSYBER	107	372.39	0.47	All
PSYBRA	1542	302.83	0.38	All
PSYGRA	104	181.52	0.29	SB2
RHEPOR	44	72.16	0.83	EV1
SCHMOR	123	196.85	0.42	All
SIMTUL	104	96.30	0.56	SB3
SLOBER	96	119.71	0.77	EV1, SB1, SB3
SWIMAC	62	249.62	0.52	SB1, SB2
SYZJAM	538	90.90	0.66	SB1, SB2, SB3
TABHET	168	167.67	0.66	All
TETBAL	76	140.50	0.53	SB1, SB3
TRIPAL	17	238.25	0.69	All

Table 2: Model parameters for the growth and survival models. Parameter values are median parameter estimates with 95% credible intervals in parentheses. Species-specific parameters (β_{ks}) are not shown.

Parameter	**Description**	**Growth model**
b_1	mean intercept	0.096 (0.078, 0.114)
b_{11}	SLA effect on intercept	0.008 (-0.011, 0.028)
b_{12}	WD effect on intercept	-0.016 (-0.035, -0.003)
σ_1	variance associated with intercept	0.004 (0.003, 0.006)
b_3	mean drought effect	-0.047 (-0.057, -0.038)
b_{31}	SLA effect on drought effect	0.008 (-0.002, 0.019)
b_{32}	WD effect on drought effect	0.009 (-0.001, 0.019)
σ_3	variance associated with drought effect	$5x10^{-4}$ ($2x10^{-4}$, $9x10^{-4}$)
b_4	mean crowding effect	-0.005 (-0.009, -0.001)
b_{41}	SLA effect on crowding effect	-0.001 (-0.005, 0.004)
b_{42}	WD effect on crowding effect	-0.001 (-0.006, 0.003)
σ_4	variance associated with crowding effect	$6x10^{-5}$ ($2x10^{-5}$, $1x10^{-4}$)
b_5	mean slope effect	-0.009 (-0.016, -0.003)
b_{51}	SLA effect on slope effect	-0.06 (-0.013, 0.001)
b_{52}	WD effect on slope effect	-0.001 (-0.008, 0.005)
σ_5	variance associated with slope effect	$2x10^{-4}$ ($9x10^{-5}$, $4x10^{-4}$)
b_6	mean curvature effect	0.001 (-0.005, 0.006)
b_{61}	SLA effect on curvature effect	0.004 (-0.003, 0.011)
b_{62}	WD effect on curvature effect	-0.004 (-0.010, 0.002)
σ_6	variance associated with curvature effect	$1x10^{-4}$ ($5x10^{-5}$, $3x10^{-4}$)
b_7	mean NCI*drought interaction	-0.004 (-0.002, -0.010)
b_{71}	SLA effect on NCI*drought interaction	-0.002 (-0.009, 0.004)
b_{72}	WD effect on NCI*drought interaction	-0.001 (-0.007, 0.006)
σ_7	variance associated with NCI*drought interaction	$3x10^{-5}$ ($8x10^{-5}$, $2x10^{-4}$)
b_8	mean slope*drought interaction	-0.005 (-0.012, 0.001)

b_{81}	SLA effect on slope*drought interaction	0.004 (-0.004, 0.012)
b_{82}	WD effect on slope*drought interaction	0.004 (-0.003, 0.011)
σ_8	variance associated with slope*drought interaction	$9x10^{-5}$ ($3x10^{-5}$, $2x10^{-4}$)
b_9	mean curvature*drought interaction	-0.009 (-0.016, -0.002)
b_{91}	SLA effect on curvature*drought interaction	-0.008 (-0.017, 0.000)
b_{92}	WD effect on curvature*drought interaction	-0.003 (-0.011, 0.003)
σ_9	variance associated with curvature*drought interaction	$3x10^{-5}$ ($1x10^{-4}$, $3x10^{-4}$)
b_{10}	mean antecedent growth effect	NA
b_{101}	SLA effect on antecedent growth effect	NA
b_{102}	WD effect on antecedent growth effect	NA
σ_{10}	variance associated with antecedent growth effect	NA
β_2	diameter effect	0.038 (0.036, 0.041)
σ_{growth}	variance in growth	0.025 (0.025, 0.025)
$\sigma_{individual}$	variance associated with individual effects (γ_i)	0.003 (0.002, 0.003)

Figure 1: Distribution of topography variables across the four plots. Note that each data point is the topography at the location of an individual tree stem.

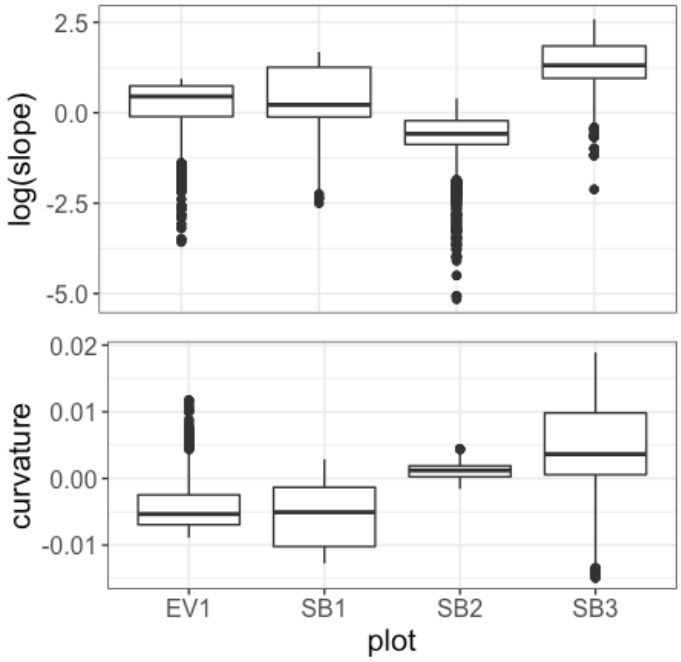

Figure 2: Observed growth across the three study years.

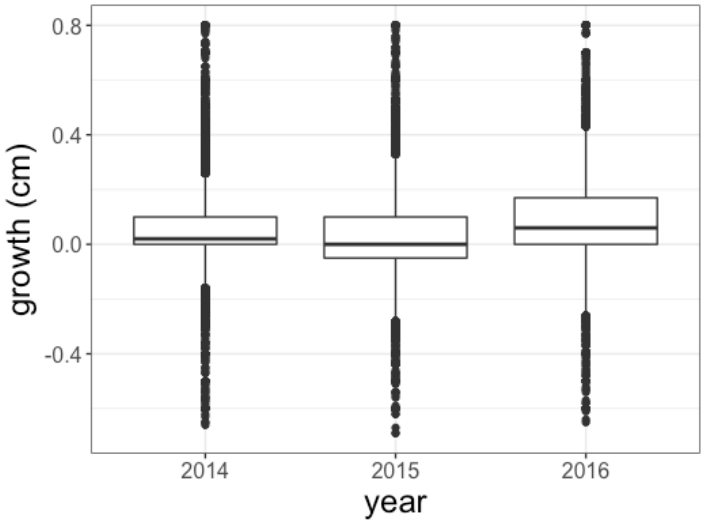

Figure 3: Replicated vs. observed growth. Red dashed line is 1:1 line. R^2 replicated vs. predicted equals 0.32.

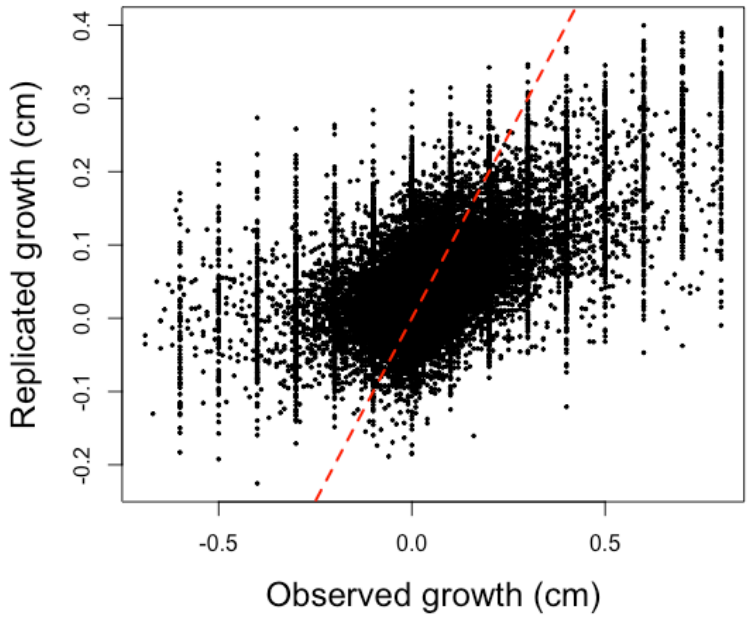

Figure 4: Predicted probability of survival vs. observed survival. R^2 predicted vs. observed equals 0.56.